Forschungszentrum Jülich
in der Helmholtz-Gemeinschaft

Institut für Bio- und Nanosysteme (IBN)
Bioelektronik (IBN-2)

Chemical Modification of Silicon Surfaces for the Application in Soft Lithography

Sandra Gilles

Jül-4249

Berichte des Forschungszentrums Jülich ; 4249
ISSN 0944-2952
Institut für Bio- und Nanosysteme (IBN)
Bioelektronik (IBN-2) Jül-4249

Vollständig frei verfügbar im Internet auf dem Jülicher Open Access Server (JUWEL)
unter http://www.fz-juelich.de/zb/juwel

Zu beziehen durch: Forschungszentrum Jülich GmbH · Zentralbibliothek, Verlag
D-52425 Jülich · Bundesrepublik Deutschland
☎ 02461/61-5220 · Telefax: 02461/61-6103 · e-mail: zb-publikation@fz-juelich.de

Chemical Modification of Silicon Surfaces for the Application in Soft Lithography

Sandra Gilles

Table of Contents

1 Introduction

In 1965 MOORE [58] predicted that the transistor density of integrated circuits would double every 2 years[1]. 40 years later this observation called Moore's law is still an ongoing trend. Enhancing computing performance while simultaneously lowering the fabrication costs is the driving force for the semiconductor industry to decrease the sizes of devices on a chip further and further. To escape from the inevitable size restrictions, efforts are made to find innovative architectures leading to new concepts in electronics. Molecular Electronics is a research field pointing in that direction. The idea to use single molecules as functional units was inspired by FEYNMAN in his speech „There's Plenty of Room at the Bottom" in 1959 [2]. Unconventional techniques are required in order to address molecules in electronics.

Conventional patterning techniques used in semiconductor processing like Photolithography or Electron Beam Lithography are limited with respect to resolution or economic viability. Therefore efforts are made to introduce alternative patterning methods such as Soft Lithography techniques [96]. It is characteristic for Soft Lithography methods that a soft polymer as stamp or mold is used for patterning a substrate by printing or molding. Surface and interface properties often play fundamental roles in the printing and molding processes. Tailor-made surface properties are required for many Soft Lithography applications. It is often sufficient to build up films of molecular monolayer thickness in order to modify the properties of a materials surface. Such monolayers can consist of physically adsorbed molecules or more stable of molecules that are able to chemically bind to the surface. Langmuir-Blodgett films and self-assembled monolayers are common possibilities for such surface coatings [89]. The two-dimensional surface film determines the new surface properties.

Commmonly silicon is the basic semiconductor material for microelectronic devices. Its production and handling is well-established. It is therefore reasonable that also in Soft Lithography techniques silicon is used as substrate for patterning procedures or as master for stamp fabrication. Hence, the chemical modification of silicon surfaces is a matter of interest for various applications in Soft Lithography. Appropriate molecules for this intention are organosilanes, which are capable to anchor to the surface in a self-limiting self-assembly process [67] [64]. They can bear a wide range of functionalities determining the new surface properties. Furthermore, they can act as interface between inorganic and organic compounds due to their characteristic structure. Further coupling of organic molecules to the interfacial silane film is possible.

[1] originally in 1965 MOORE predicted a doubling time of 12 months, but corrected his prognosis in 1975 to 24 months

[2] The speech was given at the annual meeting of the American Chemical Society at the California Institute of Technology (Caltech), a transcript is available on the internet under http://www.zyvex.com/nanotech/feynman.html

The purpose of this work was to modify silicon surfaces by chemical attachment of functional molecules, e.g. organosilane self-assembled monolayers. Especially perfluorinated and thiolterminated molecules should be used to create surfaces for specific Soft Lithography applications. The aim was to reproducibly obtain dense, stable and homogeneous films; monolayers suitable for the required demands.

A polymeric stamp, the key element for Soft Lithography techniques, generally gets in contact with a silicon surface during molding and printing procedures. The materials can stick together because of their surface properties. A release agent is required to ensure that polymer and silicon can be separated easily. The coupling of perfluorinated organosilane molecules to the silicon surface is a common method to lower its surface energy and to promote the release from the polymer. Several demands are made on such a lubricant layer. The surface property should be such that an easy release of polymer and silicon is possible. The molecules have to be well-anchored so that they stay on the surface during numerous molding processes. Furthermore, the layer should be extremely thin and homogeneous so that pattern topographies are not altered. The last point especially gains importance with respect to the down-scaling of feature sizes to the nanometer regime.

In Molecular Electronics single molecules or domains of molecules are addressed for investigation or usage as functional units. This can commonly be done by placing the molecules between two metal electrodes. This is often performed on a silicon substrate in the face of later integration into semiconductor electronics. Such metal–molecule–metal structures can be fabricated using Soft Lithography techniques. The advantage is that these are highly gentle procedures, as required for the integration of sensitive molecules like proteins. Joining silicon and metal surfaces via a printing procedure is a challenging task. The adhesion between metal and silicon has to be promoted. Nobel metals are known to have a great affinity to sulfur, hence thiolterminated molecules attached to metal on one side and silicon on the other side should be able to work as adhesion layer. This can only be possible if the molecules are fixed on the surface and are standing upright. Also, a high concentration of free thiol groups is required.

2 Theory

2.1 Soft Lithography

Microfabrication for the information technology is usually based on Photolithography as patterning technique. In Photolithography a photomask is projected onto a thin film of photoresist. Development of photoresist, lift-off and etching are possible subsequent steps for the definition of structures. In the course of downscaling the feature sizes further and further, the wavelength of the used light has to be reduced as well. This is due to the fact that the resolution in Photolithography is related to the wavelength of the irradiating light. For the fabrication of nanoscale feature sizes deep ultraviolett (UV) or even soft X-ray radiation is required. These techniques have the disadvantage that substantial efforts have to be made because of their technical specifications. So are e.g. complex reflective optics demanded. Another possibility for the creation of patterns in the nanometer range is Electron Beam Lithography. Here an electron beam is scanned over the resist film. This method has the drawback that it is, in contradiction to Photolithography, a non-parallel process. The mentioned advanced lithographic methods are indeed suitable for the fabrication of extremely small feature sizes, but their introduction into an economic mass-production seems to be difficult.

To overcome the described problems, efforts to develop innovative lithographic techniques have been made. In this context a range of innovative methods, summarized as Soft Lithography, were introduced by XIA and WHITESIDES [96] in the 1990s and further developed by others.
Soft Lithography is a non-photolithographic method for carrying out micro- and nanofabrication. Patterns are generated by the use of an elastomeric stamp or mold with patterned relief structures on its surface. This patterned stamp is the key element to soft lithography. It is usually made of a polymer. A common polymer for the application as stamp or mold is poly(dimethylsiloxane) (PDMS). PDMS is a cross-linked silicone with the general structure shown in Fig. 2.1. The degree of cross-linking can be varied at will resulting in more soft or stiff PDMS material.

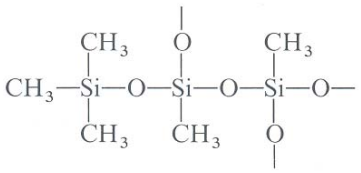

Figure 2.1: The general structure of silicones (Source: [70])

The stamp is fabricated (Fig. 2.2) using a master having relief structure on its surface. A prepolymer of the elastomer is poured over the master, cured and peeled off. The master is generally produced by common Photo- or Electron Beam Lithography. The master can be made of a silicon wafer with relief structures of photoresist, silicon, silicon oxide or silicon nitride, for instance.

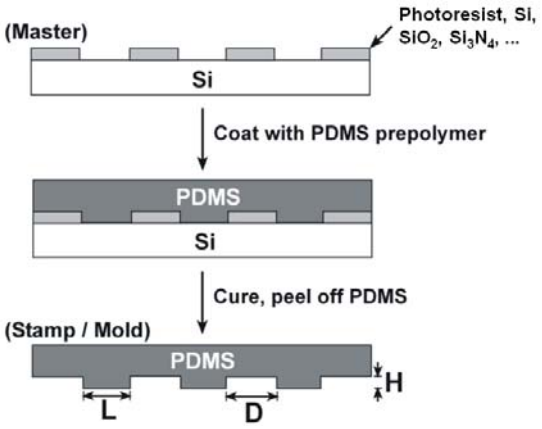

Figure 2.2: Schematic illustration of the fabrication of the topographically patterned elastomeric pattern-transfer agent (mold or stamp) by casting and curing an elastomer against a patterned relief structure (Source: [24])

The surface of a silicon master usually has to be modified so that the cured polymer can be peeled off. The surface free energy of the master has to be lowered to make it easier to separate master and polymer. A „release agent“ or „lubricant layer“ is needed. It is important for this application that the lubricant layer covers the master completely so that a complete release is guaranteed. It has to be stable so that it stays on the master and is not removed by the polymer. For feature sizes in the nanoscale range it further has to be extremely thin and homogenous in order not to change the patterns on the master. Often perfluorinated silanes, which can be covalently linked to the surface, are used as release agent (→ section 2.4).
Soft Lithography comprises a range of different techniques. Some examples are explained in the following.

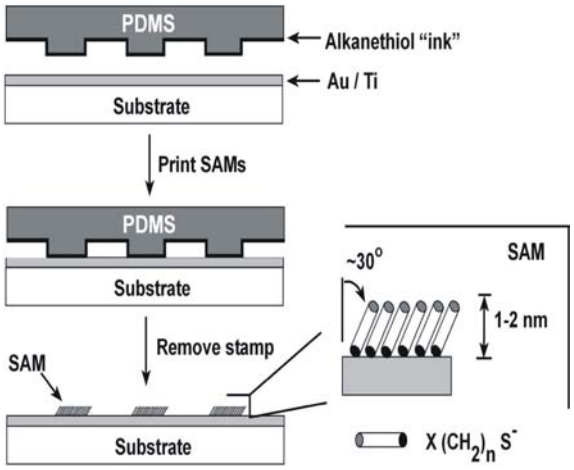

Figure 2.3: Schematic illustration of the Microcontact Printing procedure used to pattern self-assembling monolayers of alkanethiols on a gold surface (Source: [24])

Microcontact Printing (μCP) [48] is a technique for generating patterns of functional organic or inorganic layers on surfaces over large areas ($> cm^2$). The general procedure (Fig. 2.3) brings a topographically patterned elastomeric stamp, wetted („inked“) with a solution of molecules into contact with the surface of a metal, metal oxide or semicon-

ductor. The procedure is widespread with alkanethiols and derivatives on gold, silver, palladium and platinum. For these systems an ordered self-assembled monolayer (SAM) forms rapidly at the points of contact (→ section 2.2).

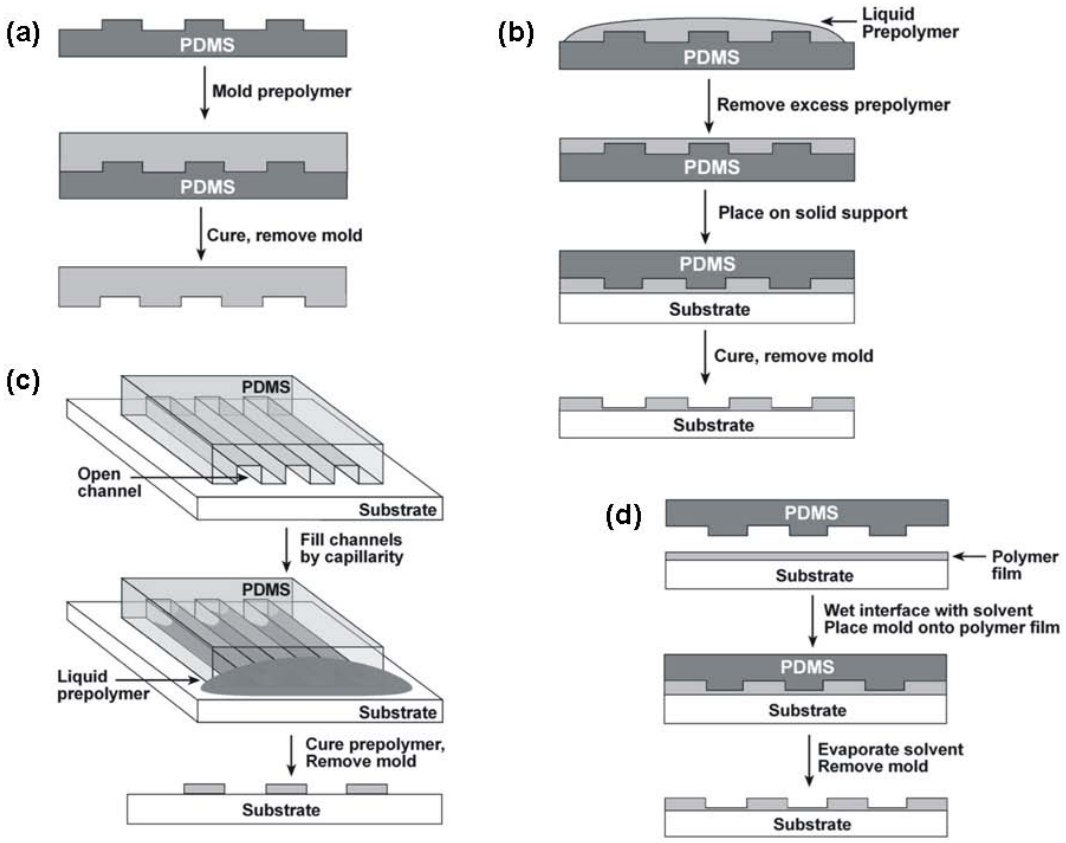

Figure 2.4: Schematic of several Soft Lithography methods (Source: [24])
(a) Replica Molding (REM)
(b) Microtransfer Molding (μTM)
(c) Micromolding in Capillaries (MIMIC)
(d) Solvent-assisted Micromolding (SAMIM)

Replica Molding (REM) [95] is a method for the duplication of the information present in the surface of a master (Fig. 2.4a). Polymer molds are prepared by casting against rigid masters and are then used as masters themselves in a second step. The resulting structures are complementary to those on the polymer mold and very similar to those on the original master.

In **Microtransfer Molding (μTM)** [99] a thin layer of liquid prepolymer is applied to the patterned surface of mold and the excess liquid is removed (Fig. 2.4b). The mold is then placed in contact with the surface of a substrate, and the prepolymer is cured to a solid by UV light or heating. Peeling away the mold leaves a patterned structure on the surface of the substrate. Often a thin residual film of polymer occurs between the raised features that has to be removed if the intent is to use the patterned structures as etch masks.

Micromolding in Capillaries (MIMIC) [44] uses a mold that is placed on the surface of a substrate to form a network of empty channels between them (Fig. 2.4c). A low-viscosity

prepolymer is then placed at the open ends of the channels, spontaneously filling them by capillary action. After curing the prepolymer into a solid and removal of the mold, a patterned structure of polymer is left on the substrate.

Solvent-assisted Micromolding (SAMIM) [45] generates relief structures in the surface of a material using a solvent able to dissolve or soften the material without affecting the mold (Fig. 2.4d). The mold is wetted with a solvent and brought into contact with the surface of the substrate, typically an organic polymer. The solvent dissolves a thin layer of the substrate, and the resulting fluid is molded against the relief structures in the mold. When the solvent dissipates and evaporates, the fluid solidifies and forms a patterned relief structure complementary to that in the surface of the mold.

Nanotransfer Printing (nTP), introduced by LOO et al. [53], is a method to transfer metal structures by a patterned elastomeric stamp. In Fig. 2.5 the technique is illustrated by the example of transferring gold to a GaAs surface modified by an alkanedithiol monolayer. A gold layer is deposited onto a polymer stamp (here PDMS) with relief structures. The gold-coated stamp is brought into contact with the substrate. S-Au bonds are formed spontaneously between the thiol groups of the substrate and the gold layer on the raised features of the stamp. Removing the stamp leaves only the chemically anchored gold patterns on the surface.

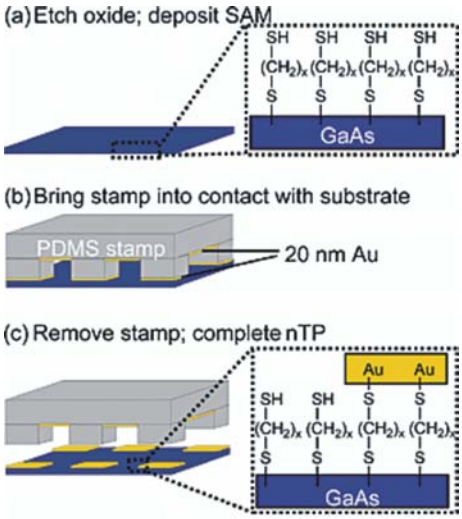

Figure 2.5: Schematic of the Nanotransfer Printing (nTP) procedure: (a) Alkanedithiols are deposited on a GaAs substrate. (b) Gold-coated elastomeric PDMS stamp with appropriate relief features is brought into contact with the treated substrate. (c) Removal of the stamp from the substrate completes the printing process. Au on the raised part of the PDMS stamp is bonded and transferred to the dithiol-coated GaAs. (Source: [53])

Shuttle-Transfer Printing (STP), a technique similar to nTP, was introduced by SCHWAAB [75]. The general idea is the definition of metal patterns with a high resolution process on a first substrate followed by transfer of the patterns onto a target substrate using a polymeric substrate as shuttle (Fig. 2.6). Resist patterns on the first substrate are defined by lithography (e.g. Photo-, Electron Beam or Nanoimprint Lithography). Then a

lubricant layer is deposited, only bonding to the parts of the substrate which are not covered by resist. Subsequently a metal layer is deposited. A following lift-off step removes the resist. After that only the lubricant and the metal inside the former resist patterns stay on the substrate. A transfer-mediating layer is immobilized onto the metal surface, e.g. by self-assembly of an alkanethiol. Further a polymer is brought into conformal contact with the first substrate. By removing the polymer the metal and the transfer-mediating layer stick to the polymer, the lubricant layer stays on the first substrate. The polymer surface with the metal patterns can then be contacted with a second substrate. This substrate can already have some metal patterns or functional layers. Before or after contacting both surfaces, a solvent can be applied to weaken the adhesion between metal and polymer. Finally the polymer is removed and the metal stays on the second substrate.

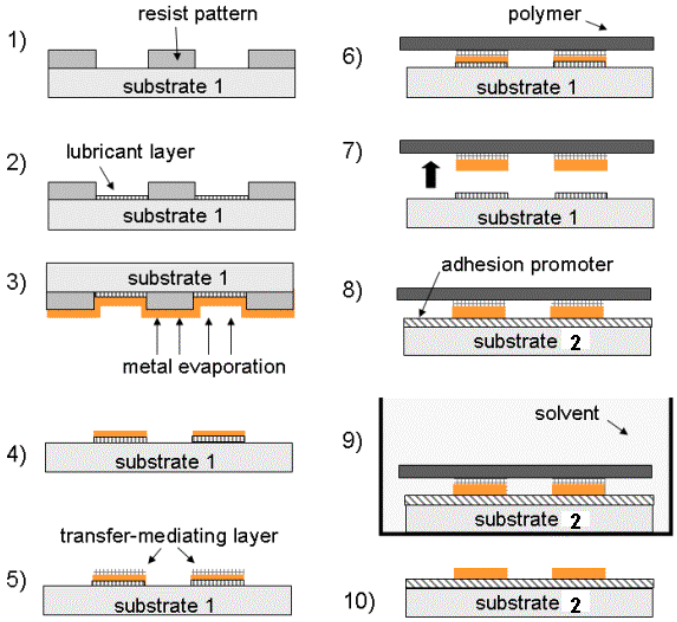

Figure 2.6: Schematic of the Shuttle-Transfer Printing (STP) process: (1) Resist patterning (2) Deposition of lubricant layer (3) Deposition of metal layer (4) Removal of resist (5) Immobilization of a transfer-mediating layer onto the metal surface (6) Contacting a polymer substrate with the first substrate (7) Removing the polymer together with the gold (8) Contacting the polymer surface with the metal patterns with a second substrate (9) Application of solvent (10) Stripping off the polymer (Source: [75])

The key to obtain reproducible well-defined patterns is a system substrate–shuttle–substrate with a gradient of metal adhesion. The adhesion between metal and the first substrate should be very low; the adhesion between metal and polymer should be higher in order to ensure the transfer from substrate to polymer. Finally the adhesion between metal and the second substrate should be even higher. The system proposed by SCHWAAB includes perfluorinated molecules as lubricant layer on the first substrate (low adhesion to metal), polyolefin plastomer (POP) as shuttle material (medium adhesion to metal) and thiolterminated molecules as adhesive layer on the second substrate (high adhesion to metal). Appropriate organosilane molecules can be used as lubricant and adhesive layer (→ section 2.4). The proposed polymer POP is a copolymer of ethylene and an α-olefin such as butene or octene. The polymer consists of long chains that are

not cross-linked. The stiffness of POP is usually higher than that of PDMS.

The fabrication of metal patterns with Soft Lithography techniques (as shown with nTP and STP) is of special interest for the application in Molecular Electronics, a research field dealing with electronic properties of molecules. Two main parts are existent in Molecular Electronics which are closely linked. On one hand discovering the electronic properties of different molecules is of interest, on the other hand the application of appropriate molecules as functional units is desired. For investigating properties like electric conductivity and switching behavior, a functional molecule or domains of molecules are positioned between two metal electrodes (metal–molecule–metal structure). The arrangement of electrodes and molecules can be of various kinds. Break junctions or crossbars are common techniques.
A break junction can be prepared by gluing a notched metal wire onto a flexible substrate and fracturing the wire by bending the substrate [59] [69]. After that an adjustable tunneling gap can be established and molecules of interest can be brought in between the break junction. The two broken parts of the metal wire are used as electrodes for investigating the electrical properties of the molecules. Similar electrodes spaced by a few nanometers can also be prepared by electrochemical etching. Single molecules can be placed in such junctions and investigated.
In the case of crossbar junctions domains of molecules are addressed. Crossbars consist of metal electrodes (e.g. nanowires) crossing each other on a substrate (Fig. 2.7). The first (bottom) electrode can be covered by a molecular layer. The second (top) electrode is brought on top, perpendicular to the bottom electrode. In that way the molecular interlayer in the area of crossing electrodes (junction) can be examined by applying a current to bottom and top electrode. Shuttle-Transfer Printing was introduced as a possibility for the fabrication of crossbar electrodes for Molecular Electronics.

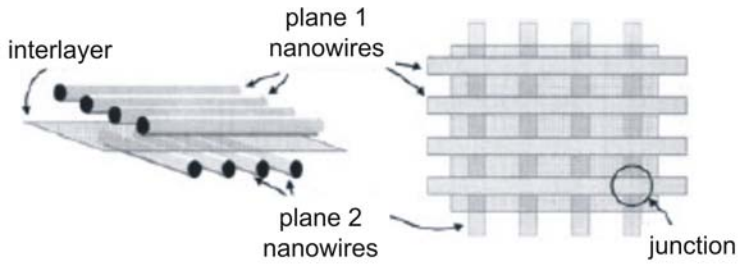

Figure 2.7: Schematic view of nanoelectronic crossbars from two different perspectives (Source: [80])

In the case of several parallel crossed electrodes, it is spoken of crossbar arrays. Crossbar arrays are a promising approach for an alternative computer architecture as suggested by HEATH et al. [31]. The crossbar architecture provides a high defect-tolerance and is considered as a potential substitute for conventional CMOS[3] technology.

[3]Complementary metal oxide semiconductor

2.2 Self-Assembled Monolayers

Thin films of only a few nanometers in thickness are able to change the surface properties of a substrate completely while the surface topography is conserved. The first approach to create indeed two-dimensional surface films was the Langmuir-Blodgett technique. Amphiphilic molecules are brought onto a liquid surface and assemble well-ordered at the liquid-air interface. The molecules are deposited onto a solid substrate by displacing the substrate from the liquid while the amphiphilic molecule film at the liquid–air interface is compressed. [89]

Another method is the formation of self-assembled monolayers (SAMs). SAMs are molecular assemblies that are formed spontaneously on the surface of an appropriate substrate. Therefore the substrate has to be exposed to the molecules (e.g. in terms of liquid, solution or vapor). The substance forms a surface coating consisting of a single layer of molecules. Since excess molecules cannot bind to the surface or the monolayer the process is self-limiting.

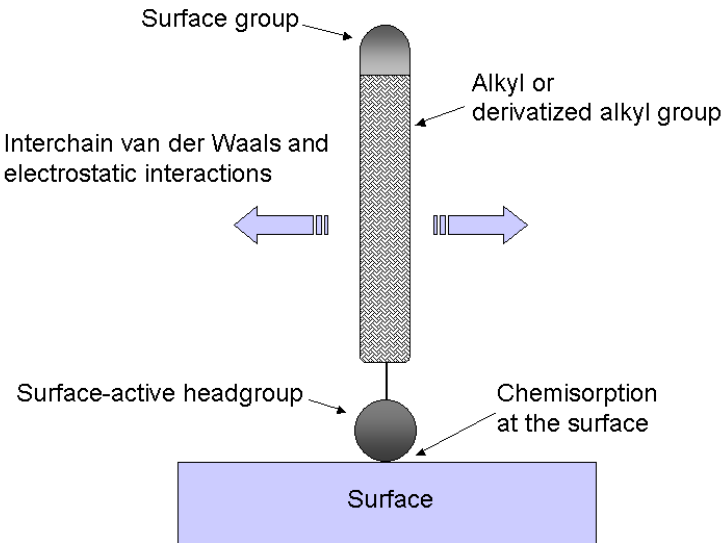

Figure 2.8: A schematic view of a typical self-assembling surfactant molecule (Source: [89])

According to ULMAN [89] a self-assembling surfactant molecule consists of three parts (see Fig. 2.8) from the energetic point of view. The head group provides the most exothermic process, the chemisorption on the substrate. The head group reacts with specific sites on the surface creating an attachment through a chemical bond. The energies associated with the chemisorption are at the order of hundreds of kJ/mol. As a result of the exothermic head group – substrate interactions, molecules try to occupy every available binding site on the surface. In this process they push together molecules that have already adsorbed.

The second molecular part is the alkyl chain. The energies associated with its interchain van der Waals interactions are at the order of a few kJ/mol (exothermic) per CH_2 unit. Van der Waals interactions are restricted to short-range; self-assembly cannot be possible given only the interactions among the alkyl chains. The first and most important process

is chemisorption. Only after molecules are put in place on the surface, formation of an ordered and closely packed assembly can start. In the case of alkyl chains (C_nH_{2n+1}) van der Waals interactions are the main forces whereas long-range electrostatic interactions dominate when a polar bulky group is substituted into the alkyl chain. [89]
The third molecular part is the terminal functionality. It determines the properties of the SAM surface, e.g. wettability and reactivity. The surface groups are often thermally disordered at room temperature.

The most well known and extensively studied SAMs are alkanethiols on gold. The high affinity of the thiol group to gold leads to a spontaneous formation of an Au–S bond. The formation of alkanethiols on gold is often presented as a model system of self-assembled monolayers.
Organosilanes can be used as SAM system for hydroxylated substrates or substrates with a thin water layer. An appropriate substrate for the formation of silane SAMs is an oxidized silicon surface. A further description of this process is given in section 2.4. According to ONCLIN et al. [64] the expression „self-assembled monolayers“ was first mentioned in an anonymous article concerning the self-assembly of organosilanes on silicon oxide [3].
The chemisorption can also result in an ionic bond, as it is the case for the assembly of carboxylic acids on AgO/Ag. The acid molecules are attached to the surface by $CO_2^- Ag^+$ coordination.

2.3 Surface Chemistry of Silicon and Silicon Oxide

In silicon crystals the atoms are sp^3 hybridized and bonded to four nearest neighbors in tetrahedral coordination. That means, silicon crystals have the diamond structure. When the crystal is cut or cleaved, bonds are broken, creating dangling bonds at the surface. The number and direction of these dangling bonds will depend on the direction of the surface normal (Fig. 2.9).

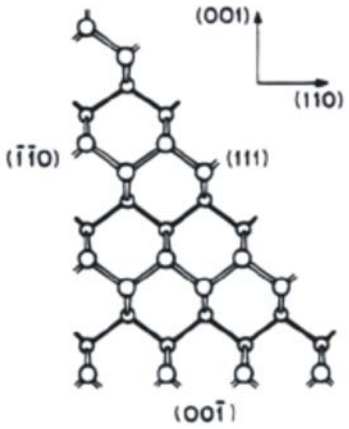

Figure 2.9: The dangling bond formation on the unreconstructed surfaces of the three low index planes of Si. Each Si atom in the bulk is tetrahedrally bonded to four nearest neighbors. Coplanar atoms are shown as the same size. (Source: [29])

The surface energy is lowered by reducing the number of dangling bonds by rebonding. Reconstructed silicon surfaces evolve, for instance with surface dimers (Fig. 2.10). Dangling bonds are the source of the chemical activity of silicon surfaces. [61]

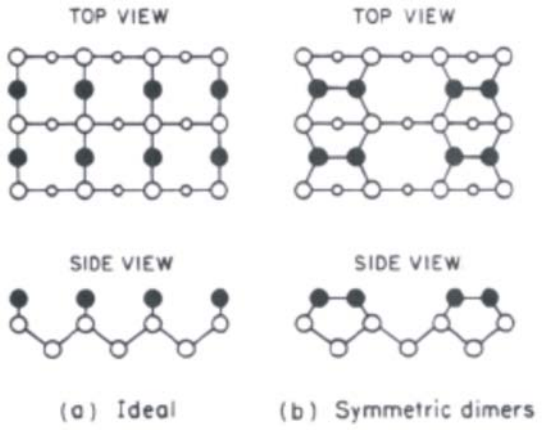

Figure 2.10: Top and side views of the ideal and reconstructed Si(100) surface (Source: [61])

The interaction of silicon surfaces with oxygen gas can lead to either production of a silicon oxide film on the surface (passive oxidation):

$$\mathrm{Si_{(s)}} + \mathrm{O_2} \rightarrow \mathrm{SiO_{2(s)}} \tag{2.1}$$

or to etching of the surface (active oxidation):

$$\mathrm{Si_{(s)}} + \frac{1}{2}\mathrm{O_2} \rightarrow \mathrm{SiO_{(g)}} \tag{2.2}$$

Which oxidation process takes place depends on surface temperature and oxygen pressure. Active oxidation dominates at high temperatures, while passive oxidation dominates at high oxygen pressures. [61]

Fresh cleaned silicon surfaces are oxidized by atmospheric oxygen under the formation of a native oxide layer of about 3 nm. SiO_2 layers of any thickness can be produced by methods like wet oxidation in a chemical etching environment, or by exposure of the clean silicon surface held at elevated temperatures to oxygen (dry oxidation) or water vapor (steam oxidation) under vacuum. The oxidation rate is greater for steam than for wet oxidation while for dry oxidation the rate is considerably less. Steam or wet oxidations are less reproducible and the oxides are less homogeneous and have a high pinhole density. SiO_2 tends to form a flexible but chemically saturated vitreous network. It has a local atomic configuration as present in crystalline SiO_2 (short-range order) but without long-range order. [18]

The configuration of oxygen in crystalline silicon oxide is a bridging position between two silicon atoms. Each silicon atom is surrounded by four oxygen atoms in a tetrahedral configuration in the bulk SiO_2. The Si–O bond length is about 1,6 Å for the SiO_2 modifications α- and β-quartz as well as α- and β-cristobalite [35].

Fresh prepared and water containing SiO_2 exhibits silanol groups Si–OH on the surface.

After some time the silanol groups undergo a condensation reaction, forming more stable siloxane groups Si–O–Si [35]. Therefore fresh or refreshed silicon oxide surfaces are more reactive than old ones.
Considering the SiO_2 surface, exemplary Si–O bonds to the upward tetradydra are cut (Fig. 2.11). Saturation of the surface Si sites with H results in three OH groups in a hexagon. These hydroxyl groups are pointing normal to the surface. The density of OH groups present on the surface is calculated to be $1/22\,\text{Å}^2$. [81]

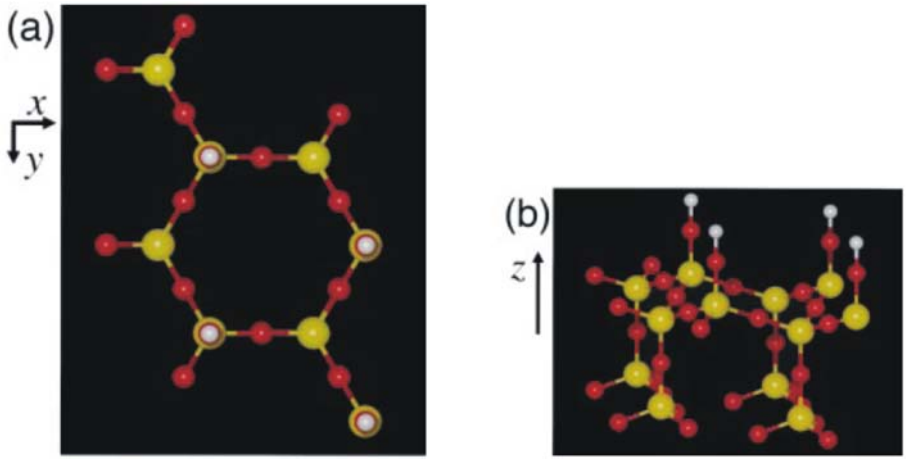

Figure 2.11: 3D representation of the silicon oxide surface showing O (red), Si (yellow) and H (white) atoms.
(a) Projection perpendicular to the surface shows a hexagonal lattice. The hydroxyls form a triangular sublattice
(b) Side view with hydroxyl groups pointing upward.
(Source: [81])

During storage silicon wafers become contaminated by organic materials in the atmosphere of a laboratory (e.g. organic solvents) and also by outgassing organic residues from the storage boxes after a few hours [85]. The organic substances easily adsorb to the silicon surface. As an effect of that process one can observe a more hydrophobic surface of a stored wafer in comparison to the perfectly hydrophilic surface of a fresh wafer. Since the organic contaminants covering the wafer inhibit surface reactions they are usually removed prior to further use. Most effective techniques for removing organic adsorbents are UV cleaning and plasma enhanced cleaning [16] [15]. It was found by CHOI et al. that ECR[4] oxygen plasma is more effective than the UV/O_3 cleaning for the removal of organic contaminants but can cause substantial damage to the silicon surface [15].

[4]Electron cyclotron resonance

2.4 Self-Assembly of Organosilanes on Silicon Oxide

As pointed out in section 2.2 various surfaces can be modified by self-assembled monolayers. The preparation of SAMs on silicon oxide surfaces is of special interest for semiconductor technology. Changing the surface properties (e.g. promoting adhesion to or assisting the release from another material) can be an application. SAMs on silicon oxide can also be used for pattern creation during the process of micro- and nanofabrication.
For the modification of silicon oxide (or often generally titled hydroxylated surfaces) organosilanes are suitable. Organosilanes are alkylsilane derivatives with the general structure $RSiX_3$, R_2SiX_2 or R_3SiX, where X is chloride or alkoxy and R is a carbon chain that can bear different functionalities [89]. A wide range of functionalities for diverse applications have been described in literature. Some examples are given in Table 2.1.

Table 2.1: Applications of functional organosilane self-assembled monolayers

End group functionality	Application examples	References
Perfluorinated alkyl chain	Release agent in Soft Lithography	
$-(CF_2)_n-CF_3$	→ Stamp fabrication	[96]
	→ Shuttle-Transfer Printing	[75]
	Avoidance of soil adhesion to a surface	[84]
	Friction/stiction control in micromachines	[54]
Amino group	Immobilization of biomolecules	
$-NH_2$	→ Enzymes	[6]
	→ DNA	[30]
	Chromatography	[93] [8]
Thiol group	Metal adhesion promotion	
-SH	→ Evaporated gold layers	[56]
	→ Gold nanoparticles	[47] [38]
Vinyl group	Preparation of defined multilayers	[63]
$-CH=CH_2$		

Although silanized surfaces are widely used, several details of the SAM formation mechanism are still a matter of research [64]. First a silanization mechanism was proposed by LEE [49] and further developed by ZISMAN [100]. They suggested, that in a first step the silane is hydrolyzed by water present in the liquid phase or at the substrate surface followed by the chemisorption process to the surface. Hydroxyl groups present on the surface were believed to interact with the hydrolized silane molecules via hydrogen bonds. The last step proposed was cross-linking between the adsorped silane molecules forming a stable network on the surface.

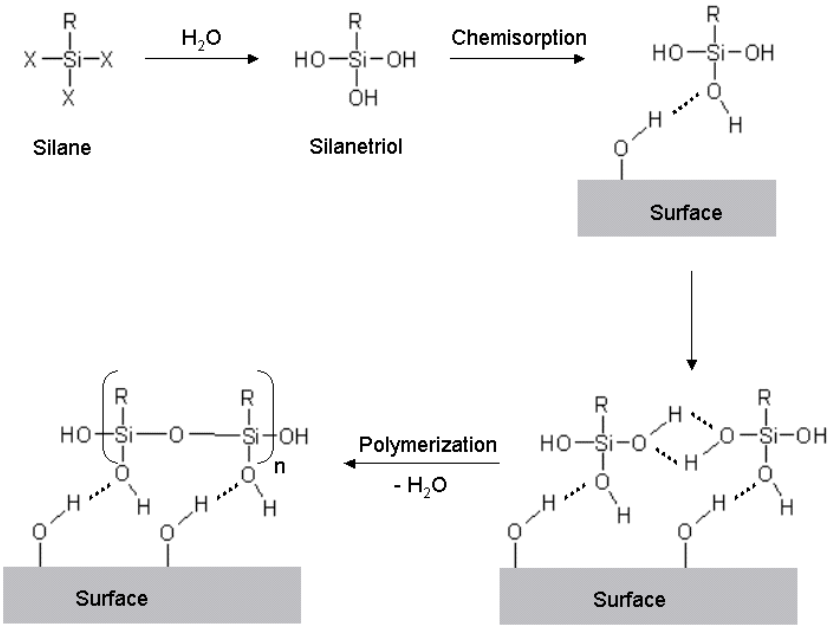

Figure 2.12: Mechanism of SAM formation of organosilane on a hydroxylated surface (Source: [100])

Further pioneering work concerning this topic was performed by SAGIV and NETZER in the early 1980s [73] [63]. They referred to the proposed model and showed a mechanism with cross-linking between molecules as well as coupling to the surface. It should be noted that they pointed out, that this can only be considered as an idealized model. It was already suggested by these authors that the real structure might contain organosilane molecules bonded covalently to the substrate, while forming only hydrogen bonds with adjacent silane molecules, or vice versa. Nevertheless, since then many authors dealing with the silanization procedure refer to the idealized model.
Later it was found to be more likely that the chemisorption takes place with a thin water layer on the substrate (Fig.2.13) and not directly with the hydroxyl groups present there [78] [87]. That is in agreement with the observation that silane SAMs can also be formed on surfaces where no or few hydroxyl groups are available like gold [21] [5], mica [43] [11] or dehydrated silica [50].

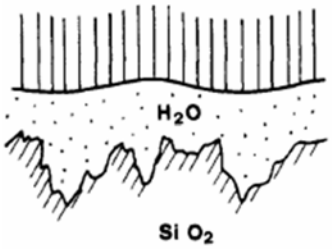

Figure 2.13: Schematic of silane network attached to the water layer on a silicon oxide substrate (Source: [78])

A theoretical consideration about the mechanism was done by STEVENS [81]. He pointed out that cross-polymerization in a well ordered alkylsilane SAM cannot occur due to

steric effects. Since the Si–O distance is too short, parallel arranged aliphatic tails would overlap in a cross-linked monolayer at full coverage. An illustration of the problem is shown in Fig. 2.14 taken from RYE et al. [71] [72]. The crystalline SiO_2 surface is drawn in the plane of the paper. The circles show the overlapping van der Waals radii of all-trans configured alkyl chains without taking the hydrogen atoms into account. STEVENS concluded that the alkyl chains cannot be parallel but must be splayed apart like crabgrass if cross-linking occurs. These theoretical thoughts are in agreement with the results of FONTAINE et al. [22], who found that the order of an octadecyltrimethoxysilane (OTMS) monolayer on a water surface is a decreasing function of the number of cross-links.

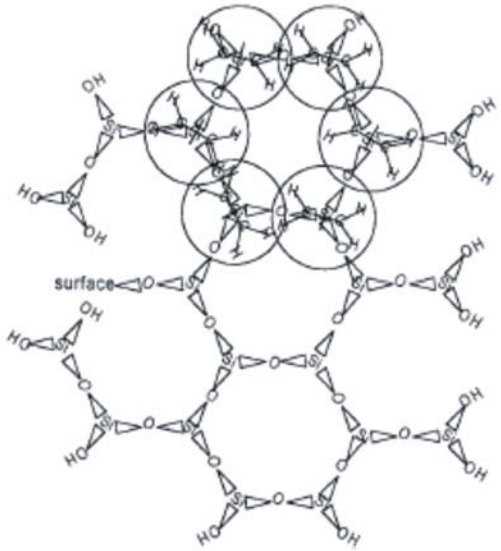

Figure 2.14: Model structure of SiO_2 surface in the plane of the paper with circles representing alkylchains pointing normal to the surface (Source: [71])

The above presented models have in common that water is required in the mechanism. This is in agreement with consistent observations that organosilane SAMs are only formed in the presence of water. The role of water was shown in numerous publications. The tenor is that a minimum amount of water is needed in the silanization process. In the case of perfectly dry conditions silane films of low quality are formed [7] or no reaction at all takes place [27]. With increasing availability of water the films reach a higher quality [87] [50]. An oversupply of water on the other hand can lead to unwanted polymerization of the silane molecules resulting in thick inhomogeneous films. The silanization procedure is often carried out under inert atmosphere to decrease the degree of polymerization in the silane liquid and on the sample surface caused by excess water presence. A deposition procedure at the laboratory atmosphere typically leads to cluster formation as can be seen in Fig 2.15.

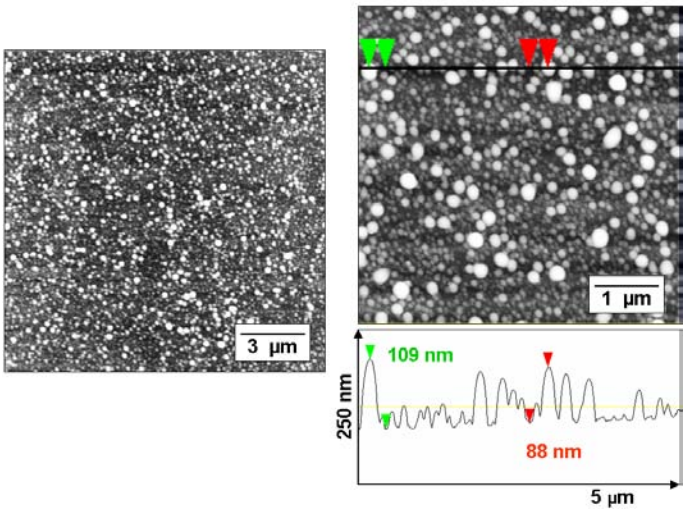

Figure 2.15: AFM image of a silicon wafer surface silanized at the laboratory atmosphere Contrast scale: 200 nm (left image) and 250 nm (right image)

Commonly, two different procedures are employed for creating organosilane SAMs on a surface: Liquid phase deposition (LPD) or vapor phase deposition (VPD). In liquid phase deposition the silane is diluted in an organic solvent and the substrate stays in the solution for a certain time. In case of vapor phase deposition the silane is evaporated (by reducing the pressure and/or heating) and the substrate is exposed to the vapor. It was found that the LPD tends to lead to clustered multilayers whereas high quality monolayers can be achieved by VPD [41] [34] [93]. JUNG et al. [41] found additionally that several cycles of vapor phase deposition with alternating silane and water deposition led to satisfying monolayers.
Various instruments and associated methods for the vapor phase deposition are reported. The VPD can be done by placing substrates and silane liquid in a vessel, sealing and leaving it for a certain time at ambient [25] or elevated temperature. The chamber can be also evacuated before sealing [93] [8]. An additional approach is to evacuate the vessel with substrates and silane inside room temperature. Furthermore silane molecules can be transported via an inert gas into the chamber where the substrates are placed [91] [68]. Several patents concerning the silanization process are applied. SHEU [77] invented a device in which a plasma is generated to clean substrate surfaces and subsequently vapor of organosilane compounds are introduced to silanize the cleaned surface. The substrates can be cured by a baking process in the same chamber. An apparatus with even more features was patented by HOFFMANN et al. [33]. The method includes cleaning of the substrate by a plasma, hydrating the substrate with steam, drying the substrate and silanization of the substrate by deposition of alkyl silane from the gas phase. All process steps are performed in the closed chamber.

Besides the role of water, several other parameters in the silanization process are investigated, for instance the effects of temperature, silane age, deposition time, solvent (in case of liquid phase deposition) and pressure (in case of vapor phase deposition). In some publications the use of catalytic substances for the silanization process is reported. Tri-

ethylamine is a typical catalyst used in the formation of aminoterminated silane SAMs [92] [42].
Temperature can have manifold effects on the silanization process. It was found that an increasing reaction temperature is associated to less ordered films for deposition out of a liquid [78]. Further the existence of a critical temperature T_c near room temperature was proven above which no ordered monolayers are formed [13] [12] [65].
The VPD is often carried out at elevated temperatures to ensure the evaporation of the silane molecules. Reaction temperatures in the range of 70–200 °C are reported [93] [8] [17].
A different effect of the temperature is sometimes utilized in an annealing step subsequent to the silanization procedure. Often such a curing step is listed in the protocol without mentioning the motivation [51] [23] [98] [97]. KESSEL and GARNICK [43] found that a postbake of silanized mica substrates is necessary to give a well-anchored and stable layer. BRITT and HLADY [10] found a negative effect of annealing. They cured surfaces modified with alkyl silane at 115 °C and observed the formation of molecule domains having increasing diameters with growing annealing time.

2.5 Characterization Methods

2.5.1 Atomic Force Microscopy

In Atomic Force Microscopy (AFM) [55] [9] a cantilever (a small tip mounted on a lever) is moved over a sample surface (or vice versa) and bends under the force between tip and surface atoms (Fig. 2.16). The sample (tip) is attached to fine piezoelements for scanning it against the tip (surface). The detection of the applied force is usually realized with the light pointer principle. The beam of a light emitting diode is reflected at the end of the cantilever onto a 2D position sensitive detector. The deflection is a measurement for the present force.

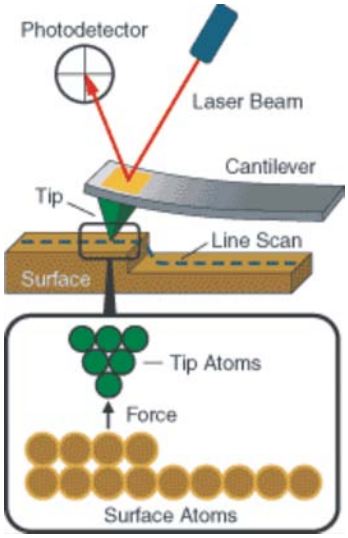

Figure 2.16: Schematic of Atomic Force Microscopy
(Source: http://www.molec.com/what_is_afm.html)

Attractive as well as repulsive forces are existent between tip and sample atoms. The variation of the force as a function of distance is shown in Fig. 2.17.

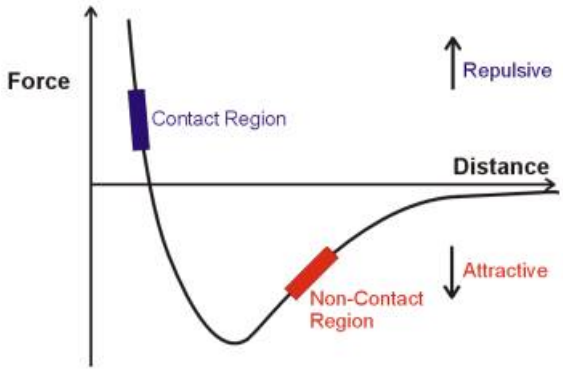

Figure 2.17: Plot of the forces between tip and sample (Source: http://www.tu-darmstadt.de)

AFM measurements in different modes are possible.
Contact mode: In contact mode the tip is brought into contact with the surface and the cantilever deflection is kept constant during scanning by a feedback loop. The measured

surfaces of constant force represent the topography. Because the tip is permanently in contact with the surface while scanning, a considerably shear force can be generated, causing damage to the sample, especially on very soft specimens. Atoms or molecules can be pulled out of the surface which leads to a modified surface topography and uncontinuous imaging conditions.

Tapping mode: In tapping mode (also: intermittent contact mode) the tip is not constantly in contact with the sample. The cantilever is stimulated to vibrate near its resonance frequency and scans the surface in a distance of typically 1 to 100 nm. The tip touches the surface only intermittently. Interaction between sample and tip leads to a damping of the tip oscillation and a reduction of the amplitude (Fig. 2.18). The oscillation amplitude is maintained constant by a feedback loop. The short tip – sample contact time prevents inelastic surface modification.

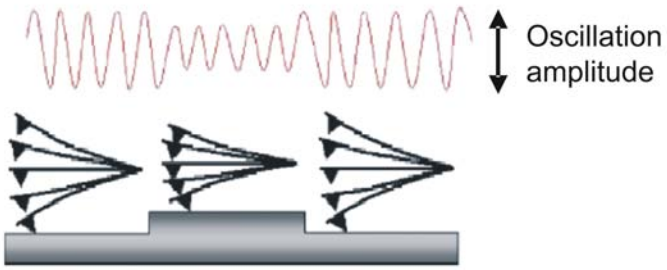

Figure 2.18: Schematic representation of an AFM tip operating in the tapping mode (Source: [4])

Non-contact mode:
In non-contact mode the cantilever is oscillating near its resonance frequency, like in tapping mode, and brought into proximity of the surface, however without touching it. The van der Waals attractive forces are sensed. Again, the oscillation amplitude acts as feedback parameter.

2.5.2 Ellipsometry

Ellipsometry [20] [60] is a very sensitive optical method to derive information about surfaces. It makes use of the fact that the polarization state of light may change when the light beam is reflected from a surface. Ellipsometry is often used in thin film analysis since the entire system substrate/film influences the change in polarization. Thereby it is possible to deduce information about the film properties, e.g. the film thickness. The name of the method is derived from the fact that in general the state of the light polarization, especially after reflection, is elliptic.
Light can be considered as an electromagnetic wave. The electric field $\mathbf{E}$ of a plane wave is described by:

$$\mathbf{E}(\mathbf{r}, t) = \mathbf{E}_0 e^{(i\mathbf{k}\mathbf{r} - i\omega t)} \tag{2.3}$$

Plane waves are typically referenced to a local coordinate system (x, y, z) where z is the propagation direction and x and y are directions parallel (p) and perpendicular (s), re-

spectively, to the plane of incidence. Now the E vector can be described by two harmonic oscillations along x and y with the same frequency but different amplitude and phase. As a result, at a fixed point in space the E vector moves along an ellipse. If the phase of the x and y oscillation is equal, the resulting ellipse transforms into a straight line. If the phase difference is +/-90° the ellipse becomes a circle. Thus, the linear and the circular polarizations are limiting cases of the general elliptical state. For all other phase differences, a „true“ ellipse evolves.

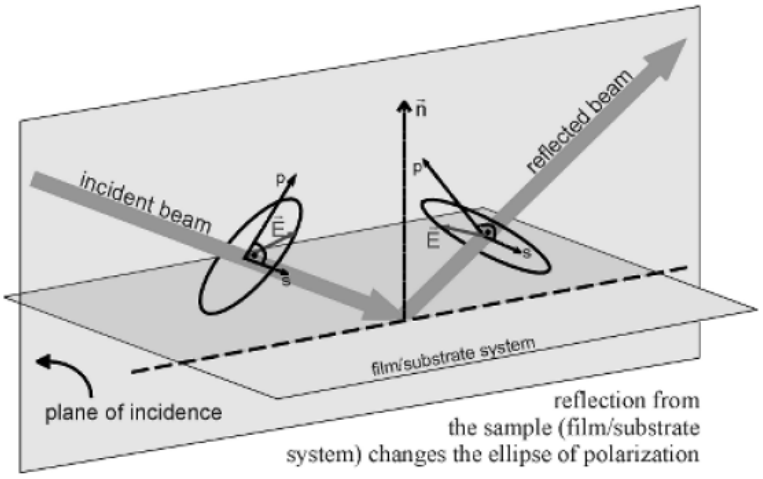

Figure 2.19: Schematic process of ellipsometry (Source: [60])

In an ellipsometric measurement monochromatic, polarized light is reflected by the surface of a sample (Figure2.19). The electromagnetic wave interacts with the sample to finally form the reflected light wave with an altered state of polarization. The known state of polarization χ^i is transformed into χ^0 after reflection according to:

$$\rho = \frac{\chi^0}{\chi^i} = \frac{r_p}{r_s} \tag{2.4}$$

where r_p and r_s are complex reflections for p- and s-polarized light, respectively. The complex reflection ratio ρ can also be represented by the angles Ψ and Δ:

$$\rho = \tan\Psi e^{i\Delta} \tag{2.5}$$

The meaning of Ψ is an angle whose tangent gives the ratio of amplitude change for the p and s component, while Δ denotes the relative phase shift of the p and s component upon reflection.

Nulling Ellipsometry: When linear polarized light is reflected by a sample, the reflected light will in general exhibit an elliptical state of polarization. The other way around, the same elliptical state of polarization (but with reversed sense of rotation) incident on the surface will generate a linear polarized reflection. As a consequence it is possible to detect this particular state by using a second polarizer as an analyzer in the reflected beam. Two linear polarizers at an angle of 90° („crossed polarizers“) do not transmit light. Therefore it is possible to extinguish a linear polarized light beam by setting the second polarizer

to a 90° position with respect to the axis of the linear polarization. Doing this is called „finding the Null“ or „nulling“.

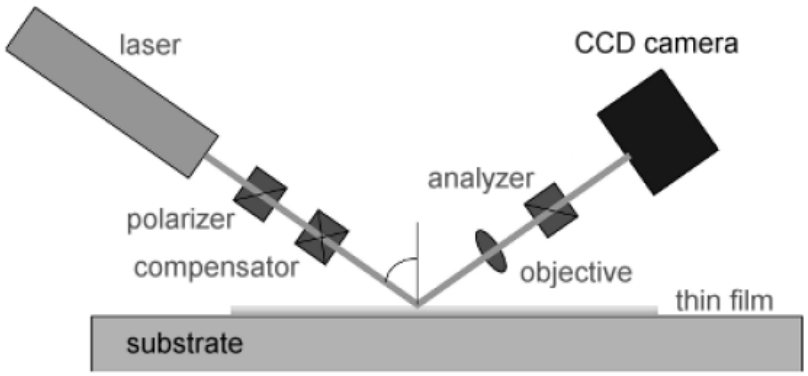

Figure 2.20: Schematic setup of ellipsometry (Source: [60])

Measurement Setup: The typical setup of Ellipsometry is shown in Figure 2.20. The light beam is usually produced by a Laser and polarized by a polarizer. After reflection by the sample the electromagnetic wave is led through an analyzer and into the detector. As detector a CCD[5] camera can be used.

2.5.3 X-Ray Photoelectron Spectroscopy

[62] [19] A well established method for surface analysis is X-Ray Photoelectron Spectroscopy (XPS), also known as Electron Spectroscopy for Chemical Analysis (ESCA). It is based on the photoelectric effect shown in Figure 2.21.

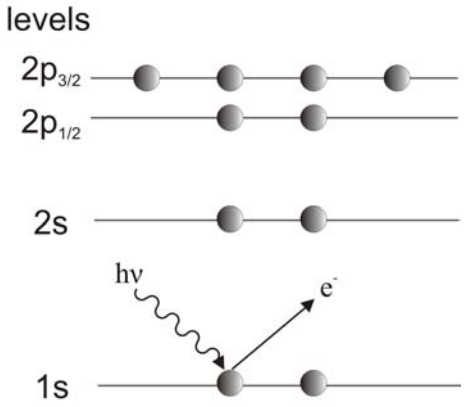

Figure 2.21: Principle of X-ray Photoelectron Spectroscopy

Induced by X-ray irradiation core-level electrons are able to escape from the material with a certain kinetic energy E_K, which is measured by the spectrometer. With the knowledge of the X-ray energy $h\nu$ the electron binding energy E_B can be calculated according to:

$$h\nu = E_B + E_K + \Phi \tag{2.6}$$

[5]Charge-coupled device

The energy of the irradiating photons is determined by PLANCKs constant h[6] and the X-ray frequency ν. The parameter Φ is the work function, the energy needed to remove the electron from the solid.
XPS measurements are carried out in ultra high vacuum to avoid contamination of the sample and interaction of X-rays and electrons with gas molecules. Usually the vacuum in the spectrometer chamber is between 10^{-6} and 10^{-8} Pa.
For generating the inciting X-rays mostly Al or Mg anodes are used. The energies of the K_α-lines are 1486,6 and 1253,6 eV respectively. A monochromator can be placed between the X-ray source and the sample to obtain X-rays of a defined wavelength.
The emitted electrons enter the electrostatic hemispherical analyzer consisting of two hemispherical electrodes with applied voltages V_1 and V_2 (Fig. 2.22). The electrons travel between the hemispheres, repelled by V_2 and attracted by V_1. By altering the voltages electrons with different kinetic energies reach the detector. An electron multiplier can be used as detector.

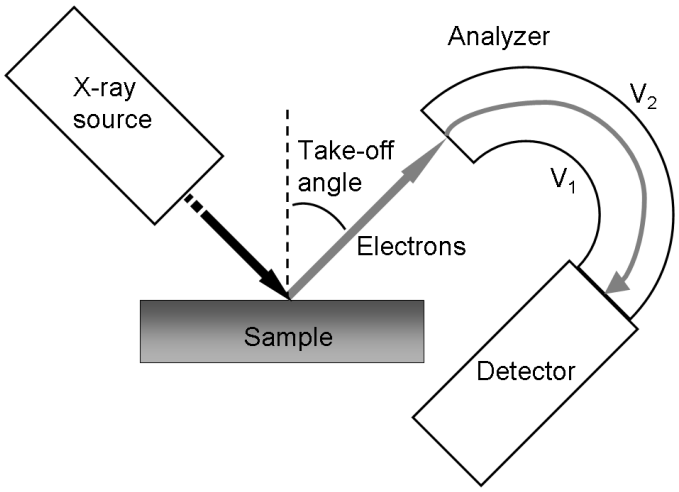

Figure 2.22: Schematic setup of X-ray Photoelectron Spectroscopy

XPS is a method sensitive to the first surface layers. The majority of the signal electrons that reach the detector originate from a depth of several nanometers below the surface. This is due to scattering processes of the electrons travelling through the solid. Only electrons near the surface are able to escape into the vacuum. The maximum information depth is obtained if the detector, is normal to the surface. With decreasing the take-off angle (Fig. 2.22), the angle between surface normal and analyzer, the information depth decreases. This leads to a higher surface sensitivity which is important for certain applications, so for analysis of monolayers.
In XPS, elements are identified by the characteristic binding energies of their core-level electrons. For each element of the periodic table at least one signal can be observed in the spectrum (except hydrogen and helium). Besides the identification of the element itself also information about its oxidation state and its chemical environment can be obtained. Generally a higher electron density surrounding the atom core leads to a lower effective

[6] $h = 6,62608 \cdot 10^{-34}$ Js

coulomb potential and therefore a lower binding energy is observed. The difference in the energy positions according to the different chemical environment of the atoms emitting the signal electrons is called a chemical shift.

2.5.4 Contact Angle Measurement

A characteristic of a surface is its free energy. The shape of a liquid drop lying on the surface is effected by the surface free energy and is therefore suitable for measuring surface properties.
The contact angle Θ is the angle at which a liquid/gas interface meets a solid surface (Fig. 2.23). It is a measure for the wettability of a surface with a specific liquid phase. The smaller the contact angle, the better the wettability. The contact angle Θ reflects the similarity in the nature of the contacting phases.

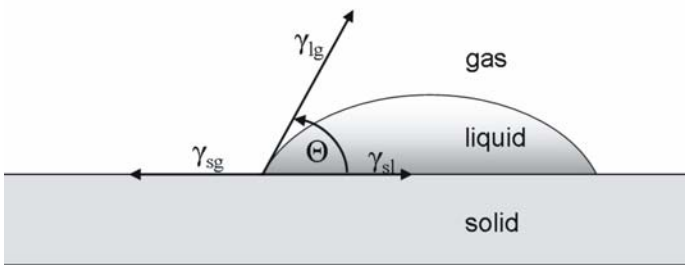

Figure 2.23: Contact angle Θ of the three phase system solid/liquid/gas with the interfacial energies of solid/gas γ_{sg}, solid/liquid γ_{sl} and liquid/gas γ_{lg}

Based on the magnitude of the contact angle, the following three cases can be distinguished [76]:

1. Wetting of the surface by the liquid („good wetting“) when $\Theta < 90\,^\circ$
2. Non-wetting („poor wetting“) when $\Theta > 90\,^\circ$
3. Spreading („absolute wetting“) when no equilibrium contact angle establishes, and the drop spreads into a thin film.

Often the contact angle of water on a solid is of interest. A water drop spreads completely on extreme hydrohphilic surfaces. Large water contact angles ($> 90\,^\circ$) indicate a hydrophobic surface.
The relationship between contact angle and thermodynamic properties of the involved phases is given by Young's equation:

$$\cos\Theta = \frac{\gamma_{\mathrm{sg}} - \gamma_{\mathrm{sl}}}{\gamma_{\mathrm{lg}}} \tag{2.7}$$

with the interfacial energies of solid/gas (γ_{sg}), solid/liquid (γ_{sl}) and liquid/gas (γ_{lg}) interface.

A possibility to measure the contact angle is the sessile drop method. It is based on the investigation of the shape of a liquid drop lying on the solid surface. The image of the drop is analyzed and thus the contact angle is determined.

3 Materials and Methods

3.1 Chemicals and Materials

The chemicals were used as received without further purification. Physical properties of the chemicals are noted if relevant.

- 1H,1H,2H,2H-Perfluorooctyltrichlorosilane (FOTCS), 97 %, ABCR

  Boiling point: Bp $=$ 192°C [2]

  Refractive index: $n_D^{20} = 1.352$ [2]

- 3-Aminopropyltriethoxysilane (APTES), 99%, Aldrich

  Boiling point: Bp $=$ 217°C [86]

  Refractive index: $n_D^{20} = 1.4210$ [86]

- 3-Mercaptopropyltriethoxysilane (MPTES), 95%, ABCR

  Boiling point: Bp $=$ 210°C [1]

  (The refractive index of MPTES was not known, however the refractive index of 3-mercaptopropyltriethoxysilane able to form identical monolayers is 1.4412 [86])

- Potassium hydroxide (KOH) solution, 10 %, prepared by dilution of potassium hydroxide pellets (Merck) in water

- Ammonium hydroxide solution, 10 %, prepared by dilution of ammonium hydroxide solution with $30 - 33$ % NH_3 (Riedel-de Haën) with water

- Ammonium thioglycolate solution, $\sim$ 60 % in water, Fluka

- Phosphate buffer solution pH 8.0, a mixture of 96.9 mL of 66 mM solution of disodium hydrogen phosphate dihydrate (prepared by dilution of $Na_2HPO_4 \cdot 2H_2O$, $>$ 99 %, Merck, in water) and 3.1 mL of 66 mM solution of potassium dihydrogen phosphate (prepared by dilution of a 1 M KH_2PO_4 solution, Sigma-Aldrich, with water)

- Trifluoroacetic acid, 99%, Sigma-Aldrich

- Triethylsilane, 99 %, Sigma-Aldrich

- α-Tritylthio-ω-carboxy succinimidyl ester poly(ethylene glycol), M $=$ 3000 Da, Iris Biotech

- 2-Propanol, $>$ 99.8 %, KMF

- Water, deionized with a Millipore Milli-Q water purification system, specific resistance 18.2 MΩ (if the usage of water is mentioned, it always refers to this deionized water)

- Argon 5.0, purity $\geq$ 99.999 %

- Oxygen 5.0, purity $\geq 99.999\,\%$
- Silicon wafers, $\langle 100 \rangle$, p-doped, $1 - 10\,\Omega$cm
- PDMS: Sylgard 184, Dow Corning

  The PDMS was purchased as two-part kit, consisting of a base and a curing agent. Base and curing agent were mixed in a ratio of 10:1, the mixture was poured in a flat dish and cured in an oven at 60 °C for 12 h and subsequent at 110 °C for 1 h. The upper side was used as contact side in printing processes.
- POP: Affinity VP8770, Dow Chemical

  The POP material was purchased as resin and pressed into slabs by the Institute of Plastics Processing at RWTH Aachen University. Pieces of slabs were cleaned in 2-propanol and pressed against an unpatterned silicon wafer at elevated temperature ($\sim 85\,°$) to obtain a flat surface as contact side for printing processes. This was done in a Hot Embossing device, described by SCHWAAB [75].
- Scotch Tape: Scotch Magic Tape 810

3.2 Devices and Methods

- AFM measurements were performed with a Nanoscope IV Multimode atomic force microscope of Veeco Instruments in tapping mode. Veeco tapping mode cantilevers RTESP5 (1–10 Ωcm n-doped silicon, ${f_0}^7 = 251 - 287$ kHz) were used.
- Layer thicknesses were determined using a Nanofilm EP^3 ellipsometer with Nd:YAG Laser ($\lambda = 532$ nm) and EP^3 View 2.05 software. The angle of incidence was usually 70°. Substrates with an artificial SiO_2 surface layer of about 100 or 10 nm were used for ellipsometric analysis, fabricated by wet or dry oxidation, respectively.

  Calculations of film thicknesses were always carried out assuming a single homogeneous nonabsorbing film with the refractive index of silicon oxide (n = 1.46). This method can be applied for organic films on silicon oxide because of the similarity of the refractive indices of SiO_2 and the monolayer [28] [37] [50] [14]. The thickness of the silicon oxide layer was determined before silanization and subtracted from the measured layer.

  At least two different regions on the sample were measured. The average value was used as result, the standard deviation as error, but at least 0.1 nm.
- X-Ray Photoelectron Spectroscopy was done with a Physical Electronics XPS 5600 using AlKα radiation for excitation. The electron take-off angle was changed in order to improve the analytical sensitivity if required. Binding energies were calibrated to the binding energy of Si at 99.3 eV. Quantification of the components is

[7] Resonance frequency

given in atom % with a relative error of $\pm$ 15 %. XPS analysis was carried out by the Central Division of Analytical Chemistry of the Research Center Jülich.

The assignment of signals was done with the aid of NIST X-ray Photoelectron Spectroscopy Database, NIST Standard Reference Database 20, Version 3.4, available on the internet at http://srdata.nist.gov/xps/

- A DataPhysics OCA instrument was used for determination of contact angles. Water was always used as measuring liquid. A water droplet of 5 μL was placed on the surface and the focused drop was analyzed after $\sim$ 10 sec with the aid of DataPhysics SCA 202 software. If the water drop spread on the surface and could not be calculated, it was defined to be 0 °.

  Contact angles were measured on at least two different regions on the sample. The average value was used as result, the standard deviation as error, but at least 1 °.

- Optical microscopy was done with a Zeiss Axioplan 2. Images were taken with an AxioCam MRc5.

- A plasma oven 100E from Technics Plasma GmbH was used with oxygen as plasma gas. The plasma oven was used with an oil-free scroll pump from Leybold.

- Experiments under inert atmosphere were performed in a MBRAUN MB200B glovebox filled with argon.

4 Experimental Section

The aim of this work was to introduce specific functionalities on silicon surfaces. This is possible with organosilane SAMs. High quality organosilane SAMs are useful for numerous tasks. The wide range of possible silane functionalities causes application in many different fields like Soft Lithography, Chromatography and Micromaching. Hydroxylated or water containing surfaces, like silicon oxide or glass, can be modified with organosilane SAMs. A major intention of this work was to investigate the silanization process on oxidized silicon and, if possible, to enhance the quality of the thin films. Besides the general aim to create reproducible and satisfying monolayers, this work was motivated by specific applications related to Soft Lithography. An auspicious and challenging field is the fabrication of complex electrode architectures like crossbar arrays by the means of Soft Lithography. In this context organosilane SAMs might be used as *adhesive layer*. Silanized surfaces are capable to also bear the opposite functionality, i.e. to work as a *lubricant layer*. This ability is used in the fabrication of stamps in Soft Lithography to ensure release between master and polymer material after the molding process or in the formation of lithographical patterns during Shuttle-Transfer Printing.

In the scope of this work both kinds of silane layers were a matter of optimization. For this reason the experimental section is divided into two main parts. In the first part, not only the silanization for the application as lubricant is developed, but the molecules also serve as a model system for the investigation of the silanization process in general. Connected to the examination of the lubricant layer was the construction of a new silanization device. This device should also improve the quality of the adhesive layer, if necessary. The investigation of the adhesive layer formation is reported in the second part.

4.1 Lubricant Layer

During the stamp fabrication for Soft Lithography an elastomer is molded against a patterned (silicon) master generating structures on the stamp. To ensure an easy release between master and stamp after the mold process, it is required to lower the surface free energy of the master. Often perfluorinated alkyl silanes are used for this purpose as lubricant layer or release agent [96]. These molecules are capable of forming a self-assembled monolayer on a hydroxylated silicon surface. With down-scaling the pattern size it becomes more and more important for the lubricant layer to be thin and homogeneous, a true monolayer. Structures in the nanometer regime would be altered significantly by agglomerated silanes. Furthermore, the layer requires to be stable so that no silane molecules are transferred to the stamp during the molding process. The SAM should stay on the master for further molding processes.
During this work 1H,1H,2H,2H-perfluorooctyltrichlorosilane (FOTCS) (Fig. 4.1) was used.

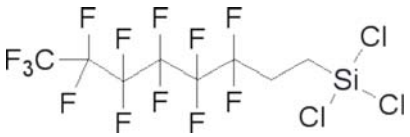

Figure 4.1: 1H,1H,2H,2H-perfluorooctyltrichlorosilane (FOTCS)

SCHWAAB [75] discovered that the silanization setup at hand was generally appropriate to gain suitable lubricant film qualities except of irregularities in few cases. A new device was required to achieve results with higher reproducibility and to investigate the influence of several parameters on the procedure. Preliminary experiments with the existent apparatus were performed to find out which factors should be enhanced. Further the new silanization device was built according to the results of the preliminary experiments and what is known from the literature.

4.1.1 Conventional Silanization with Perfluorosilane

Cleaning of silicon wafers

In order to start with a defined and reproducible substrate, silicon wafers with a native silicon oxide surface were used. They were cleaned by rinsing with water, blowing dry with argon and application of an oxygen plasma (200 W, 1.5 mbar, 30 sec). The purpose of the plasma treatment was also the activation of the surface by refreshment of surface silanol groups. The time of 30 sec was chosen according to the results of CHOI et al. [16] [15] as an optimum between removal of organic contaminants and surface roughness. A stored wafer had a water contact angle of more than 40 ° (Fig. 4.5 a). This is in agreement with the results of TAKAHAGI et al. [85] who found out that this is due to organic contaminations coming from the laboratory atmosphere and the polymeric storage boxes. After the plasma treatment, the oxide surface was perfect hydrophilic (Fig. 4.5 b), water spread on the surface. After one hour storage in a wafer box, the surface was still hydrophilic, the water contact angle could not be measured. After storage over night, the water contact angle increased again to 15 °. Therefore the substrates were always cleaned immediately before use.

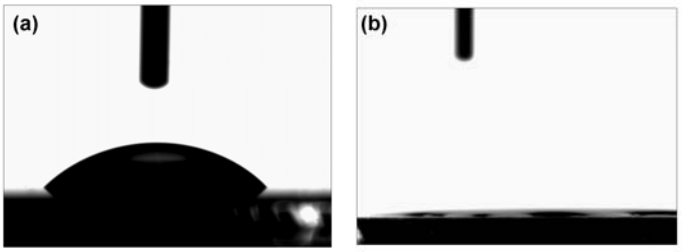

Figure 4.2: Stored wafer (a) before and (b) after plasma treatment

To judge the quality of the silane films, it is important to have information about the original surface. Therefore the topography of plasma-cleaned substrates was investigated by Atomic Force Microscopy. The recorded images (Fig. 4.3) reveal a root-mean-square

(rms) surface roughness of 0.11 nm for a 2.25 μm^2 area. Peak to peak heights of 0.4 nm were measured. This value is below the size of FOTCS molecules (1.06 nm [37] – 1.2 nm [94]). The surface seems to be suited for the silanization procedure.

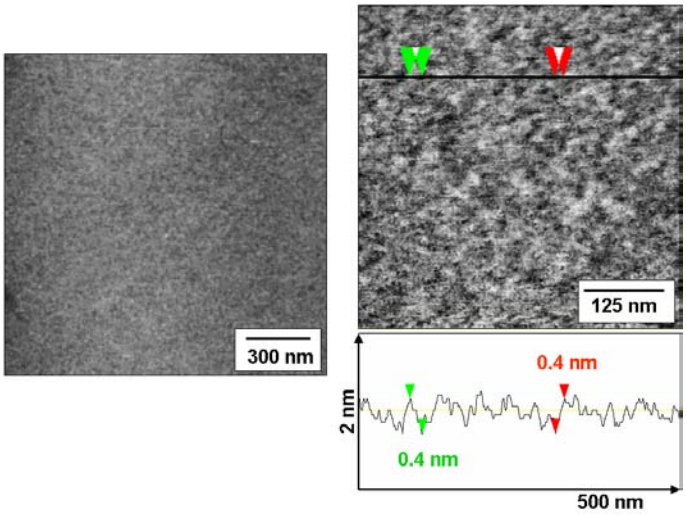

Figure 4.3: Silicon wafer with a native silicon oxide surface, cleaned by oxygen plasma
Contrast scale: 5 nm (left image) and 2 nm (right image)

Silanization with FOTCS

The silanization procedure was done by vapor phase deposition. High quality monolayers are known to be easier achieved by this technique in comparison to deposition from a solution [41]. The VPD was performed in a setup designed by SCHWAAB [75]. It is schematically shown in Fig. 4.4. The substrates were lying on a sample holder in a desiccator. 40 μL of silane was placed in a dish, covered by a half open beaker as splash guard. The desiccator was closed and connected to a vacuum pump. The pressure inside the desiccator was controlled by a pressure gage and adjusted by opening a dosing valve to an argon line. An adsorption trap was installed in line to avoid the presence of oil residues from the vacuum pump in the silanization process.

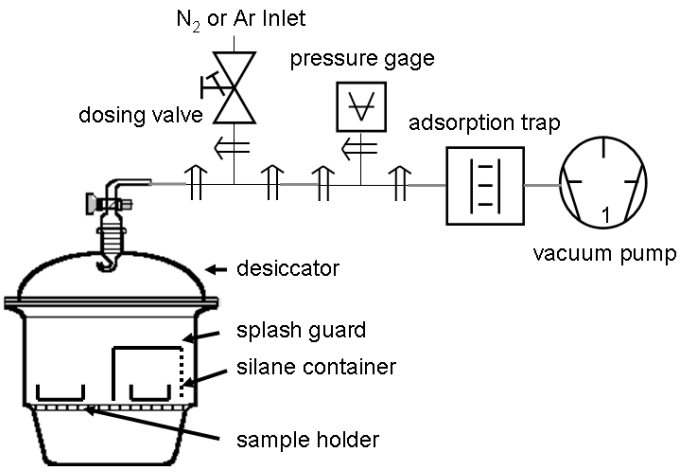

Figure 4.4: Schematic setup of silanization procedure (Source: [75])

The silanization setup was situated inside a glovebox with argon atmosphere to avoid exposure of the water sensitive silane to air humidity. The silane chemicals were solely opened inside the glovebox to avoid hydrolysation and polymerization of the molecules. After plasma-cleaning, the substrates were removed from the plasma chamber and passed into the glovebox. The substrates were exposed to air for about 2 min between cleaning and inserting them into the glovebox. In some cases the storage time between cleaning and silanization expanded up to 30 min. Usually the silanization was done for 1 h at a pressure of 45 mbar.
After that treatment the surface was hydrophobic (Fig. 4.5) as a consequence of the successful deposition of FOTCS on the wafer. The hydrophobicity indicates a low surface free energy as required.

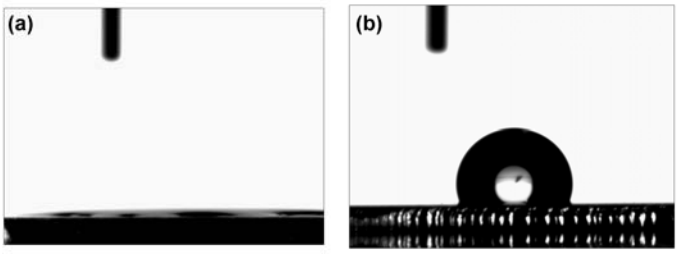

Figure 4.5: Water contact angle (a) after plasma-cleaning and (b) after silanization with FOTCS

Contact angle values in the range of 84 ° to 107 ° were obtained for silanized surfaces. Values higher than 100 ° are required for a satisfying hydrophobicity of the surface. This was usually achieved for a short delay time ($\sim$ 2 min) between cleaning and silanization. Comparing ellipsometric and contact angle data revealed, that high contact angle values corresponded to a layer thickness of around 0.7 nm. The thickness is below a monolayer of upright standing molecules. Even lower layer thicknesses of about 0.4 nm to 0.6 nm were measured for samples showing also low contact angle values. These results were obtained in general for samples that were stored under ambient condition for a period of $10 - 30$ min. A reason for the decreasing layer thickness might be an increasing contamination of the surface with organic substances during storage deterring the formation of a closed monolayer by occupying binding sites. The altering storage times also could lead to a difference in water content on the surface. Since water is known to be crucial for the procedure, a lack of water as well as excess water could result in low quality coatings. The storage time could be controlled in contrast to the humidity of the environment. It was taken care of the reaction to be carried out immediately (< 2 min) after cleaning the surface. The minimization of the time between cleaning and silanization could only be seen as a small step into the direction of reproducibility. The cause of the irregularities was not erased in this way.
Element analysis of the silanized surface was done by X-Ray Photoelectron Spectroscopy. The survey spectra of a cleaned and a FOTCS covered surface are shown in Fig. B.1 (appendix). It clearly shows that a fluor peak appears for the silanized sample which was not present before silanization.

Relative surface concentrations of the relevant elements are given in Table 4.1.

Table 4.1: Results of XPS analysis of a bare silicon wafer with a native oxide layer and a FOTCS covered surface

Element	F	O	C	Si
Si wafer with native SiO_2 (relative concentration [atom %])	0	52.7	5.3	42.0
Si wafer with native SiO_2 modified with FOTCS (relative concentration [atom %])	26.7	29.5	14.4	29.4

The spectrum of the bare silicon wafer mainly reveals the presence of silicon (from substrate and native oxide layer) and oxygen (from native oxide layer). A small amount of carbon was also found, most likely because of few contamination from the laboratory atmosphere. The ratio Si : C was about 8 : 1. After silanization the ratio Si : C decreased to about 2 : 1, which means the surface concentration of carbon increased significantly. This is reasonable for the surface covered with FOTCS molecules, containing alkyl chains. The relative concentrations of about 30 % for silicon and oxygen after silanization are in good agreement with values of 32.8 atom % (Si) and 27.6 atom % (O) for surfaces covered with similar molecules reported by HOZUMI et al. [37]. They found these values for a sub monolayer coverage.

The detail C 1s, F 1s, O 1s and Si 2p XP spectra of the silanized surface were recorded and are shown in Fig. B.2 (appendix). The peak values, relative concentrations and chemical assignments are summarized in Table 4.2.

Table 4.2: XPS results of a FOTCS covered surface

Element	Binding energy [eV]	Relative concentration [atom %]	Chemical assignment
F 1s	689.2	23.2	CF_2, CF_3
	688.4	3.5	CH_2-CF_2
O 1s	533.0	27.1	SiO_2, org. O
	532.0	2.4	org. O
C 1s	294.0	1.7	CF_3
	291.8	5.9	C*F_2-CF_2
	291.1	2.0	C*F_2-CH_2
	287.4	0.3	COC, C=O
	286.1	2.2	C*H_2-CF_2
	285.0	2.3	C*H_2-CH_2
Si 2p	103.3	9.7	SiO_2
	99.3	19.7	SiO_2

The oxygen signals are assigned to silicon oxide and to O in organic compounds (org. O). Besides the appearance of the fluor peak, also in the C 1s spectrum the presence of the perfluorinated molecules on the surface is evident. The carbon peaks can be correlated very well. The chemical environments of the carbon atoms are assigned to the peaks at different binding energies in Fig. 4.6. The peaks assigned to contamination (see below) are labelled in grey.

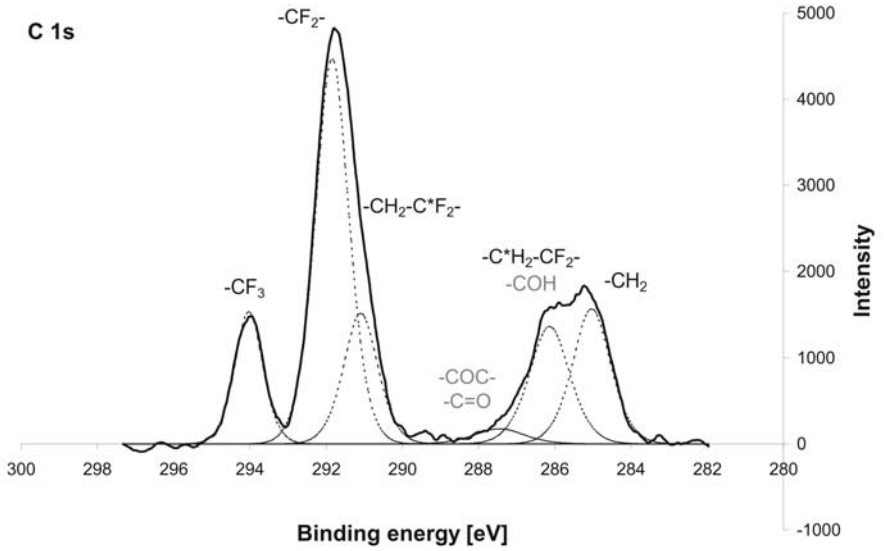

Figure 4.6: C 1s spectra of a FOTCS covered surface

The spectrum is similar to those reported by others [26] [94] [36] [37]. The rates of carbon in CF_2 (7.9 atom%) and CF_3 (1.7 atom %) groups are in good agreement with the theoretic 5 : 1 proportion in the CF_3-$(CF_2)_5$-$(CH_2)_2$-$SiCl_3$ molecule. The amount of carbon present in CH_2 groups (signals at 285.0 and 286.1 eV) is with 4.3 atom% (2.0 + 2.3) higher than theoretically expected. This is probably due to organic impurities bearing as well CH_2 groups and functionalities as COH, typically producing signals at similar binding energies. The small peak at 287.2 eV can be attributed to ether and carbonyl groups, most likely also coming from impurities. Such impurities are not unusual for a surface prepared outside ultra-high vacuum.

Fig. 4.7 shows examplarily AFM images of a FOTCS covered surface. The surface roughness of a 1 μm^2 area was 0.21 nm. It has little increased in comparison to the cleaned surface, but is rather flat for a silanized surface. In Fig. 4.7 c a wavelike topography can be seen with elevation between „trough“ and „crest“ of about the length of a single FOTCS molecule. Possibly these are structures of silane molecules with the tails spread aside as mentioned by STEVENS [81] due to steric hindrances among the tails. It is reasonable that such a coverage is lower than a complete monolayer coverage. This is in agreement with the results of Contact Angle Measurement, Ellipsometry and X-Ray Photoelectron Spectroscopy.

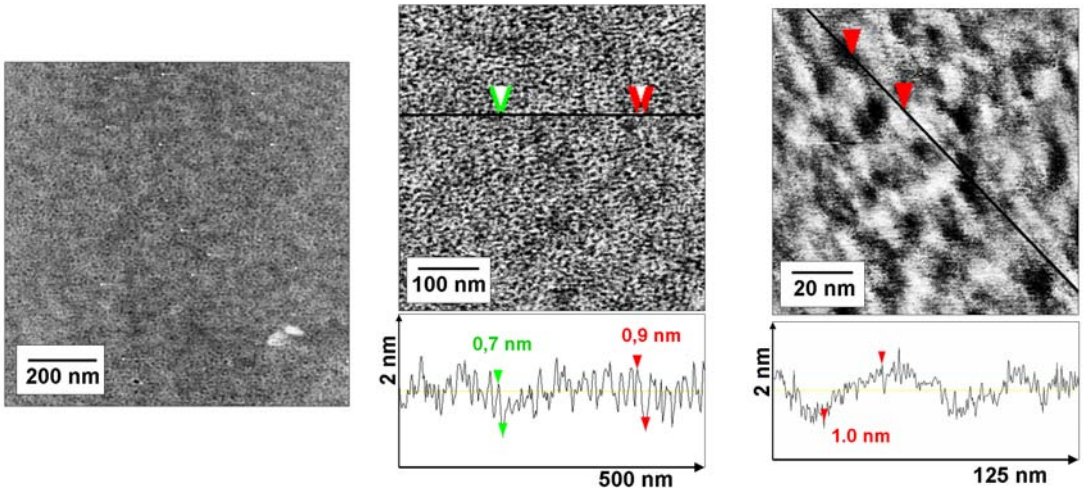

(a) Contrast scale: 5 nm (b) Contrast scale: 2 nm (c) Contrast scale: 2 nm

Figure 4.7: Silicon wafer coated with FOTCS by vapor phase deposition in a desiccator

Such layers are acceptable for the application as release agent in Soft Lithography as long as the surface free energy of the modified surface is low enough to ensure the release between stamp and master. For other applications it might be more important to achieve true monolayers with upright standing molecules. To erase the problems of contamination and uncontrolled process conditions an advanced silanization setup was required.

4.1.2 New Silanization Device

Designing the new silanization device

The preliminary results showed that an optimization of the silanization procedure was necessary. A new silanization device was designed in the style of apparatuses described in literature [77] [33].

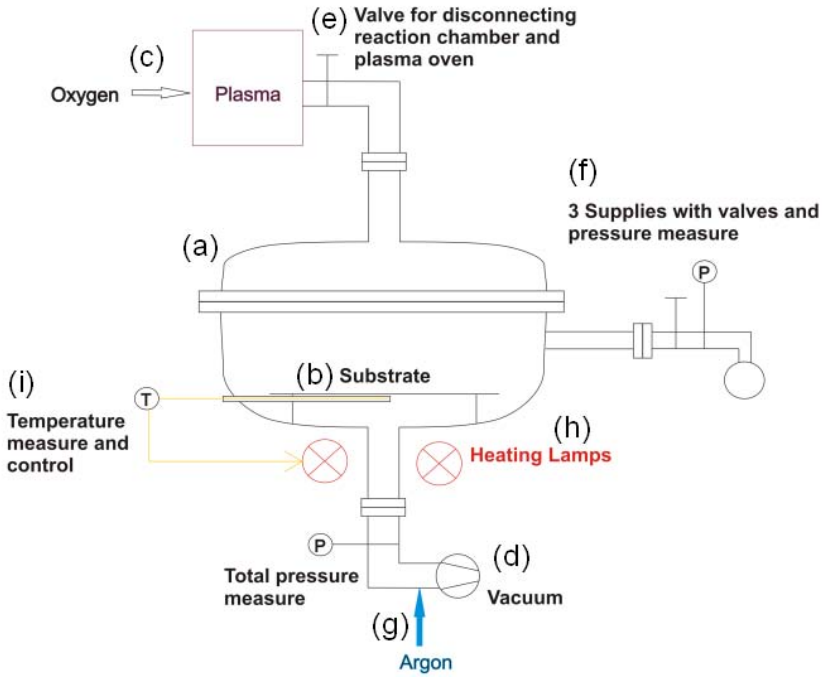

Figure 4.8: Scheme of the new silanization device

An important demand was to carry out the cleaning step and the silanization step in a closed device without exposing the substrates to the atmosphere in between. In the preliminary results it had been turned out that an increasing time between cleaning and silanization led to a decreasing quality in surface coverage. Contamination and uncontrolled water content on the surface are possible reasons for the variation. Both influences were left to chance with the old silanization setup. By combining the cleaning and silanization in one device, it should be possible to avoid contamination and to tune the water content present on the substrate in a controlled manner. Therefore a special device was constructed (Fig. 4.8). It consists of a main reaction chamber (a) fabricated of glass with several attached components. For placing the substrates, a table was mounted at the bottom of the chamber (b). On top of the chamber, a gas inlet could be connected to the outlet of a plasma oven. The outlet of the reaction chamber was connected to a vacuum pump (d). An oil-free scroll pump was used as vacuum pump to avoid the presence of oil in the system. For cleaning and activating the substrates, the oxygen plasma (c) created inside the plasma chamber could be pumped through the reaction chamber and over the substrates. Plasma contains highly activated species such as electron, ions and radicals. Radicals can be isolated from the plasma because of their longer lifetime than electrons and ions. This effect is used in the so-called remote plasma treatment, which is known

to be less aggressive than conventional plasma. JIERONG et al. [40] found that the surface of samples in a remote plasma at a distance of 800 mm from the inductance center is still effected by the plasma. They claim that free radicals are present which improve the hydrophilicity of the surface whereas the short-lived ions and electrons do not reach the sample so that almost no etching and sputtering occurs. In the new silanization device the distance between plasma center and samples was about 800 mm. After the cleaning step, the connection between plasma oven and main reaction chamber could be closed by a valve (e). The intention of constructing a remote plasma device was not only to clean the substrates prior to silanization. Another aim was the ability to clean the whole device after use. In the vapor deposition process, the evaporated silane molecules occupy the reaction chamber. They do not only react with the substrate surface but also with the inner walls of the reaction container made of glass. Hints were found for undesired cluster formation of silane in an often used desiccator in an experiment described in another context (p. 54). Physisorbed molecules might detach from the wall during a silanization process and deposit on the wafer surface. To avoid the agglomeration of silane molecules on the inner walls of the reaction chamber, cleaning with the remote plasma after each use should be performed.
Liquid reservoirs (f) were attached to the device. Here the silane chemicals, water and catalytic additives could be filled in. From the attached reservoirs the liquids could be allowed to enter the reaction chamber in form of vapor. To control the inlet from the reservoirs in a reproducible way, the pressure in the attachments was measured. The inlet regulation could be done with the aid of dosing valves.
For the preparation of stable monolayers the attachment of molecules via chemical binding was desired. One should be able to remove only physisorbed molecules and also those that are lying on top of an already existing monolayer. Heating of the substrate after silanization was thought to be appropriate for that demand. In several publications heat treatment is also reported as annealing step of silanized surfaces for the formation of chemical binding between surface silanol groups and silane molecules. Infrared (IR) lamps should be added to the apparatus as heating equipment (h). It was planned to mount the IR lamps onto reflectors beneath the reaction chamber. (i) The temperature could be measured by a Pt 100 thermocouple. The performance of the heating lamps could be controlled holding the temperature at a set constant value via a temperature control unit.
In order to distinguish the new silanization device from former silanization apparatuses like the desiccator in the glovebox, it was called **C**leaning **A**nd **S**ilanization **IN** **O**ne device, abbreviated as CASINO device. A picture of the constructed CASINO device is shown in Fig. 4.9.

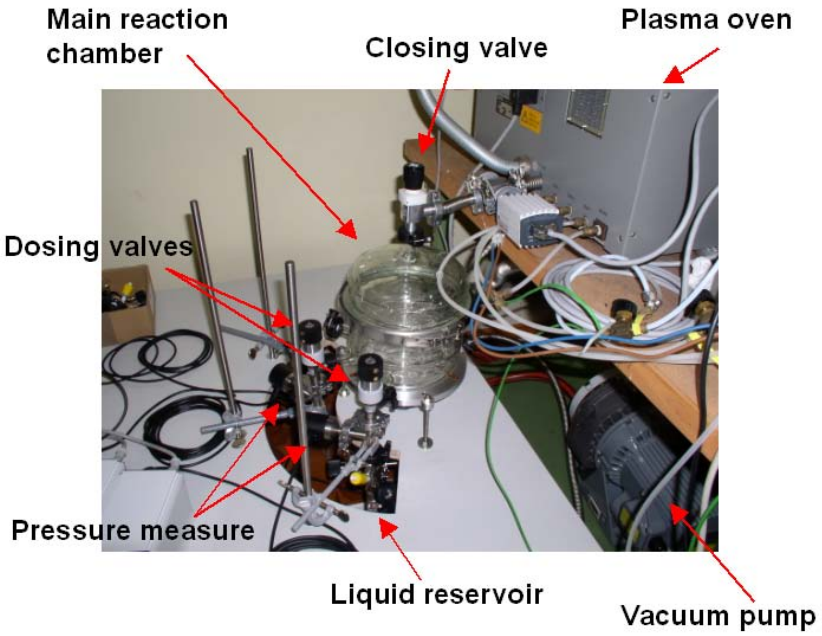

Figure 4.9: The new silanization device

Adjustment of parameters in the new device

Since the setup of the CASINO device differs from the former procedure, the process parameters had to be adjusted. The adjustment should ensure that the results are comparable to those of the experiments performed in the desiccator.
Firstly, the process step of cleaning the substrates was optimized. For comparison, cleaning inside the plasma chamber provides satisfying results after 30 sec (see section 4.1.1). In the CASINO device the substrates are placed in the chamber behind the plasma oven, where only few reactive species arrive. The samples are cleaned by a remote plasma. The time needed to clean the substrates in the remote plasma was examined with silicon wafers stored in wafer boxes (untreated). A second test sample was a „defined contaminated“ wafer. For the latter a silanization procedure with FOTCS was performed as described in section 4.1.1.
The oxygen plasma was created in the plasma oven with maximum possible power (280 W) and at an oxygen pressure of 1.5 mbar. The remote plasma was applied to the substrates for various times. Water contact angles of the surfaces were measured in the beginning and after remote plasma treatment as an indicator for the cleaning effect. The results are shown in Fig. 4.10. In the beginning (time = 0), the stored wafer revealed a contact angle in the range of $40 - 50\,°$. This value dropped during cleaning in the remote plasma. After a cleaning time of 30 min the Contact Angle Measurement showed absolute wetting indicating a clean surface. For the FOTCS coated surface the curve starts at a contact angle value of about 100 °. During the cleaning process the surface bonded FOTCS molecules have to be destroyed by the plasma. As expected it took a longer time (at least 90 min) to reach a contact angle of 0 ° (water drop spread on the surface).

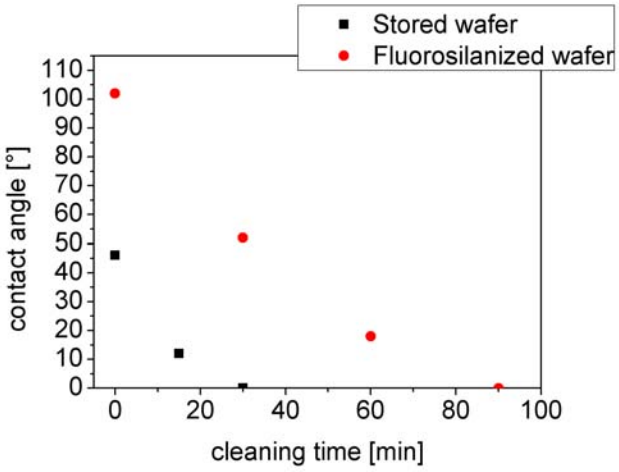

Figure 4.10: Contact angles measured of stored and fluorosilanized surfaces after several cleaning times

To be on the safe side, a cleaning time of 45 min in the remote plasma prior to silanization was chosen. In order to clean the contaminated reaction chamber after silanization, remote plasma was applied for at least 90 min.

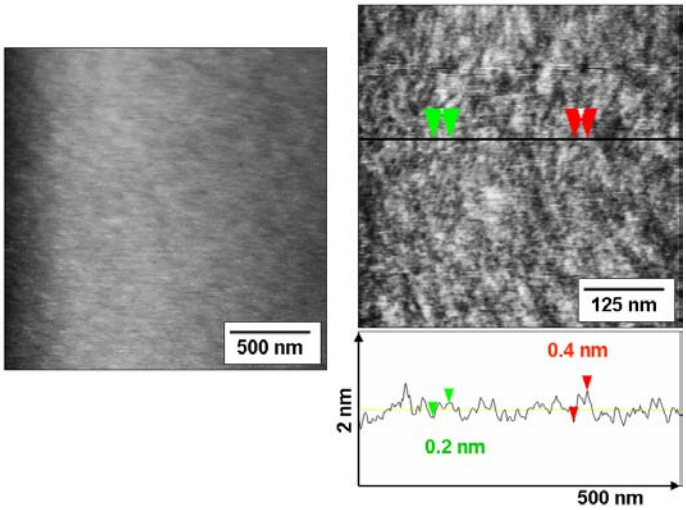

Figure 4.11: AFM image of a silicon oxide surface cleaned in remote plasma for 45 min
Contrast scale: 4 nm (left image) and 2 nm (right image)

A surface of a stored wafer cleaned by remote plasma was characterized by Atomic Force Microscopy (Fig. 4.11). An extremly flat surface (rms: 0.06 nm for a 3 μm^2 area) was observed. That the roughness of that surface is lower than that of a wafer cleaned inside the plasma oven shows that it is a highly gentle procedure. Most likely only few free radicals but no electrons and ions are present so that no etching or sputtering effect occurs as expected from the results of JIERONG et al. [40].

Another important parameter was the chamber pressure during silane deposition since it defines the partial pressure of silane molecules in the glass vessel. The formerly sufficient

pressure of 45 mbar did not lead to equivalent results in the new device. The silanization resulted in a less hydrophobic surface than expected. A measured water contact angle of (37±1) ° was much lower compared to contact angles of around 100 ° for surfaces prepared in the desiccator. Obviously the new geometry required a different reaction pressure. A pressure test series was done in order to establish a pressure appropriate for the silanization process. The motivation was to find the pressure needed in the CASINO device that leads to comparable surface coverages as in the desiccator. Therefore the pretreatment was chosen the same as used with the desiccator. The substrates were rinsed with water, blown dry with argon and cleaned in the plasma oven for 30 sec. After removing from the plasma chamber, they were left at the atmosphere for $1-2$ min before placing them in the CASINO reaction chamber. The deposition of FOTCS was then carried out at various pressures for 1 h, respectively. In this step the connection to the silane reservoir was completely open. The chamber was purged for 5 min at the reaction pressure, while the connection to the silane reservoir was closed. This was done to ensure the absence of FOTCS in the chamber when it was opened afterwards to remove the samples. Evaluating the results was done by measuring water contact angle and layer thickness. The results are summarized in Table 4.3.

Table 4.3: Silanization at different pressures after cleaning inside the plasma oven

Silanization pressure [mbar]	5	1.1	1.0	0.9	0.1
Contact angle [°]	88 ± 3	104 ± 1	104 ± 1	104 ± 1	105 ± 1
Silane layer thickness [nm]	0.6 ± 0.1	1.0 ± 0.1	1.1 ± 0.1	1.1 ± 0.1	5.5 ± 0.1

A silanization base pressure of 5 mbar led to a contact angle of 88 ° and a layer thickness of 0.6 nm. Both measured values indicate a sub monolayer coverage. This means that a pressure of 5 mbar is still too high. A deposition at 0.1 mbar seemed to be inappropriate as well, leading indeed to an adequate hydrophobicity with a contact angle of 105 °, but also to a thickness of 5.5 nm pointing to a multilayer formation. A surface with a FOTCS layer equivalent in wettability and thickness to former experiments was obtained at a reaction pressure of 1 mbar. The result was verified by performing the same procedure at a pressure of 1.1 and 0.9 mbar, respectively. The obtained results confirmed that silanization with a pressure of 1 mbar (even with 10 % deviation) in the CASINO device leads to a silane layer comparable in wettability and thickness to those prepared in the desiccator. A pressure of 1.0 mbar was chosen for further experiments with FOTCS in the CASINO device.

The reason for the lower pressure needed was probably the different geometry of the setups. Whereas in the desiccator the silane was placed in an open dish, it was here situated in a reservoir separated from the chamber by a needle valve. The evaporating molecules have to pass this bottle-neck. The probability that molecules reach the substrate surface

is lower here than in the case where the chemical is placed directly inside the reaction chamber. By decreasing the chamber pressure, the number of evaporating molecules is increased. Therefore also the feasibility that molecules pass the bottle-neck and reach the substrates increases.

Silanization in the CASINO device

The knowledge of appropriate cleaning and silane deposition conditions were used in the following experiments.

Water rinsed and argon dried substrates were placed in the CASINO device. The chamber was evacuated to 1.5 mbar (pressure regulation by opening/closing oxygen line) and an oxygen plasma of 280 W was created in the plasma oven. The remote plasma was applied for 45 min. After the cleaning step, the connection to the plasma oven was closed. The chamber pressure was reduced to 1.0 mbar (pressure regulation by opening/closing argon line) and the needle valve to the silane container was opened. Silanization was carried out for 1 h at 1.0 mbar. Then the connection to the silane reservoir was closed and the chamber pressure was hold at 1.0 mbar for another 5 min to remove FOTCS vapor from the chamber. The substrates were taken out and heated to 200°C on a heating plate for 5 min. Contact angles and layer thicknesses were measured before and after the heat treatment and are summarized in Table 4.4

Table 4.4: Results of silanization procedure in CASINO device with heat treatment afterwards

	After silanization	After heating
Contact angle [°]	102 ± 1	104 ± 1
Layer thickness [nm]	0.8 ± 0.1	0.5 ± 0.1

The results of the silanized surface showed that FOTCS was indeed deposited in the process. However, the thickness of the FOTCS layer of 0.8 nm after silanization indicated that a sub-monolayer was produced instead of a closed monolayer. After heating the substrate to a temperature near the boiling point of FOTCS the layer thickness was further decreased to 0.5 nm ($\sim$ 30 %). A comparison of the influence of post silanization heat treatment was done with substrates silanized by the original procedure in the desiccator. There the substrates were also heated on a heating plate to about 200 °C for 5 min after silanization. The thickness decrease was measured to be $3 - 6$ %. This decrease is in the error range of the thickness determination. Therefore it was stated that there were just minor changes in the layer thickness after heating which indicates a firm linking of almost all perfluorosilane molecules to the surface or to adjacent molecules.
The behavior of the samples prepared in the CASINO device can be explained by the conditions during the process. Initially the substrates were covered by a thin water layer, due to air humidity, when placed in the reaction chamber. A certain amount of water on the surface (in form of water layer or silanol groups) is known to be necessary for the covalent anchoring of silane molecules. The samples were not exposed to air or water va-

por between cleaning and silanization. The vacuum of 1.5 mbar was not appropriate to remove surface water completely. The influence of the remote plasma on the water layer is unknown. Presumably the remote plasma treatment created a surface with reduced water content since a certain amount of molecules could be removed by the final heating step. The fact that at least part of the FOTCS molecules were able to anchor to the surface and were not removable by the heating step indicates that the surface was not perfectly dry.

The observation is in agreement with the results of JUNG et al. [41]. They exposed silicon oxide surfaces to FOTCS vapor with and without subsequent exposure to water vapor. Under „dry“ conditions (without water vapor) they found a silane layer thickness of 0.66 nm and a water contact angle of 100 °. They further performed experiments with several cycles of silane and water exposure and obtained satisfying results after at least two cycles (layer thickness: 0.94 nm; contact angle: 112 °).

A similar experiment was done in the CASINO device. Samples were cleaned for 45 min with remote plasma and exposed to FOTCS vapor for 1 h at 1.0 mbar. Then the connection to the FOTCS reservoir was closed, the chamber was purged for 5 min and water vapor was allowed to enter the chamber at 10 mbar for 30 min. This step was again followed by 5 min purging with closed connections to the reservoirs. Then another FOTCS deposition step was performed at 1.0 mbar for 1 h. After removing the samples from the CASINO device they were heated on a heating plate to 200 °C for 5 min. Ellipsometry and Contact Angle Measurement were performed before and after the heat treatment (Table 4.5).

Table 4.5: Results of silanization procedure (two cycles) in CASINO device with heat treatment afterwards

	After silanization	After heating
Contact angle [°]	108 ± 2	106 ± 1
Layer thickness [nm]	2.7 ± 0.2	2.3 ± 0.1

The contact angle after the silanization was with 108 ° in a satisfying range. However the layer thickness of 2.7 nm indicates the formation of a doublelayer or cloudlike multilayers. After heating, the contact angle value did not change significantly. The layer thickness decreased to 2.3 nm indicating that some excess molecules were evaporated. The thickness was still in the range of double the FOTCS molecule length. Obviously the used parameters were not ideal. From the experiment under „dry“ conditions it was assumed that part of the FOTCS molecules were not chemically attached to the surface (they could be removed by heating). In the cyclic silanization experiment these molecules were not removed after the first deposition. The exposure to water vapor might have led to cluster formation of these loose molecules. It is also possible that the water content on the sample surface after the exposure to water vapor was higher than necessary, also leading to an undesired polymerization of FOTCS molecules.

A probably adequate procedure would be to perform the cyclic silanization with heat treatment subsequent to each FOTCS deposition step to ensure the controlled in situ removal of excess molecules. It seems less recommendable to remove excess molecules by rinsing with solvents since the procedure in the closed device would need to be interrupted.
The optimization of parameters (like deposition time of silane/water, deposition pressure of water, heating time, etc.) leading to satisfying and reproducible results is advisable but was beyond the scope of this thesis.

4.2 Gold Adhesive Layer

As explained in section 2.1, Shuttle Transfer Printing is a suitable method for the production of molecular electronic devices such as crossbars. A critical point is to find materials for substrate 1, shuttle and substrate 2 with increasing adhesion ability to the metal, here gold. SCHWAAB [75] suggested to use a perfluoro functionality on surface 1 (low adhesion to metal) and a thiol functionality on surface 2 (high adhesion to metal). The modification can be done by silanization with a perfluorosilane (e.g. FOTCS) and a thiol terminated silane (also named: mercaptosilane), respectively. Mainly two classes of polymer materials were proposed for this application: poly(dimethylsiloxane) (PDMS) and polyolefin plastomer (POP). The adhesion gradient of the chosen system is shown in Fig. 4.12.

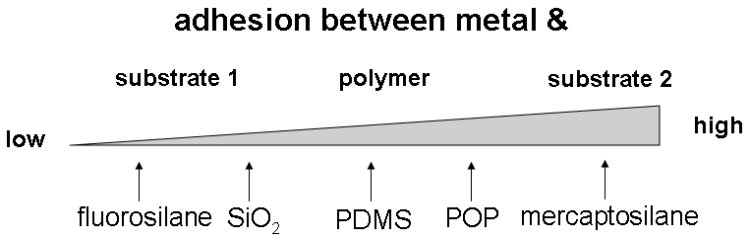

Figure 4.12: Adhesion gradient for Shuttle-Transfer Printing (Source: [75])

Au-S bonds should form immediately when gold and thiol groups get in contact. Since this binding is very strong, the gold should be transferred easily to the thiol terminated surface and stick there.
Although the system seems to be perfect for Shuttle-Transfer Printing of metal electrodes, the practical application is not straightforward. The weak point in the system is an insufficient adhesion between metal and mercaptosilanized surface. SCHWAAB [75] reported that an organic solvent was needed to weaken the adhesion between stamp material and metal. Often the presence of an organic solvent is unwanted, for instance in the case of biomolecules placed in the crossbar junction. Further the transferred gold was easily removed in subsequent processes.
A possible explanation for the lack of adhesion is the quality of the mercaptosilane layer. So the performance of the adhesion layer should be improved. Therefore the silanization procedure should be examined and enhanced for offering a surface appropriate for the attachment of gold.

3-Mercaptopropyltriethoxysilane (MPTES) (Fig. 4.13) was chosen to modify the silicon oxide surface.

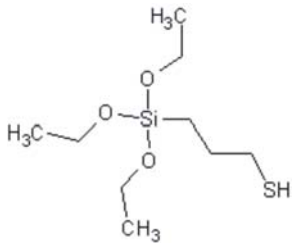

Figure 4.13: 3-Mercaptopropyltriethoxysilane (MPTES)

For a full pattern transfer from polymer to substrate a high quality of the adhesive layer is required. That means, there should not be any agglomerations of silane, but an arrangement of molecules in a dense and stable monolayer with free thiol groups pointing normal to the surface. Vapor phase silanization was performed and the surfaces were characterized.

4.2.1 Silanization with Mercaptosilane

In the preliminary experiments substrates were covered with MPTES. The modified surfaces were characterized and the printing of gold onto the surfaces was tested. The interaction between gold and mercaptosilanized surface was further investigated.

Silanization with MPTES

The silanization was performed in a desiccator placed in a glovebox. The setup is shown in Fig. 4.4. The reaction pressure was hold constant at 5 mbar for 1 h. The surface was characterized by Ellipsometry, Contact Angle Measurement, AFM and XPS.

The contact angle ranged between 34 ° and 40 °. LENIGK et al. [51] reported a contact angle value of (48.5 ± 1.5) ° for a deposited layer of 3-mercaptopropyltrimethoxysilane (MPTMS). This deviation is probably not due to the use of different molecules, because the resulting layer from deposition of MPTMS on silicon oxide should be the same as of MPTES. Methoxy as well as ethoxy groups are thought to be removed in the first step of the silanization process. It is more likely that the higher contact angle was due to the fact, that they used a deposition procedure out of a liquid with water present in the solution. They further found a layer thickness of (39 ± 7) Å and concluded to have not a monolayer but polymerized MPTMS molecules on the surface.
The layer thicknesses of the MPTES layers prepared by vapor deposition in the desiccator were measured to be $0.5 - 0.6$ nm. This is in good agreement with monolayer thicknesses reported by others of 0.5 nm [38] or 0.7 nm [39].
AFM characterization is shown in Fig. 4.14. The surface topography is similar to the one which was found for the substrates covered with FOTCS. The root-mean-square surface roughness is 0.22 nm for an area of 4 μm^2.

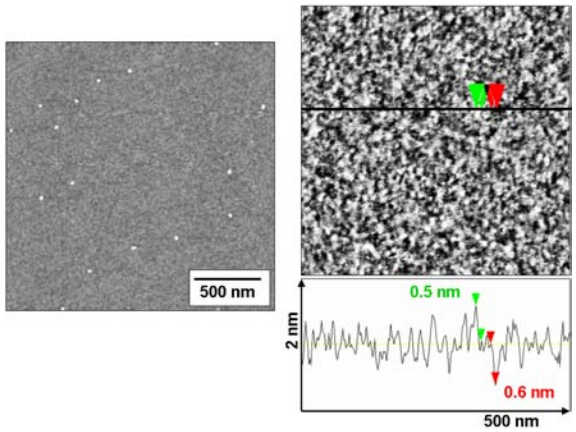

Figure 4.14: AFM images of MPTES layer on silicon oxide
Contrast scale: 10 nm (left image) and 2 nm (right image)

The composition of the MPTES layer was investigated by XPS measurements. The survey and the detail spectra are shown in the appendix (Fig. B.3, B.4). Especially the presence of sulfur was of interest. The S 2p signal was not detectable here since an interference with the dominant silicon peaks occurred. Therefore only the S 2s signal was taken into account for the analysis. The spectra were recorded with a take-off angle of 12.5 ° between the analyzer and the substrate surface normal. This was done to emphasize the sulfur signal relative to the background. The results are listed in Table 4.6.

Table 4.6: XPS results of MPTES covered surface

Element	Binding energy [eV]	Relative concentration [atom %]	∑ Relative concentration [atom %]	Chemical assignment
O 1s	532.9	56.6	56.6	SiO_2, org. O
C 1s	286.7	1.9		
	285.0	18.2	20.1	CH_2
S 2s	233.5	1.7		SO_4^{2-}
	227.6	3.2	4.9	SH
Si 2p	103.4	14.0		SiO_2
	99.3	4.4	18.4	SiO_2

The high concentration of oxygen relative to silicon (ration 3 : 1) is a sign for the increased analytical surface sensitivity. Probably the information is mainly derived from the SAM layer and the native silicon oxide layer. Two S 2s peaks were measured at 227.6 and 233.5 eV. Comparison of S 2s binding energies is difficult since little data concerning this can be found in literature. The signal at 227.6 eV can be assigned to free thiol groups. This is in agreement with XPS measurements of the sulfur containing amino acid cysteine (HS-CH_2-CH(NH_2)-COOH) [52]. The presence of a signal at 233.5 eV could be due to sulfate ions. Similar values at 233.7 eV and 233.6 eV are reported by STROHMEIER et al. for SO_4^{2-} [82] [83]. The origin of sulfate ions remains unclear. The concentration of thiol groups is

rather low in relation to the amount of carbon. This might be due to organic impurities on the surface. Additionally the concentration value of sulfur might be falsified since it was hardly extractable from the background.

Printing gold on MPTES covered surface

As found by AFM and ellipsometric measurement, the MPTES covered surface was atomically flat and the silane layer thickness was in the range of the molecule length. That indicates the formation of a MPTES monolayer. This surface should be suitable for attachment to gold via chemical binding between sulfur and gold atoms. Experiments of printing gold onto a mercaptosilanized surface using polymer stamps (PDMS and POP) were performed. The transfer of patterned gold electrodes should not be done until the printing process could be handled. For testing the adhesion properties unpatterned gold layers were transferred. 20 nm gold layers were deposited onto glass slides. The adhesion of gold to glass is known to be very weak. In the printing process the polymer stamps were pressed on the gold covered glass slide and stripped off with the intent to transfer the gold onto the stamp. The gold covered side of the stamp was then placed on the substrate. The stamp was removed. The amount of gold transferred from stamp to substrate was evaluated by sight and expressed in percentage of transfer. Chemical attachment of gold to the substrate was checked by Scotch Tape Test. This is a common method for qualitatively testing the adhesion of a thin film to a substrate. It is claimed that a Scotch Tape applied to the covered substrate and then stripped off is able to remove only the weakly bonded materials whereas films anchored by chemical binding stays on the surface. Here, Scotch Tape was applied to the surfaces with gold deposited in the printing step and stripped off. The removal of gold via this test was evaluated by sight and expressed in percentage of removal. In case of chemical binding between gold and sulfur, removal of the metal should not be possible.

With POP stamps it was easy to transfer the gold layer from glass slide to polymer. However, releasing the gold onto mercaptosilanized substrates was impossible.
To transfer the gold layer onto PDMS stamps was more difficult. Usually only parts of the gold layer adhered to the polymer surface. The transfer from PDMS stamps to substrates ranged between 50 and 100 %. The removal with Scotch Tape was always 100 %. That the transferred gold was always completely removable indicated the lack of chemical binding between thiol groups and gold.

The better adhesion of gold to POP (in comparison to PDMS) is an advantage of this material. Another convenience is the fact that POP is harder than PDMS. The relatively soft PDMS material easily bends during the printing procedure. This can lead to cracks in the transferred gold layer. This phenomena is shown in Fig. 4.15. The image was taken by Scanning Electron Microscopy (SEM) and shows a cracked gold layer on a mercaptosilanized substrate.

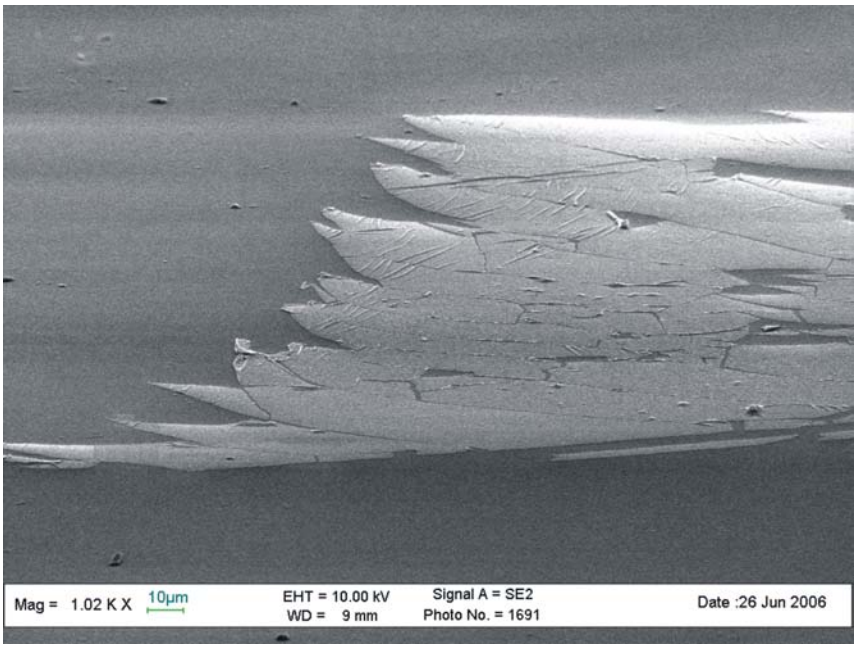

Figure 4.15: Gold printed with PDMS on MPTES covered surface

Such cracks are unwanted in the fabrication of crossbars. Therefore PDMS cannot be the material of choice for this printing procedure. The use of a stiffer material like POP is preferred to obtain crossbar electrodes without cracks.

Treatment of substrates after silanization

The failed attempt to attach the gold layer to the mercaptosilanized surface was further investigated. A possible explanation could have been that there were no free thiol groups available on the surface. Thiol groups are able to react with each other creating disulfide (S-S) bonds. Such disulfide bonds might have been formed during the deposition process reducing the number of free thiol groups and thus also reducing binding sites for gold. Another possibility was that there were excess silane molecules lying on top of a monolayer. Therefore efforts were made to remove multilayers or destroy disulfide bonds by treating the silanized surface in various ways:

- The substrates were rinsed with water, blown dry with argon (Intention: washing off excess molecules that are not bonded to the surface)
- The substrates were heated on a heating plate to $\sim 150\,^{\circ}\mathrm{C}$ for 5 min (Intention: evaporating excess molecules that are not bonded to the surface)
- The substrates were immersed in potassium hydroxide solution (10 %) for a few minutes, rinsed with water, blown dry with argon (Intention: breaking S-S bonds)
- The substrates were immersed in ammonium hydroxide solution (10 %) for a few minutes, rinsed with water, blown dry with argon (Intention: breaking S-S bonds)

- The substrates were immersed in ammonium thioglycolate solution (10 % and 60 %) for a few minutes, rinsed with water, blown dry with argon (Intention: breaking S-S bonds [57])

Printing gold onto substrates treated after silanization

All treated samples were used as substrates to transfer gold to. As in the printing tests with untreated mercaptosilanized surfaces, the transfer efficiency varied between 50 and 100 %. Also the Scotch Tape Tests failed in all cases, meaning that it was always possible to remove the transferred gold with Scotch Tape completely. So the result was that neither of the treatments improved the sticking of gold to the surface. Hence in the later experiments the mercaptosilanized surfaces were used untreated.
The failure of improvement after the different treatments indicated that neither multilayers nor disulfide bonds were responsible for the poor adhesion between gold and MPTES surface. The S 2s XP spectrum did indeed not show sulfur in disulfide bonds.

Some of the treated substrates were examined by Atomic Force Microscopy to find out which influence the treatments had on the surface topography. Images of a water rinsed sample and a heat treated sample are shown in Fig. 4.21 in comparison to an untreated surface.

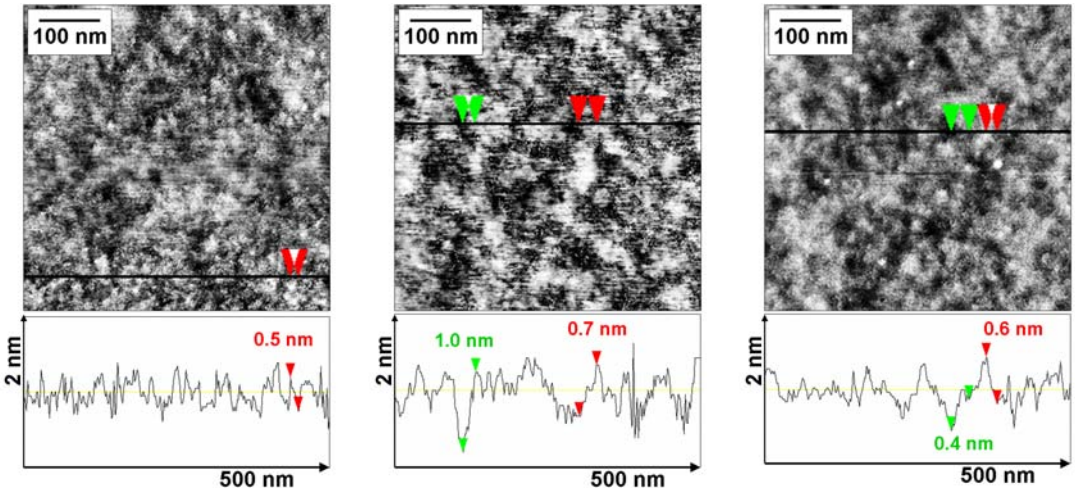

(a) untreated (b) rinsed with water (c) heated

Figure 4.16: AFM images of silicon oxide surfaces modified with MPTES after different treatments (contrast scales: 2 nm, respectively)

In addition the layer thicknesses before and after these treatments were measured by Ellipsometry. The results are summarized together with contact angle data and rms values in Table 4.7. The rms values are derived from a 4 μm^2 area.

Table 4.7: Influence of different treatments on silane layer thickness

Surface	Layer thickness [nm]	Surface roughness [nm]	Contact angle [°]
MPTES	0.6 ± 0.1	0.22	40 ± 1
MPTES rinsed with water	0.1 ± 0.1	0.32	33 ± 1
MPTES heated	0.2 ± 0.1	0.22	29 ± 1

The AFM image of the water rinsed sample revealed a slight increase in surface roughness, whereas the measured layer thickness decreased clearly. The latter observation indicates that parts of the silane film were washed off by rinsing with water. A certain amount of molecules seemed not to be covalently attached to the surface. The increase of surface roughness after the rinsing step points to the creation of aggregates. In summary, the situation might have been as follows: In the silanization procedure silane molecules were deposited on the surface resulting in a compact layer that is only partially linked. Loose molecules were then washed off or involved in increased cross-linking by the influence of water. The latter process led to a contraction of the adsorbed molecules and an increase of the surface roughness.
The results of the heated sample supports this model. Loose molecules could evaporate due to the increased temperature resulting in a layer of a lower thickness. The surface roughness did not increase because no additional water was offered for the cross-linking reaction.
The contact angle values are in agreement with the ellipsometric data. A decrease of coverage correlates to a decrease of the contact angle.

Treatment of substrates after printing of gold

An additional experiment concerning the interaction between the mercaptosilanized surface and gold was carried out by heating substrates after gold transfer to a series of temperatures. Therefore a gold layer was transferred by a PDMS stamp to the MPTES coated substrates. The substrates with the gold layer on top were then heated on a heating plate to a certain temperature for 5 min, respectively. The temperature was controlled with a thermocouple touching a reference wafer that was also lying on the heating plate. The temperature was regulated by hand. After the heat treatment the samples were cooled down for a few minutes and Scotch Tape Test was performed. The percentage of removal with Scotch Tape versus applied temperature is shown in Fig. 4.17. The error margins are due to the fact that the temperature control was done by hand.

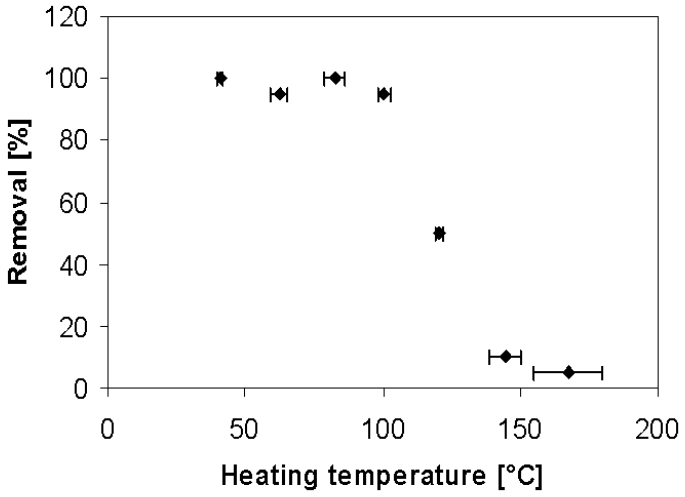

Figure 4.17: Heating of transferred gold on MPTES coated surface to various temperatures for 5 minutes, respectively

A heat treatment up to 100 °C did not lead to a change of the adhesion between gold and substrate. It was still possible to remove nearly the complete gold layer with Scotch Tape. For temperatures higher than 100 °C a decrease of the removal rate occurs. After heat treatment of around 150 °C it is almost impossible to remove the transferred gold with Scotch Tape.
A SEM image of a sample heated to 150 °C for 5 min is shown in Fig. 4.18. It reveals bubble-like structures on the gold layer. This might be due to heat-induced expansion of trapped water and/or silane between substrate and gold layer.

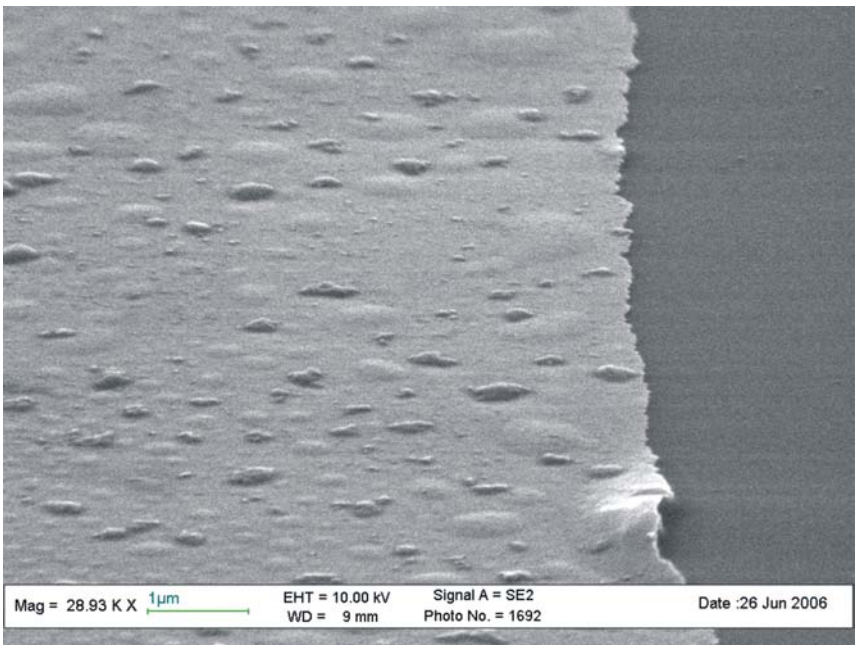

Figure 4.18: SEM image of a gold layer on a mercaptosilanized surface after heating to 150 °C for 5 min

Different reasons for the improved adhesion between gold and substrate due to heating seem possible:

1. The thin water layer on the surface, present due to air humidity, hindered the contact between gold and thiol groups. By heating the water evaporates and Au-S bonds could be formed.

2. Diffusion of gold and/or silicon took place through the thin silicon oxide layer leading to formation of alloy between silicon and gold.

3. The gold and the substrate surface could not get in touch in the first place because of a non-negligible roughness of the gold surface. By applying heat to the sample the MPTES layer and the surface gold atoms achieved a higher mobility and finally got in contact.

The influence of surface water was investigated by performing the printing procedure under dry conditions. Therefore the substrates were left in the glovebox after silanization and the stamps were passed into the glovebox as well. PDMS stamps with a gold layer on top were placed on a heating plate inside the glovebox. They were heated to about 100 °C for a few minutes in order to remove surface water completely. After cooling the stamp down, the gold covered side was brought in contact with a silanized substrate. This procedure was done with several samples. A transfer of gold to the substrates was hardly possible ($< 25\,\%$). Furthermore the few transferred pieces of gold were always removable with Scotch Tape. This indicates that the presence of a surface water layer could not have been the main reason that anchoring occurred only after heating. Another conclusion was achieved by the printing experiments in the glovebox. The transfer rate was extremely low in contradiction to printing results at the atmosphere, where usually at least 50 % of gold was transferred. This points out that transfer was rather caused by surface water changing the adhesion properties of the materials than by Au-S binding.
The possibility of diffusion was examined by depositing gold on a substrate of silicon with native silicon oxide layer, but without silane modification. The sample was heated to 150 °C and Scotch Tape Test was performed after cooling down. The gold was completely removable, diffusion did not lead to better sticking after heat treatment.
Finally the surface roughness was left as crucial parameter for the failing linkage between gold and thiol groups. The topography of a gold surface transferred to a POP stamp is shown in Fig. 4.19. Structure heights of up to 3 nm can be observed.

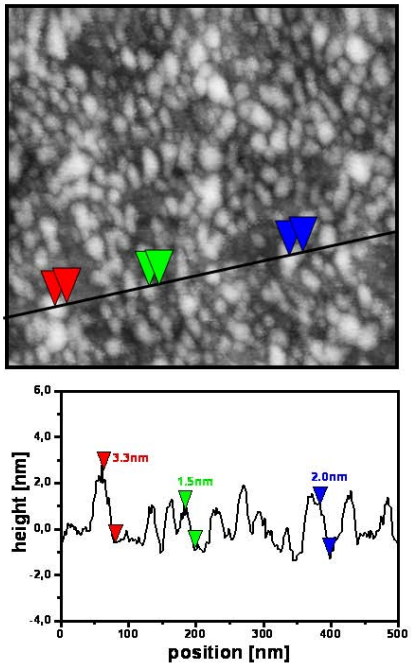

Figure 4.19: AFM image of gold surface on POP (Source: [75])Contrast scale: 5 nm

It is reasonable that a monolayer of silane molecules with a height below 1 nm is not able to compensate this roughness. In the continuative experiments efforts were made to create a thiol terminated layer that could adjust to the gold surface.

4.2.2 Coupling of Roughness Matching Adhesive Layer

As presented in the previous section, a chemical binding between gold and adhesive layer was not formed during the printing process although there were clear indications for the presence of free thiol groups available on the surface. A hindrance by surface water could be eliminated. The surface roughness of the gold remained as a possible explanation for the failure of attachment. Hence the idea to couple long and flexible molecules to the surface came up. These molecules should have a thiol termination that is able to bind to the gold, and should be long enough to compensate the roughness of the gold surface. Molecules with a poly(ethyleneglycol) (PEG) chain were chosen as deformable zone. At one end was a succinimide ester, that could be coupled to an aminoterminated surface (Fig. 4.20 (II)). In order to introduce amino groups on the surface of the silicon wafer, a silanization procedure with 3-aminopropyltriethoxysilane was performed (Fig. 4.20 (I)). The other end had a sulfur atom protected by a trityl group to avoid unwanted reaction of the thiol group. The trityl protection group could be cleaved in pure trifluoroacetic acid with triethylsilane as scavenger [46] [66] (Fig. 4.20 (III)). After cleavage, free thiol groups should be present at the surface. Such a molecule (α-tritylthio-ω-carboxy succinimidyl ester poly(ethylene glycol), Su-COO-PEG-CO-NH-C_2H_4-S-Trt) was chosen with a molecular weight of 3000 Da. This corresponds to $60 - 70$ PEG units. The length of a molecule is about $20 - 30$ nm. The length of these molecules offers the possibility to „bury“ bottom electrodes in a crossbar fabrication process. The long molecules could adjust the height of the bottom electrodes so that thiol groups and bottom electrodes are on the same level. In that way a plane surface is offered for printing the top electrodes and bending of the applied top electrodes could be avoided.

The single steps of the procedure were carried out one after another and in between the surfaces were examined to evaluate the success of the coupling reactions.

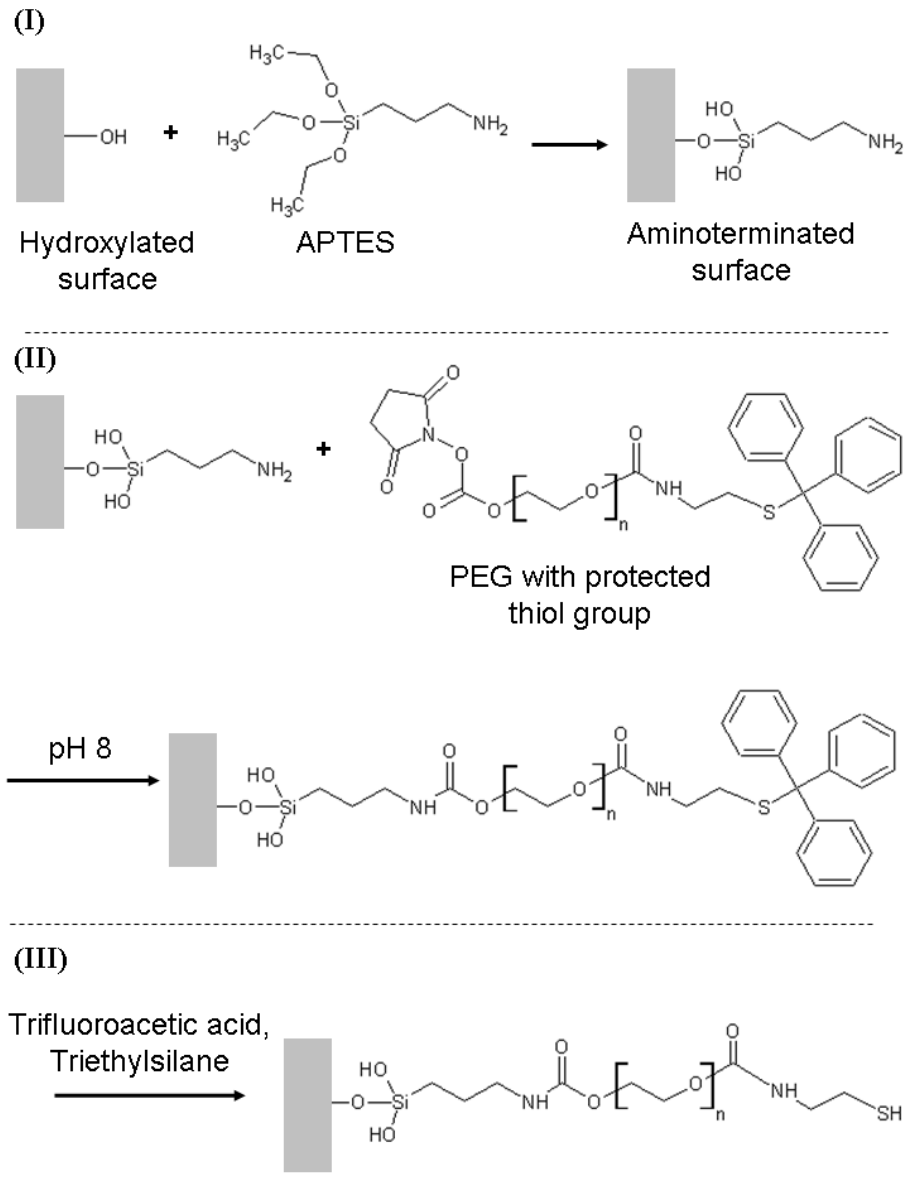

Figure 4.20: Coupling steps of the formation of a roughness matching adhesive layer

(I) Silanization with APTES

The silanization was done in a desiccator inside the glovebox for 1 hour at a pressure of 5 mbar. In the first experiments with APTES, an old desiccator was used. The vessel had been utilized for silanizations very often and might have also been used for different applications. Later a new desiccator was employed, in which only the APTES silanization was performed. The difference in APTES film quality dependent on the desiccator was investigated by AFM measurement. The substrate prepared in the new desiccator exhibits a rather flat surface (Fig. 4.21 b), similar to those modified with FOTCS or MPTES. Surface roughness was measured to be 0.20 nm for a 4 μm^2 area. In contrast, on the surface coated in the old desiccator more rough structures with heights of up to several nanometers were observed (Fig. 4.21 a). The rms value was 0.53 nm for a 5μm^2 area. The

molecules seem to be clustered together, forming agglomerations on the surface. Possibly the chemicals present on the walls inside the desiccator had this unwanted effect on the result. It is imaginable that silane molecules of several silanization processes accumulated on the glass walls in the course of time. Silane molecules could then detach again and deposit on the substrate surface in an uncontrolled manner. Considering this observation, only surfaces that were prepared in the new desiccator were used for the following coupling steps to ensure a maximum number of coupling sites.

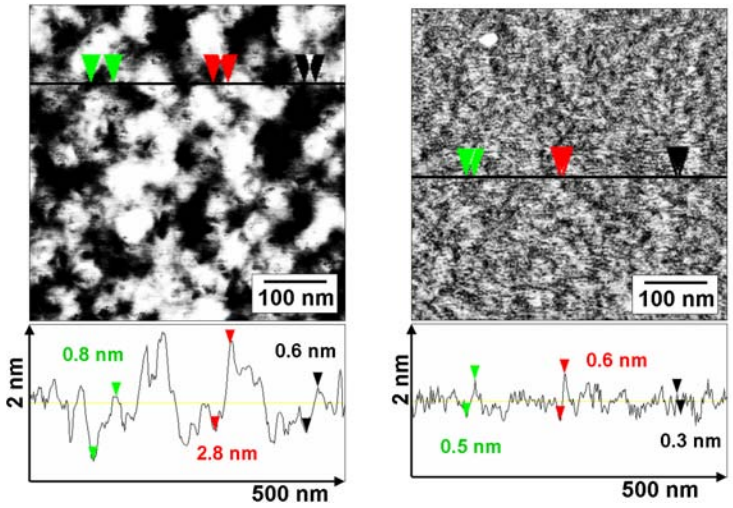

(a) (b)

Figure 4.21: APTES coated silicon surface prepared in
(a) often used desiccator
(b) desiccator exclusively used for APTES silanization
Contrast scale: 2 nm, respectively

The thickness of the APTES layer, measured several times by Ellipsometry, was $0.4 - 0.6$ nm. The thickness of a closed monolayer, supposed to be 0.7 nm [90], is slightly higher. This might be an indication that not a 100 % coverage was reached. The contact angle of the modified surface was about 48 °, which is in in good agreement with reported data in the literature for aminoterminated surfaces ($45 - 60$ ° [28] [88] [32]).

XP survey and detail spectra of the surface are shown in Fig. B.5 and B.6 (appendix). The results are summarized in Table 4.8. The XPS data show the presence of carbon and nitrogen as expected for the aminosilanized surface. However, silicon and oxygen are still the dominating signals. This indicates the formation of a very thin organic layer. This is in agreement with the ellipsometrically measured layer thickness of a few angstrom.

Table 4.8: XPS results of APTES covered surface

Element	Binding energy [eV]	Relative concentration [atom %]	∑ Relative concentration [atom %]	Chemical assignment
O 1s	532.9	37.7		SiO_2, org. O
	531.7	4.3	42.0	org. O
N 1s	402.4	0.5		NH_3^+
	400.9	0.5	2.1	NH_2 (H-bonded)
	399.9	1.1		NH_2 (free)
C 1s	289.0	0.2		
	286.9	4.9	18.6	CH_2-NH_2
	285.6	13.5		CH_2
Si 2p	103.3	14.2		SiO_2
	99.3	23.1	37.3	SiO_2

The N 1s signal was fitted to consist of three peaks. Only the peak at 399.9 eV could be assigned to free amine groups, whereas the signals at 400.9 and 402.4 eV were correlated to H-bonded and protonated amine groups, respectively [97]. The presence of different amine species besides free NH_2 groups is a known phenomenon in the case of silanization with aminoterminated silanes. The amine functionalities are assumed to compete with the alkoxy or silanol groups for surface sites during the chemisorption process. This gives rise to a variability of adsorbed species. A schematic of possible surface structures was proposed by WHITE and TRIPP [92] and is shown in Fig. 4.22.

Figure 4.22: Schematic of possibly realistic APTES covered surface (Source: [92])

The presence of H-bonded and protonated amine groups might be disadvantageous for the further coupling steps.

(II) Coupling of PEG molecules

The coupling reaction of PEG molecules was done with a 1 mM solution of PEG in phosphate buffer (pH 8.0) [74]. The amino modified substrates were immersed in the solution for 2.5 h. Subsequently they were rinsed with water and dried with argon.

The determined layer thickness was 2.6 nm. This is about 10 % of the theoretical length of the molecules consisting of $60 - 70$ PEG units. This low value of the layer thickness indicates that the coverage with PEG molecules is rather low. Possibly the PEG chains are crumbled together or lying flat on the surface instead of being outstretched perpendicular to the surface. This could lead to an inhibition of binding sites for further coupling.
XPS analysis of the surface composition was done with the modified surface. The spectra are shown in the appendix (Fig. B.7). The signals, relative concentrations and chemical assignments are summarized in Table 4.9.

Table 4.9: XPS results of PEG covered surface (before cleavage of protection group)

Element	Binding energy [eV]	Relative concentration [atom %]	∑ Relative concentration [atom %]	Chemical assignment
O 1s	533.1	38.3		SiO_2, org. O
	531.9	4.0	42.3	org. O
N 1s	402.8	0.5		NH_3^+, NH_2^+-CO
	401.8	0.1	1.1	succinimide N
	400.5	0.5		NH-CO, NH_2
C 1s	288.9	0.6		
	287.1	12.4		CO-NH, COC
	285.9	3.7	24.5	trityl C
	285.4	7.8		CH_2
Si 2p	103.4	11.6		SiO_2
	99.3	20.6	32.2	SiO_2

The ratio Si : C is decreased from 2 : 1 for the APTES covered surface to about 1.3 : 1 for the surface with coupled PEG molecules. This is reasonable since additional carbon atoms from the PEG molecules are present on the surface. The fact that silicon is still dominant confirms the observation that the thickness of the organic layer was only a few nanometers.
In the N 1s spectrum a shift in binding energies compared to the values from the APTES coated surface was measured. The NH_2 peak at 399.9 eV can not longer be observed but one at 400.5 eV. This signal can be assigned to nitrogen in the newly formed amide bond [97]. However, the presence of NH_2 cannot be excluded. The peak at 402.8 eV is assigned to protonated species. The signal at 401.8 eV might be due to unreacted succinimide groups of PEG molecules.
The carbon signals are in correlation with the derivations from the nitrogen spectrum. The peak at 287.1 eV is assigned to amide and ether C. The relation between carbon in CH_2 groups and in CH_2 groups neighboring nitrogen or oxygen was 2.7 : 1 for the APTES surface and is here 0.6 : 1. This is in correlation to the appearance of carbon in PEG units. Additionally a peak at 285.9 eV was measured,which is most likely due to carbon in the trityl protection groups.

(III) Cleavage of protection group

The cleavage of the trityl group was done with pure trifluoroacetic acid and a few drops of triethylsilane by immersing the substrates for 30 or 60 min. Since an immersion time of 60 min led to better results during the printing procedure (→ p. 59), it was mostly used in the protocol. After immersion, the samples were rinsed with water and blown dry with argon.
The determined layer thickness was 1.9 nm. The thickness decrease of 0.7 nm after cleaving the protection group is relatively high for the low coverage. This might be a hint that part of the organic layer was washed off. The contact angle of a sample after cleavage was 36 °. This in the range of MPTES modified surfaces with contact angle values of $34 - 40$ °. A blank sample was treated in the same way but without PEG molecules in the buffer solution. The measured contact angle of this sample after the procedure was 18 °. The significant difference to the PEG modified sample indicated that different molecules were present on the surface. The contact angle of the PEG modified surface could indeed be caused by thiol groups on the surface, but also by the PEG units.

Table 4.10: XPS results of PEG covered surface (after cleavage of protection group)

Element	Binding energy [eV]	Relative concentration [atom %]	∑Relative concentration	Chemical assignment [atom %]
O 1s	533.1	35.8		SiO_2
	531.7	3.0	38.8	
N 1s	402.7	0.2		NH_3^+, NH_2^+-CO
	400.4	0.6	0.8	NH-CO
C 1s	287.2	9.5		CO-NH, COC
	285.6	21.1	30.6	CH_2
Si 2p	103.5	11.3		SiO_2
	99.3	18.5	29.8	SiO_2

The XP spectra are shown in the appendix (Fig. B.8). The data are summarized in Table 4.10. Here the trityl-C signal was not found anymore, indicating that the deprotection was successful. Also the nitrogen signal assigned to the succinimide group could not be measured. Unreacted molecules might be washed off in the additional reaction step. The ratio between carbon in CH_2 and in CO-NH or COC rose again to 2.2 : 1. This might be a confirmation that part of the organic layer was washed off.

Neither before nor after the deprotection step it was possible to detect any sulfur signal. It was tried to increase the sensitivity by the use of a decreased take-off angle, but still no sulfur could be detected. This means that the sulfur concentration was below the detection limit. However the existence of sulfur on the surface can not be excluded. For surfaces modified with MPTES it was hard to detect sulfur, too. There a complete mono-

layer of MPTES molecules probably existed on the surface bearing more thiol groups than the incomplete layer of PEG molecules.

The surface topography of a PEG modified surface after the deprotection step was evaluated by AFM (Fig. 4.23). The surface was rather flat except of few agglomerations with heights of about 1.3 nm and diameters of about 50 nm. The rms value for a 4 μm^2 area was 0.18 nm.

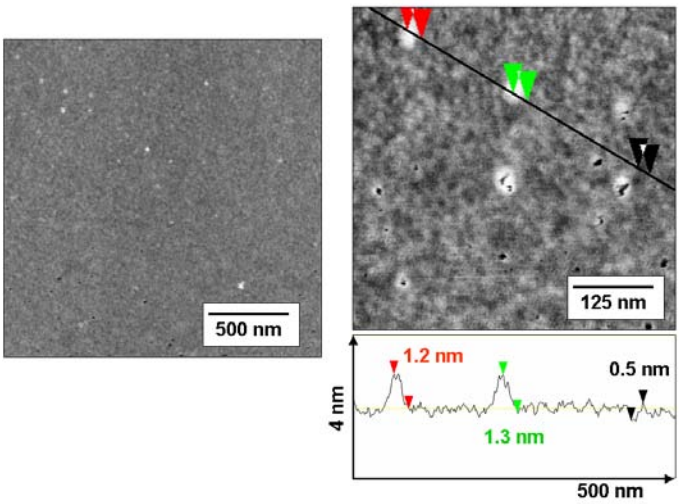

Figure 4.23: AFM images of a PEG modified surface
Contrast scale: 10 nm (left image) and 4 nm (right image)

Printing gold on PEG layer

The aim of modifying the surface with a thiol terminated PEG layer was to introduce a higher sticking efficiency between gold and surface. For this reason the transfer of gold onto the modified surfaces was tested as described earlier (p. 46). The transfer with PDMS stamps was always complete (100 %). This was also true for POP stamps. That means that the adhesion between gold and POP was overcompensated by the adhesion between gold and the PEG modified surface. Note that transfer of gold from POP was never achieved for substrates modified with MPTES. The Scotch Tape Test showed different results for changing immersion during the cleavage reaction of the protection group (III). For a cleavage time of 30 min it was possible to remove 50 % of the gold again. In the case of the substrates immersed in trifluoroacetic acid with triethylsilane for 1 h only very little ($\sim$ 5 %) of the gold could be removed with Scotch Tape.

It was also tested to print gold onto a blank sample (treated in the same way as the other samples but without PEG molecules in the buffer solution). Printing gold onto the blank sample was not successful. No transfer from POP to the sample was achieved. It was also tested to print gold on a surface modified with APTES since it is known that also amino functionalities can promote the adhesion to gold [79]. Here it was again impossible to transfer gold.

It can be concluded that the improved transfer from POP to substrate was indeed due to the thiol terminated PEG layer. The longer molecules could match to the roughness of the gold surface and the thiol groups might promote adhesion between surface and metal. However, it remains unclear what the actual conformation of the PEG molecules is. It cannot be excluded that the molecules are lying down on the surface and the adhesion is mediated by the PEG units themselves.

After the successful transfer of an unpatterned gold layer from a glass slide to the substrates, the transfer of gold patterns was tested as well. Gold electrodes on a silicon oxide substrate (with a FOTCS layer between as release agent) were used for this experiment. A lift off step with acetone was performed leaving only the gold electrodes on the wafer. A piece of POP was rinsed with 2-propanol and dried with argon before pressing on the gold structures. The stamp was applied by hand with an undefined pressure. The POP piece with the gold electrodes on the surface was then placed on the second substrate so that the gold electrodes got in contact with the adhesive layer. After pressing stamp and substrate together by hand for a few seconds, the stamp was removed. The transfer was followed by a Scotch Tape Test. Optical Microscopy images were taken to evaluate the success of the printing procedure (Fig. 4.24).

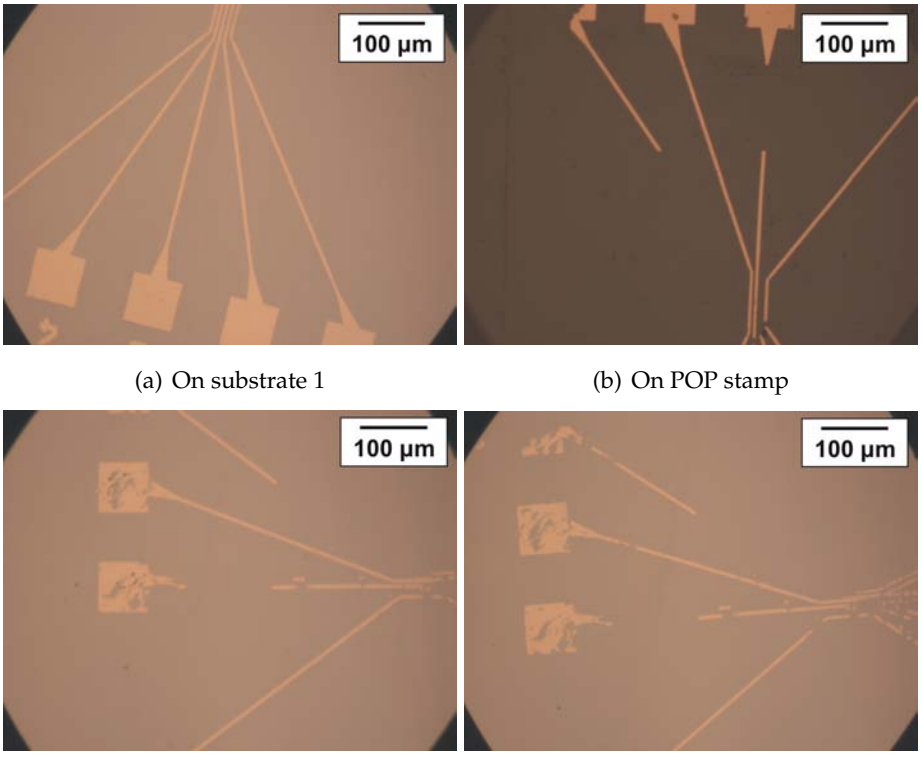

(a) On substrate 1 (b) On POP stamp

(c) On substrate 2 (d) On substrate 2, after Scotch Tape Test

Figure 4.24: Gold electrodes on different surfaces during a printing procedure

In Fig. 4.24 a the gold electrodes are shown after the lift off procedure on substrate 1. They were well defined and faultless. After the transfer to POP the structures were not

complete anymore (Fig. 4.24 b). However, no cracks were observed for the transferred structures. The uncomplete transfer might have been due to an imperfect release from substrate 1. In the next step the gold electrodes were transferred to substrate 2. Again a loss of features occurred (Fig. 4.24 c). The structures which were finally transferred to the second substrate could not be removed with Scotch Tape (Fig. 4.24 d). This implies that the successfully transferred parts of gold were indeed transferred because of chemical binding to the surface. The incomplete transfer to substrate 2 might be caused by the low amount of thiol terminations on the surface.

For reliable application further investigation and improvement of the system seems to be necessary. A higher yield of the coupling reactions should be aimed in order to achieve a higher concentration of thiol groups on the surface. This should improve the transfer from stamp to substrate. Another possibility to establish a flexible surface layer with a high amount of anchor groups could be the use of especially synthesized molecules for this purpose. A custom-made molecule with a silane termination at one end (for binding to silicon oxide), a chain of the required length and flexibility (PEG, or others) and a thiol group at the other end (for binding to gold). Thereby the PEG layer could be coupled to the silicon oxide surface directly, an unnecessary coupling step could be eliminated.

If the here described Shuttle-Transfer Printing process is used for the fabrication of cross-bars for Molecular Electronics the introduction of the PEG molecules offers interesting opportunities. Not only the ability of adhesion promotion but also the feature to work as a spacer molecule might be advantageous. A possible procedure with the here used PEG molecules as example is shown in Fig. 4.25.

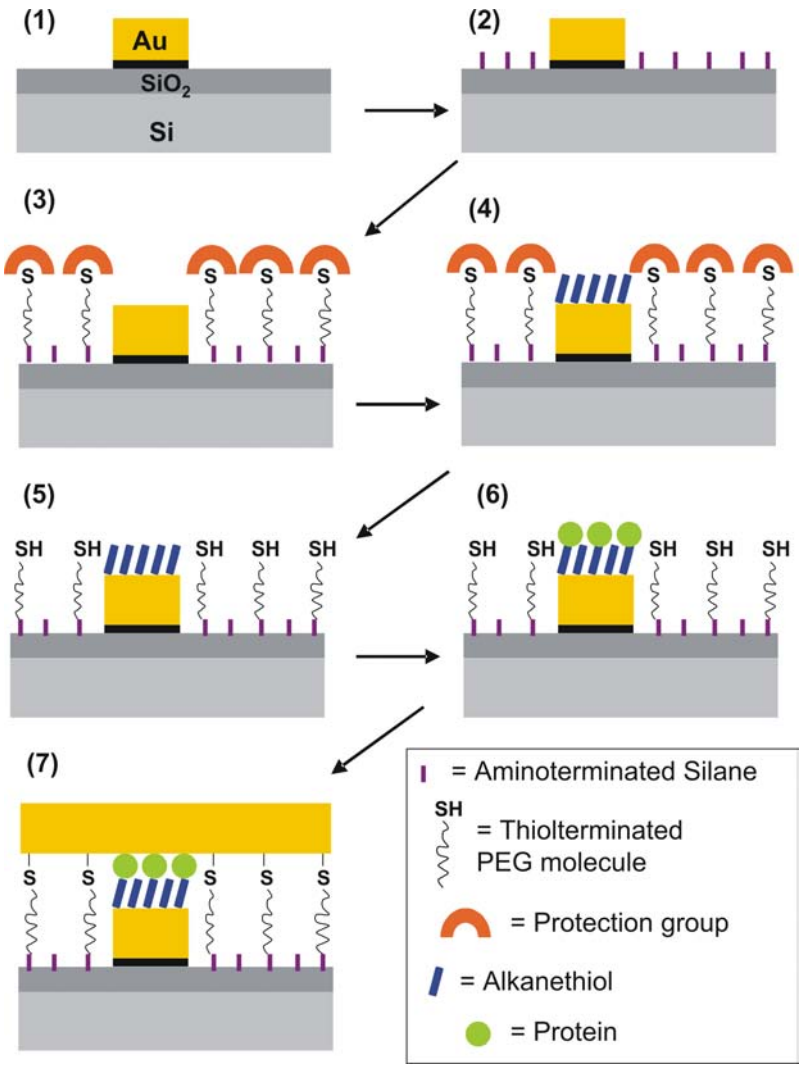

Figure 4.25: Possible Shuttle-Transfer Printing procedure with PEG adhesive layer

(1) Gold bottom electrodes are fabricated on a silicon wafer with silicon oxide surface. An adhesion layer between gold and silicon oxide might be used, e.g. titanium. The height of the gold electrode is usually about 20 nm.
(2) The silicon oxide surface is modified by silanization with an aminoterminated silane, e.g. APTES. The silane reacts only with the silicon oxide surface.
(3) The PEG molecules are coupled to the APTES layer. In this step it is important that the thiol groups of the PEG molecules are protected via a protection group (e.g. a trityl group). Otherwise the thiol groups could bind to the bottom electrode.
(4) A self-assembling monolayer of alkanethiols (e.g. γ-modified alkanethiols as anchor molecules for proteins) is deposited on the gold bottom electrode. Here again the protection of the PEG thiol groups is advantageous, avoiding the formation of disulfide bonds between the PEG molecules and the alkanethiols.
(5) The protection groups are cleaved, leaving free thiol groups on the surface. In the case of trityl as protection group the cleavage is performed with concentrated trifluoroacetic acid and triethylsilane.
(6) Proteins are deposited on the alkanethiol SAM. (Most likely it is recommended to

carry out the deprotection before the deposition of the proteins. Many proteins are known to denature under acid conditions.)
(7) The gold top electrode is printed via STP perpendicular to the bottom electrode. Alkanethiols and Proteins are present in the junction between the two electrodes. The thiol groups of the PEG molecules ensure a good transfer of the top electrode and also that it stays on the surface. In the case of upright standing PEG molecules the height of this layer should be $20 - 30\,\text{nm}$. That means the bottom electrode is „buried“ in the PEG layer. PEG thiol groups and proteins should be more or less on the same height. Thereby an unrequired deformation of the top electrode could be avoided.
The exact order of fabrication steps is not necessarily as presented above, but depends on the used system.

5 Summary and Outlook

The objective of this work was to chemically modify silicon surfaces by anchoring functional molecules. A major part was devoted to the investigation and improvement of the self-assembly process of organosilanes on oxidized silicon surfaces. Silane molecules with perfluoro, thiol, and amino functionalities were employed. These particular molecules were chosen for specific applications in Soft Lithography, namely as release agent, as gold adhesive layers, and as interface for the coupling of roughness matching gold adhesive layers, respectively.

The formation of a release agent layer with perfluorinated alkylsilanes was performed by vapor phase deposition. First an apparatus at hand was used and the modified surfaces were examined by AFM, Ellipsometry, XPS, and Contact Angle Measurement as characterization methods. It was observed that the silanization often led to uncompletely covered surfaces. Further the results showed a lack of reproducibility. Especially surface contamination and an undefined water content seemed to be critical. An advanced vapor phase deposition device, called CASINO device, was built to enhance the qualities of the thin films. The device is equipped with multiple features. It is possible to carry out cleaning and silanization in a closed chamber without exposing the samples to air in between. Thereby surface contamination is avoided. The samples can be exposed to water vapor under controlled pressure to tune the water content on the surface. Further attachments are installed for the controlled inlet of silane and catalyst vapor.
Experiments with the new device were performed following examples given in literature. A procedure with no or a low amount of water present resulted in surfaces with a low coverage. Furthermore, the molecular film produced under these (almost) dry conditions showed a lack of stability. It was possible to remove parts of the layer by heating the substrate after the coating procedure. This is in agreement with the common assumption that water plays a crucial role in the chemisorption mechanism.
Another procedure with subsequent exposure of the sample to silane, water and again silane vapor led to the formation of a silane film with an extremely low surface energy as required for the use as release agent. Ellipsometry analysis showed that the silane film probably consisted of bi- or multilayers. This might have been due to the fact that excess molecules were not removed between the reaction steps. To optimize the silanization process in the CASINO device, it was also planned to apply heat treatment of the sample during or after the deposition process. Excess molecules which are not anchored to the surface could be removed by heating. The installation of the heating equipment could not be finished during this work.
The CASINO device provides the opportunity to develop a silanization protocol to obtain dense, stable and homogeneous monolayers. The way to gain reproducible results is made available due to the controlled process conditions. Optimization of the silanization procedure with the new setup is not restricted to perfluorinated silanes. The quality of various kinds of functional organosilane layers can be enhanced with the CASINO device.

Surface layers of thiolterminated and of aminoterminated molecules were investigated as adhesive layer for the linkage of metal structures to silicon surfaces, e.g. Shuttle-Transfer Printing with gold crossbar electrodes. First, thiol- and aminoterminated organosilane SAMs were tested as adhesive layers for gold. It was found that gold did not stick to surfaces modified with such molecules. The surface modified with thiolterminated silane molecules was further examined. Neither attempts to evaporate or wash off excess molecules nor to break eventually existing disulfide bonds led to a satisfying adhesion between the modified silicon surface and gold. Adhesion was promoted only after heat treatment of a thiolmodified silicon substrate with a gold layer on top. Several explanations of this behavior were examined leading to the conclusion that the short silane molecules were not able to adjust to the roughness of the gold layer until their mobility was increased by the elevated temperature. Efforts were made to overcome the roughness induced contact failure. Long and flexible PEG molecules were coupled to an aminoterminated SAM on silicon oxide. Thereby, the adhesion to gold was promoted. The once impossible transfer of gold from a polyolefin plastomer stamp to a modified substrate could now be performed in a promising way.
Analysis of the modified surfaces during the coupling procedure indicated a low coverage with adhesive molecules. Further enhancement of the coupling reactions seems to be possible. The CASINO device could be put into action to improve the quality of the aminosilane SAM as the first layer in the system. The efficiency of the subsequent reaction steps could be increased by the use of other molecules, custom-made for this purpose.

The developed procedure of coupling long, flexible molecules to the silicon surface provides an improved opportunity to fabricate metal–molecule–metal devices on silicon substrates via Soft Lithography. For the example of gold crossbars, it is possible to bury bottom electrodes by organic molecules and subsequently apply top electrodes to the flat and levelled adhesive layer.

References

[1] ABCR: Datasheet of 3-mercaptopropyltriethoxysilane.

[2] Fluka: Datasheet of 1H,1H,2H,2H-perfluorooctyltrichlorosilane.

[3] Monolayer films that assemble themselves. *New Scientist*, 98(1352):20, 1983.

[4] ALESSANDRINI, A.; FACCI, P. AFM: a versatile tool in biophysics. *Measurement Science and Technology*, 16(6):R65, 2005.

[5] ALLARA, D.L.; PARIKH, A.N.; RONDELEZ, F. Evidence for a Unique Chain Organization in Long Chain Silane Monolayers Deposited on Two Widely Different Solid Substrates. *Langmuir*, 11(7):2357, 1995.

[6] ALMEIDA, A.T.; SALVADORI, M.C.; PETRI, D.F.S. Enolase Adsorption onto Hydrophobic and Hydrophilic Solid Substrates. *Langmuir*, 18(18):6914, 2002.

[7] ANGST, D.L.; SIMMONS, G.W. Moisture Absorption Characteristics of Organosiloxane Self-Assembled Monolayers. *Langmuir*, 7:2236, 1991.

[8] BASIUK, V.A.; CHUIKO, A.A. Gas-phase synthesis, properties and some applications of acylamide stationary phases for high-performance liquid chromatography. *Journal of Chromatography*, 521:29, 1990.

[9] BRAGA, P.C. *Atomic Force Microscopy: Biomedical Methods and Applications*. Humana Press, 2004.

[10] BRITT, D.W.; HLADY, V. An AFM Study of the Effects of Silanization Temperature, Hydration, and Annealing on the Nucleation and Aggregation of Condensed OTS Domains on Mica. *Journal of Colloid and Interface Science*, 178:775, 1996.

[11] BRUNNER, H.; VALLANT, T.; MAYER, U.; HOFFMANN, H. Substrate Effects on the Formation of Alkylsiloxane Monolayers. *Langmuir*, 15(6):1899, 1999.

[12] BRZOSKA, J.B.; AZOUZ, I.B.; RONDELEZ, F. Silanization of Solid Substrates: A Step toward Reproducibility. *Langmuir*, 10(11):4367, 1994.

[13] BRZOSKA, J.B.; SHAHIDZADEH, N.; RONDELEZ, F. Evidence of a transition temperature for the optimum deposition of grafted monolayer coatings. *Nature*, 360:719, 1992.

[14] CHANG, Y.-C.; FRANK, C.W. Vapor Deposition-Polymerization of α-Amino Acid *N*-Carboxy Anhydride on the Silicon(100) Native Oxide Surface. *Langmuir*, 14(2):326, 1998.

[15] CHOI, K.; EOM, T.-J.; LEE, C. Comparison of the removal efficiency for organic contaminants on silicon wafers stored in plastic boxes between UV/O_3 and ECR oxygen plasma cleaning methods. *Thin Solid Films*, 435:227, 2003.

[16] CHOI, K.; GHOSH, S.; LIM, J.; LEE, C.M. Removal efficiency of organic contaminants on Si wafer by dry cleaning using UV/O_3 and ECR plasma. *Applied Surface Science*, 206:355, 2003.

[17] DUCHET, J.; CHABERT, B.; CHAPEL, J.P.; GÉRARD, J.F.; CHOVELON, J.M.; JAFFREZIC-RENAULT, N. Influence of the Deposition Process on the Structure of Grafted Alkylsilane Layers. *Langmuir*, 13:2271, 1997.

[18] BALK, P. (editor). *The Si-SiO_2 System*. Elsevier, 1988.

[19] CARLSON, TA (editor). *X-Ray Photoelectron Spectroscopy*. Dowden, Hutchington & Ross, Inc., 1978.

[20] MATACOTTA, F.C.; OTTAVIANI, G. (editors). *Science and Technology of Thin Films*. World Scientific, 1995.

[21] FINKLEA, H.O.; ROBINSON, L.R.; BLACKBURN, A.; RICHTER, B.; ALLARA, D.; BRIGHT, T. Formation of an Organized Monolayer by Solution Adsorption of Octadecyltrichlorosilane on Gold: Electrochemical Properties and Structural Characterization. *Langmuir*, 2(2):239, 1986.

[22] FONTAINE, P.; GOLDMANN, M., RONDELEZ, F. Influence of Headgroup Cross-Linking on Chain Packing in Langmuir Monolayers of *n*-Alkyltrialkoxysilanes. *Langmuir*, 15(4):1348, 1999.

[23] GAO, Y.; MASUDA, Y.; YONEZAWA, T.; KOUMOTO, K. Site-Selective Deposition and Micropatterning of $SrTiO_3$ Thin Film on Self-Assembled Monolayers by the Liquid Phase Deposition Method. *Chemical Materials*, 14(12):5006, 2002.

[24] GATES, B.D.; XU, Q.; LOVE, C.; WOLFE, D.B.; WHITESIDES, G.M. Unconventional Nanofabrication. *Annual Review of Materials Research*, 34:339, 2004.

[25] GENZER, J.; EFIMENKO, K.; FISCHER, D.A. Molecular Orientation and Grafting Density in Semifluorinated Self-Assembled Monolayers of Mono-, Di-, and Trichloro Silanes on Silica Substrates. *Langmuir*, 18(24):9307, 2002.

[26] GE, S.; TAKAHARA, A.; KAJIYAMA, T. Aggregation structure and surface properties of immobilized organosilane monolayers prepared by the upward drawing method. *J. Vac. Sci. Technol. A*, 12(4):2530, 1994.

[27] HAIR, M.L.; TRIPP, C.P. Alkylchlorosilane reactions at the silica surface. *Colloids and Surfaces A*, 105:95, 1995.

[28] HALLER, I. Covalently Attached Organic Monolayers on Semiconductor Surfaces. *Journal of the American Chemical Society*, 100(26):8050, 1978.

[29] HANEMAN, D. Surfaces of Silicon. *Reports on Progress in Physics*, 50(8):1045, 1987.

[30] HAN, Y.; OFFENHÄUSSER, A.; INGEBRANDT, S. Detection of DNA hybridization by a field-effect transistor with covalently attached catcher molecules. *Surface and Interface Analysis*, 38:176, 2006.

[31] HEATH, J.R.; KUEKES, P.J.; SNIDER, G.S.; WILLIAMS; R.S. A Defect-Tolerant Computer Architecture: Opportunities for Nanotechnology. *Science*, 280:1716, 1998.

[32] HEISE, A.; MENZEL, H. Grafting of Polypeptides on Solid Substrates by Initiation of N-Carboxyanhydride Polymerization by Amino-Terminated Self-Assembled Monolayers. *Langmuir*, 13(4):723, 1997.

[33] HOFFMANN, P.; KULIG, G.; BARBIERI, L. Patent US2005247120: Gas phase deposition of perfluorinated alkyl silanes, 2005.

[34] HOFFMANN, P.W.; STELZLE, M.; RABOLT, J.F. Vapor Phase Self-Assembly of Fluorinated Monolayers on Silicon and Germanium Oxide. *Langmuir*, 13(7):1877, 1997.

[35] HOLLEMAN, A.F.; WIBERG, E. *Lehrbuch der Anorganischen Chemie*. deGruyter, 1985.

[36] HOQUE, E.; DEROSE, J.A.; HOFFMANN, P.; MATHIEU, H.J. Robust perfluorosilanized copper surfaces. *Surface and Interface Analysis*, 38:62, 2006.

[37] HOZUMI, A.; USHIYAMA, K.; SUGIMURA, H.; TAKAI, O. Fluoroalkylsilane Monolayers Formed by Chemical Vapor Surface Modification on Hydroxylated Oxide Surfaces. *Langmuir*, 15(22):7600, 1999.

[38] HUANG, X.; HUANG, H.; WU, N.; HU, R.; ZHU, T.; LIU, Z. Investigation of structure and chemical states of self-assembled Au nanoscale particles by angle-resolved X-ray photoelectron spectroscopy. *Surface Science*, 459:183, 2000.

[39] HU, M.; NODA, S.; OKUBO, T.; YAMAGUCHI, Y.; KOMIYAMA, H. Structure and morphology of self-assembled 3-mercaptopropyltrimethoxysilane layers on silicon oxide. *Applied Surface Science*, 181:307, 2001.

[40] JIERONG, C.; JING-LIAN, Y.; YUN-ZE, Z. Surface modification of medical pvc by remote oxygen plasma. *Composite Interfaces*, 11(2):123, 2004.

[41] JUNG, G.-Y.; LI, Z.; WU, W.; CHEN, Y.; OLYNICK, D.L.; WANG, S.-Y.; TONG, W.M.; WILLIAMS, R.S. Vapor-Phase Self-Assembled Monolayer for Improved Mold Release in Nanoimprint Lithography. *Langmuir*, 21:1158, 2005.

[42] KALLURY, K.M.R.; MACDONALD, P.M.; THOMPSON, M. Effect of Surface Water and Base Catalysis on the Silanization of Silica by (Aminopropyl)alkoxysilanes Studied by X-ray Photoelectron Spectroscopy and ^{13}C Cross-Polarization/Magic Angle Spinning Nuclear Magnetic Resonance. *Langmuir*, 10(2):492, 1994.

[43] KESSEL, C.R.; GRANICK, S. Formation and Characterization of a Highly Ordered and Well-Anchored Alkylsilane Monolayer on Mica by Self-Assembly. *Langmuir*, 7:532, 1997.

[44] KIM, E.; XIA, Y.; WHITESIDES, G.M. Polymer microstructures formed by moulding in capillaries. *Nature*, 376(6541):581, 1995.

[45] KIM, E.; XIA, Y.; ZHAO, X.-M.; WHITESIDES, G.M. Solvent- Assisted Microcontact Molding: A Convenient Method for Fabricating Three-Dimensional Structures on Surfaces of Polymers. *Advanced Materials*, 9(8):651, 1997.

[46] KOCIENSKI, P.J. *Protecting Groups*. Thieme, 2005.

[47] KULINOWSKI, K.M:; JIANG, P.; VASWANI, H.; COLVIN, V.L. Porous Metals from Colloidal Templates. *Advanced Materials*, 12(11):833, 2000.

[48] KUMAR, A.; WHITESIDE, G.M. Features of gold having micrometer to centimeter dimensions can be formed through a combination of stamping with an elastomeric stamp and an alkanethiol „ink“ followed by chemical etching. *Applied Physics Letters*, 63(14):2002, 1993.

[49] LEE, L.-H. Wettability and Conformation of Reactive Polysiloxanes. *Journal of Colloid and Interface Science*, 27(4):751, 1968.

[50] LE GRANGE, J.D.; MARKHAM, J.L.; KURKJIAN, C.R. Effects of Surface Hydration on the Deposition of Silane Monolayers on Silica. *Langmuir*, 9(7):1749, 1993.

[51] LENIGK, R.; CARLES, M.; IP, N.Y.; SUCHER, N.J. Surface Characterization of a Silicon-Chip-Based DNA Microarray. *Langmuir*, 17(8):2497, 2001.

[52] LLOPIZ, P.; MAIRE, J.-G. Étude infrarouge et ESCA de quelques complexes métallique de la cystéine. *Bulletin de al Socété chimique de France*, 11:I–457, 1979.

[53] LOO, Y.L.; LANG, D.; ROGERS, J.A.; HSU, J.W.P.:. Electric Contacts to Molecular Layers by Nanotransfer Printing. *Nanoletters*, 3:913, 2003.

[54] MABOUDIAN, R.; HOWE, R.T. Adhesion in surface micromechanical structures. *Journal of Vacuum Science & Technology B*, 15(1):1, 1997.

[55] MAGONOV, S.N.; WHANGBO, M.-H. *Surface Analysis with STM and AFM*. VCH, 1996.

[56] MAHAPATRO, A.K.; SCOTT, A.; MANNING, A.; JANES, D.B. Gold surface with sub-nm roughness realized by evaporation on a molecular adhesion monolayer. *Applied Physics Letters*, 88:151917, 2006.

[57] MANUSZAK, M.A.; BORISH, E.T.; WICKETT, R.R. The kinetics of disulfide bond reduction in hair by ammonium thioglycolate dithioglycolic acid. *Journal of the Society of Cosmetic Chemists*, 47:49, 1996.

[58] MOORE, G.E. Cramming more components onto integrated circuits. *Electronics*, 38(8), 1965.

[59] MULLER, C.J.; VAN RUITENBEEK, J.M.; DE JONGH, L.J. Experimental observation of the transition from weak link to tunnel junction. *Physica C*, 191:485, 1992.

[60] Nanofilm Surface Analysis. *Operating instructions EP*^{3}.

[61] NEERGARD WALTENBURG, H.; YATES, J.T. Surface Chemistry of Silicon. *Chemical Reviews*, 95(5):1589, 1995.

[62] NEFEDOV, V.I. *X-Ray Photoelectron Spectroscopy of Solid Surfaces*. VSP, 1988.

[63] NETZER, L.; SAGIV, J. A new approach to construction of artificial monolayer assemblies. *Journal of the American Chemical Society*, 105(3):974, 1983.

[64] ONCLIN, S.; RAVOO, B.J.; REINHOUDT, D.N. Gestaltung der Siliciumoxidoberfläche durch selbstorganisierte Monoschichten. *Angewandte Chemie*, 117:6438, 2005.

[65] PARIKH, A.N.; ALLARA, D.L.; AZOUZ, I.B.; RONDELEZ, F. An Intrinsic Relationship between Molecular Structure in Self-Assembled *n*-Alkylsiloxane Monolayers and Deposition Temperature. *Journal of Physical Chemistry*, 98(31):7577, 1994.

[66] PEARSON, D.A.; BLANCHETTE, M.; BAKER, M.L.; GUINDON, C.A. Trialkylsilanes as Scavengers for the Trifluoroacetic Acid Deblocking of Protecting Groups in Peptide Synthesis. *Tetrahedron Letters*, 30(21):2739, 1989.

[67] PLUEDDEMANN, E.P. *Silane coupling agents*. Plenum Press, 1982.

[68] POPAT, K.C.; JOHNSON, R.W.; DESAI, T.A. Characterization of vapor deposited thin silane films on silicon substrates for biomedical microdevices. *Surface and Coatings Technology*, 154:253, 2002.

[69] REED, M.A.; ZHOU, C.; MULLER, C.J.; BURGIN, T.P.; TOUR, J.M. Conductance of a Molecular Junction. *Science*, 278:5336, 1997.

[70] RIEDEL, E. *Anorganische Chemie*. deGruyter, 2002.

[71] RYE, R.R. Transition Temperatures for *n*-Alkyltrichlorosilane Monolayers. *Langmuir*, 13(9):2588, 1997.

[72] RYE, R.R; NELSON, G.C.; DUGGER, M.T. Mechanistic Aspects of Alkylchlorosilane Coupling Reactions. *Langmuir*, 13(11):2965, 1997.

[73] SAGIV, J. Organized Monolayers by Adsorption. 1. Formation and Structure of Oleophobic Mixed Monolayers on Solid Surfaces. *Journal of the American Chemical Society*, 102:92, 1980.

[74] SCHOLL, M.; SPRÖSSLER, C.; B, DENYER, M.; KRAUSE, M.; NAKAJIMA, K.; MAELICKE, A.; KNOLL, W.; OFFENHÄUSSER, A. Ordered networks of rat hippocampal neurons attached to silicon oxide surfaces. *Journal of Neuroscience Methods*, 104:65, 2000.

[75] SCHWAAB, D. *Surface patterning by means of Soft Lithography for Molecular and Bio-Electronics*. PhD thesis, Rheinisch-Westfälische Technische Hochschule Aachen, 2006.

[76] SHCHUKIN, E.D.; PERTSOV, A.V.; AMELINA, E.A.; ZELENEV, A.S. *Colloid and Surface Chemistry*. Elsevier, 2001.

[77] SHEU, M.-S. Patent US2005048219: Surface silanization, 2005.

[78] SILBERZAN, P.; LÉGER, L.; AUSSERRÉ, D.; BENATTAR, J.J. Silanation of Silica Surfaces. A New Method of Constructing Pure or Mixed Monolayers. *Langmuir*, 7(8):1647, 1991.

[79] SIQUEIRA PETRI, D.F.; WENZ, G.; SCHUNK, P.; SCHIMMEL, T. An Improved Method for the Assembly of Amino-Terminated Monolayers on SiO_2 and the Vapor Phase Deposition of Gold Layers. *Langmuir*, 15(13):4520, 1999.

[80] SNIDER, G; KUEKES, P.; HOGG, T.; WILLIAMS, R.S. Nanoelectronic architectures. *Applied Physics A*, 80:1183, 2005.

[81] STEVENS, M.J. Thoughts on the Structure of Alkylsilane Monolayers. *Langmuir*, 15:2773, 1999.

[82] STROHMEIER, B.R.; HERCULES, D.M. Surface Spectroscopic Characterization of Mn/Al_2O_3, Catalysts. *Journal of Physical Chemistry*, 88(21):4922, 1984.

[83] STROHMEIER, B.R.; HERCULES, D.M. Surface spectroscopic characterization of the interaction between zinc ions and γ-alumina. *Journal of Catalysis*, 86(2):266, 1984.

[84] TADA, H.; NAGAYAMA, H. Chemical Vapor Surface Modification of Porous Glass with Fluoroalkyl-Functional Silanes. 1. Characterization of the Molecular Layer. *Langmuir*, 10(5):1472, 1994.

[85] TAKAHAGI, T.; SHINGUBARA, S.; SAKAUE, H.; HOSHINO, K.; YASHIMA, H. Study on Adsorption Behavior of Organic Contaminations on Silicon Surface by Gas Chromatography/Mass Spectrometry. *Journal of Applied Physics*, 35(7A):L818, 1996.

[86] Taylor & Francis Group. Combined Chemical Dictionary, 2006.

[87] TRIPP, C.P.; HAIR, M.L. An Infrared Study of the Reaction of Octadecyltrichlorosilane with Silica. *Langmuir*, 8(4):1120, 1992.

[88] TSUKRUK, V.V.; BLIZNYUK, V.N. Adhesive and Friction Forces between Chemically Modified Silicon and Silicon Nitride Surfaces. *Langmuir*, 14(2):446, 1998.

[89] ULMAN, A. *An Introduction to Ultrathin Organic Films*. Academic Press, 1991.

[90] VANDENBERG, E.T.; BERTILSSON, L.; LIEDBERG, B.; UVDAL, K.; ERLANDSSON, R.; ELWING, H.; LUNDSTRÖM, I. Structure of 3-Aminopropyl Triethoxy Silane on Silicon Oxide. *Journal of Colloid and Interface Science*, 147(1):103, 1991.

[91] WANG, Y.; FERRARI, M. Surface Modification of Micromachined Silicon Filters. *Journal of Materials Science*, 35:4923, 2000.

[92] WHITE, L.D.; TRIPP, C.P. Reaction of (3-Aminopropyl)dimethylethoxysilane with Amine Catalysts on Silica Surfaces. *Journal of Colloid and Interface Science*, 232:400, 2000.

[93] WIKSTRÖM, P.; MANDENIUS, C.F.; LARSSON, P.-O. Gas Phase Silylation, a rapid Method for Preparation of High-Performance Liquid Chromatography Supports. *Journal of Chromatography*, 455:105, 1988.

[94] WU, K.; BAILEY, T.C.; WILLSON, C.G.; EKERDT, J.G. Surface Hydration and its Effects on Fluorinated SAM Formation on SiO_2 Surfaces. *Langmuir*, 21(25):11795, 2005.

[95] XIA, Y.; KIM, E.; ZHAO, X.-M.; ROGERS, J.A.; PRENTISS, M.; WHITESIDES, G.M. Complex Optical Surfaces Formed by Replica Molding Against Elastomeric Masters. *Science*, 273(5273):347, 1996.

[96] XIA, Y.; WHITESIDES, G.M. Soft Lithography. *Annual Review of Materials Research*, 28:153, 1998.

[97] ZHANG, F.; SRINIVASAN, M.P. Self-Assembled Molecular Films of Aminosilanes and Their Immobilization Capacities. *Langmuir*, 20(6):2309, 2004.

[98] ZHANG, Z.; HU, R.; LIU, Z. Formation of a Porphyrin Monolayer Film by Axial Ligation of Protoporphyrin IX Zinc to an Amino-Terminated Silanized Glass Surface. *Langmuir*, 16(3):1158, 2000.

[99] ZHAO, X.-M.; XIA, Y.; WHITESIES, G.M. Fabrication of Three-Dimensional Micro-Structures: Microtransfer Molding. *Advanced Materials*, 8(10):837, 1996.

[100] ZISMAN, W.A. Surface chemistry of plastics reinforced by strong fibers. *I&EC Product Research and Development*, 8(2):98, 1969.

Appendix

A Abbreviations

AFM	Atomic Force Microscopy
APTES	3-Aminopropyltriethoxysilane
Bp	Boiling point
CASINO	Cleaning and silanization in one
CCD	Charge-coupled device
CMOS	Complementary metal oxide semiconductor
ESCA	Electron Spectroscopy for Chemical Analysis
FOTCS	1H,1H,2H,2H-Perfluorooctyltrichlorosilane
IR	Infrared
LPD	Liquid phase deposition
MPTES	3-Mercaptopropyltriethoxysilane
MPTMS	3-Mercaptopropyltrimethoxysilane
MIMIC	Micromolding in Capillaries
μCP	Microcontact Printing
μTM	Microtransfer Molding
nTP	Nanotransfer Printing
PEG	Poly(ethyleneglycol)
PDMS	Poly(dimethylsiloxane)
POP	Polyolefin plastomer
REM	Replica Molding
rms	root-mean-square
SAM	Self-assembled monolayer
SAMIM	Solvent-assisted Micromolding
SEM	Scanning Electron Microscopy
STP	Shuttle-Transfer Printing
UV	Ultraviolett
VPD	Vapor phase deposition
XPS	X-Ray Photoelectron Spectroscopy

B XP-Spectra

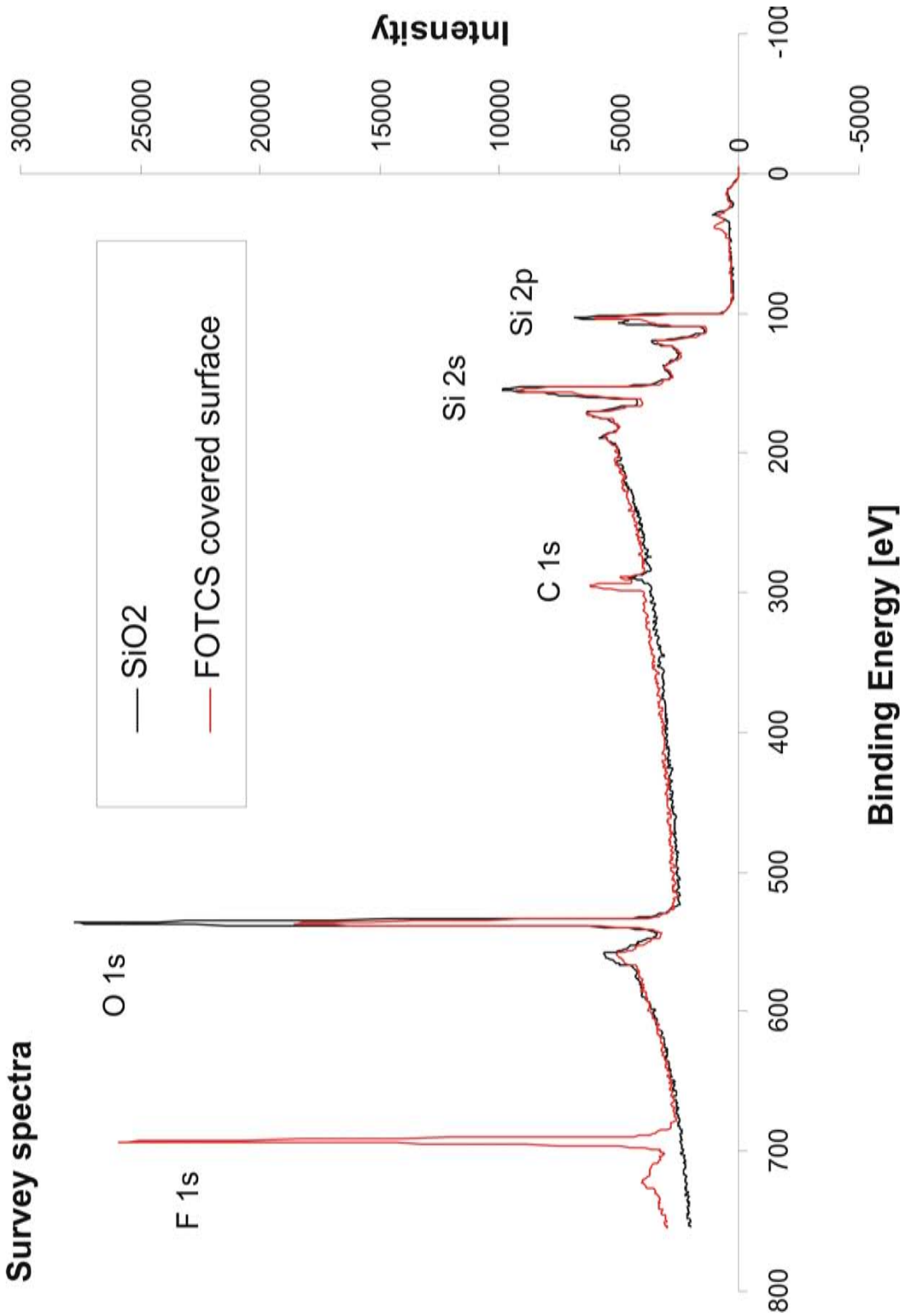

Figure B.1: Survey spectrum of a silicon wafer with native silicon oxide layer and after silanization with FOTCS

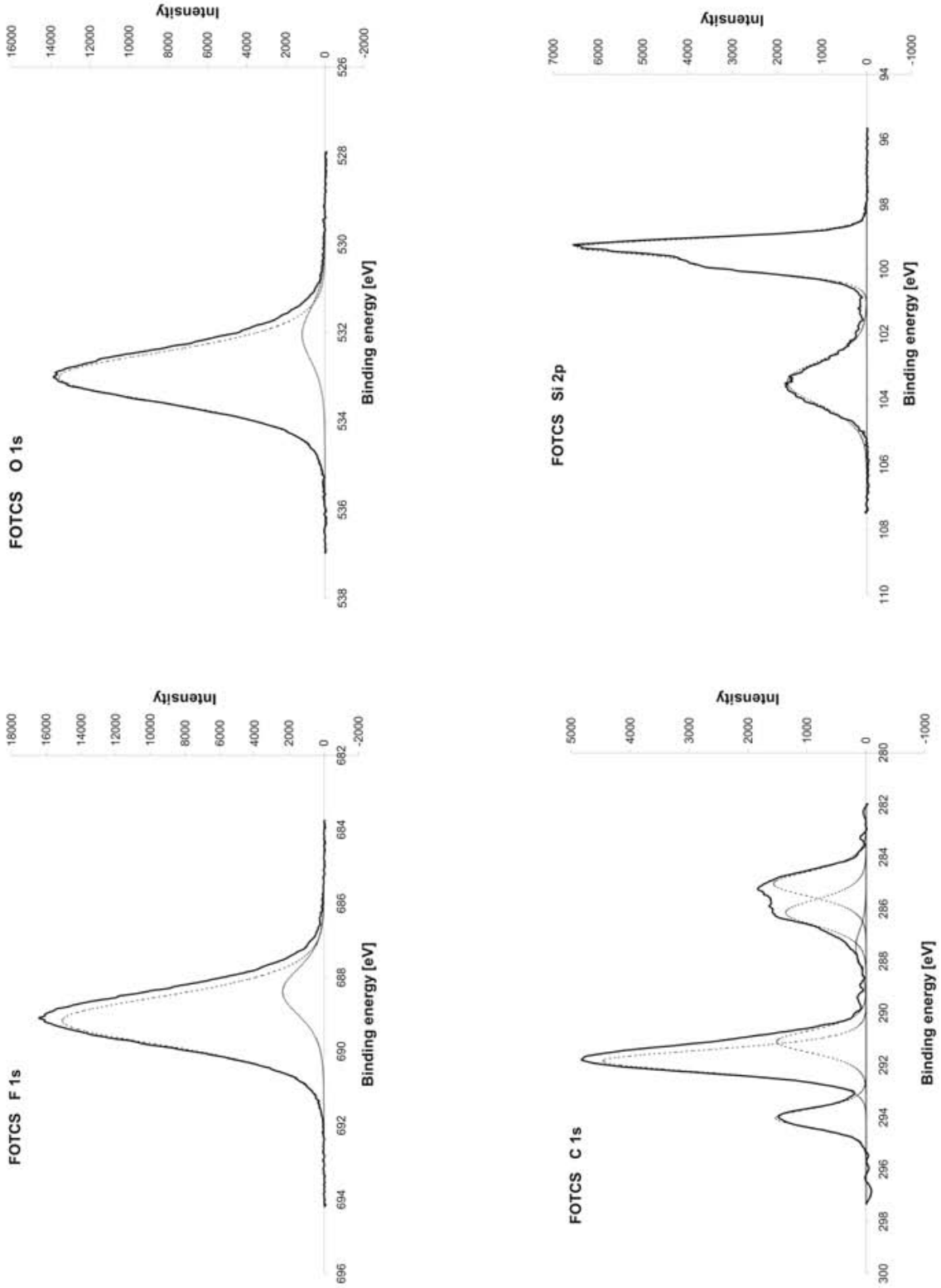

Figure B.2: Spectra of a silicon wafer after silanization with FOTCS

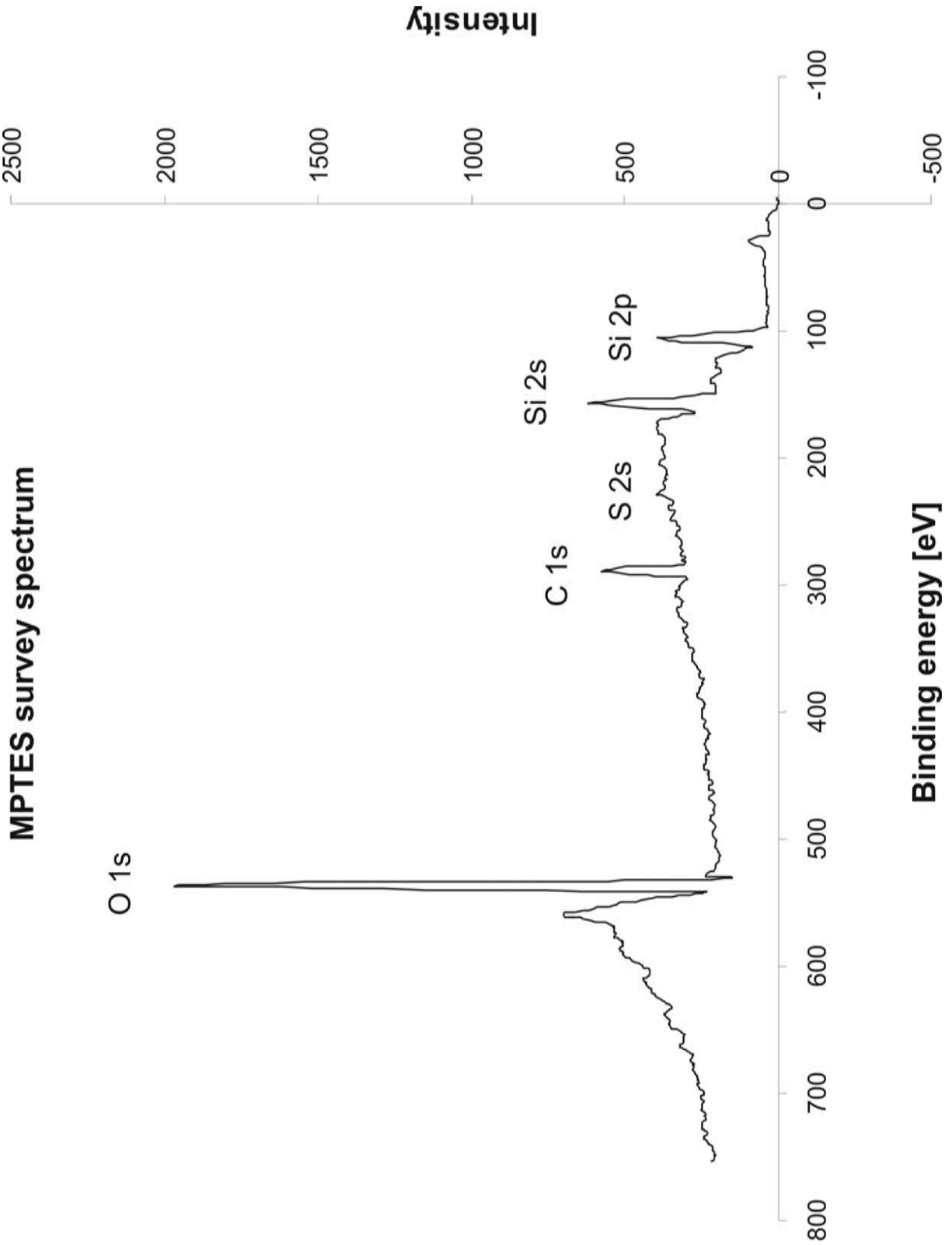

Figure B.3: Survey spectrum of a silicon wafer after silanization with MPTES

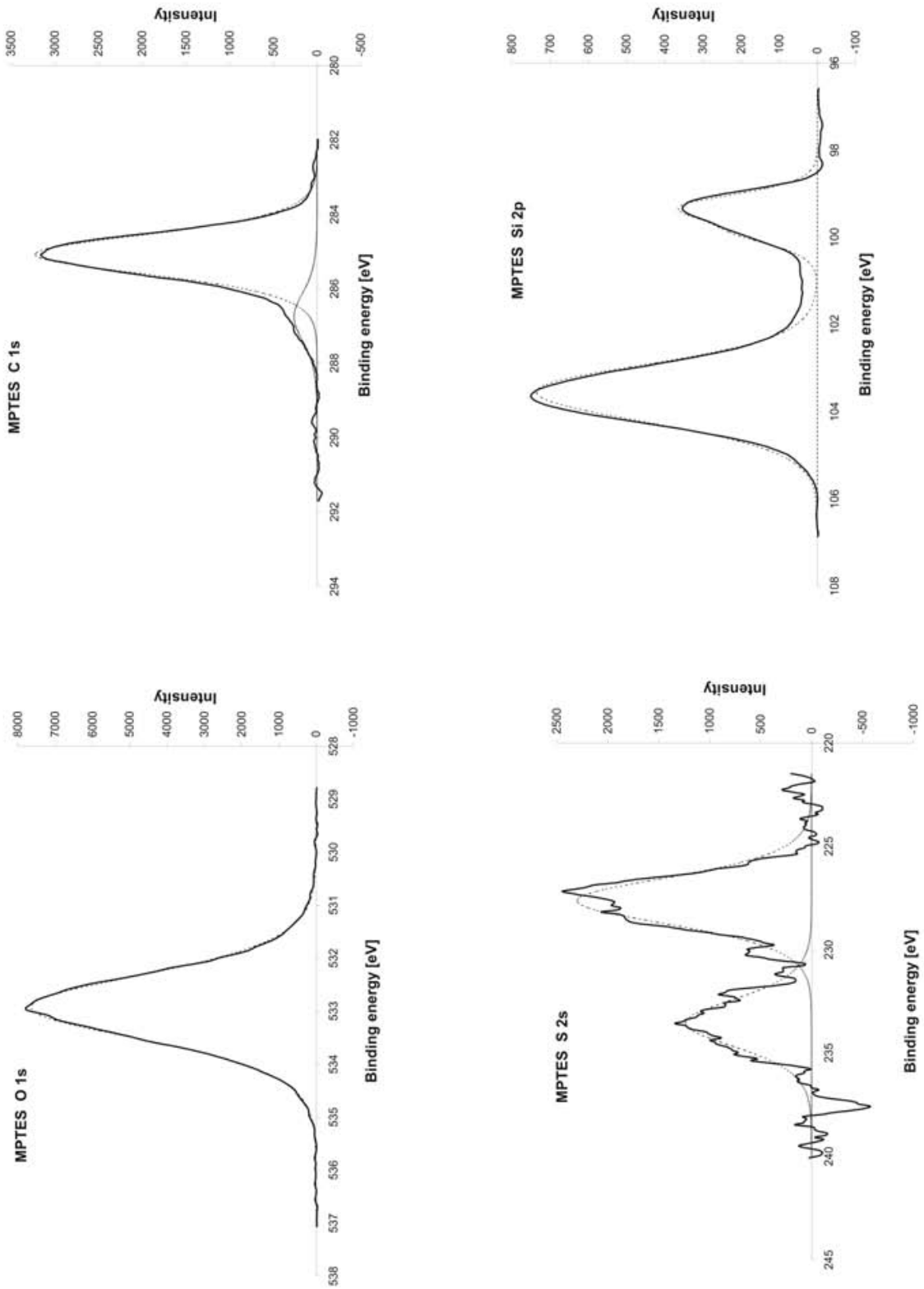

Figure B.4: Spectra of a silicon wafer after silanization with MPTES

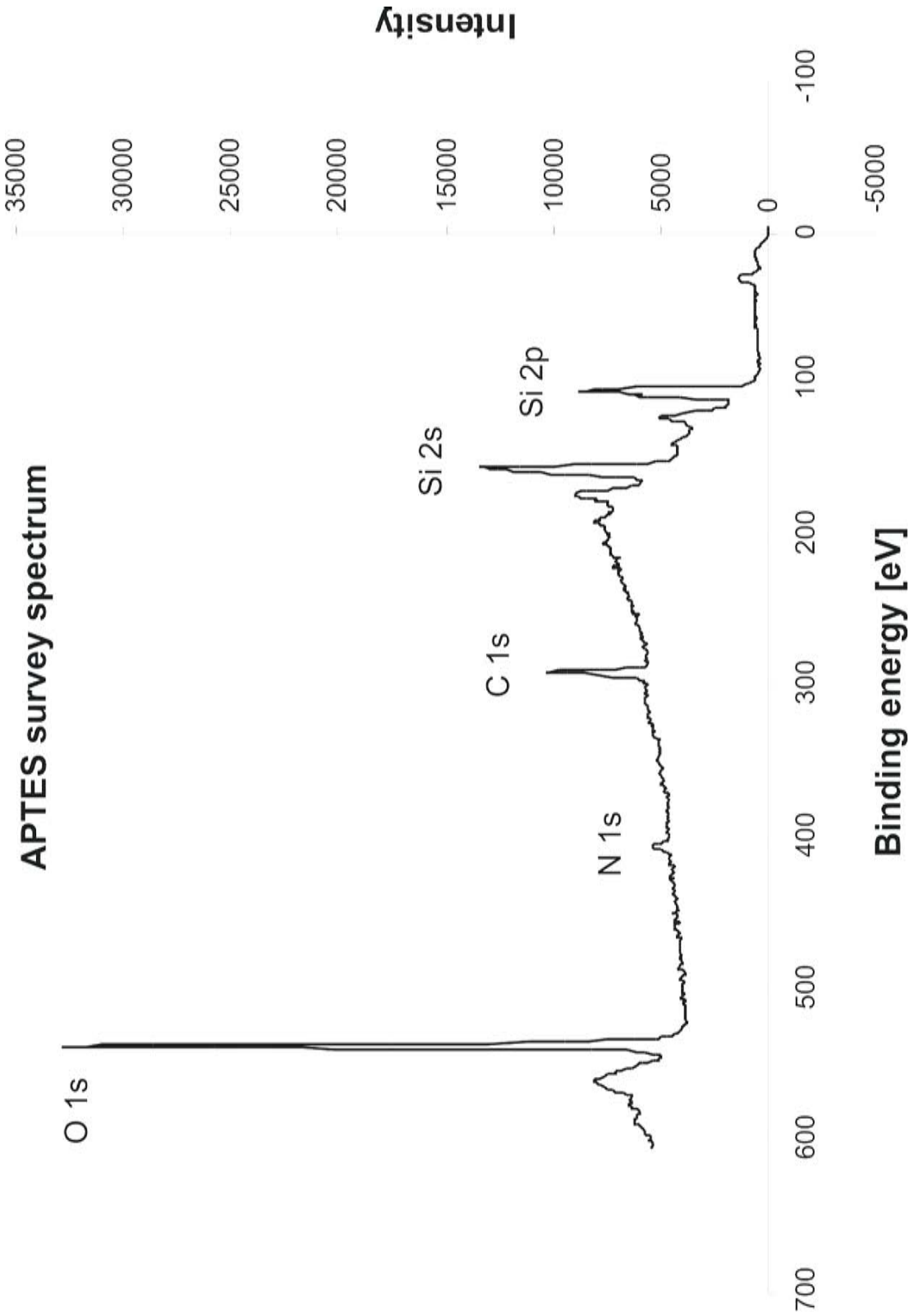

Figure B.5: Survey spectrum of a silicon wafer after silanization with APTES

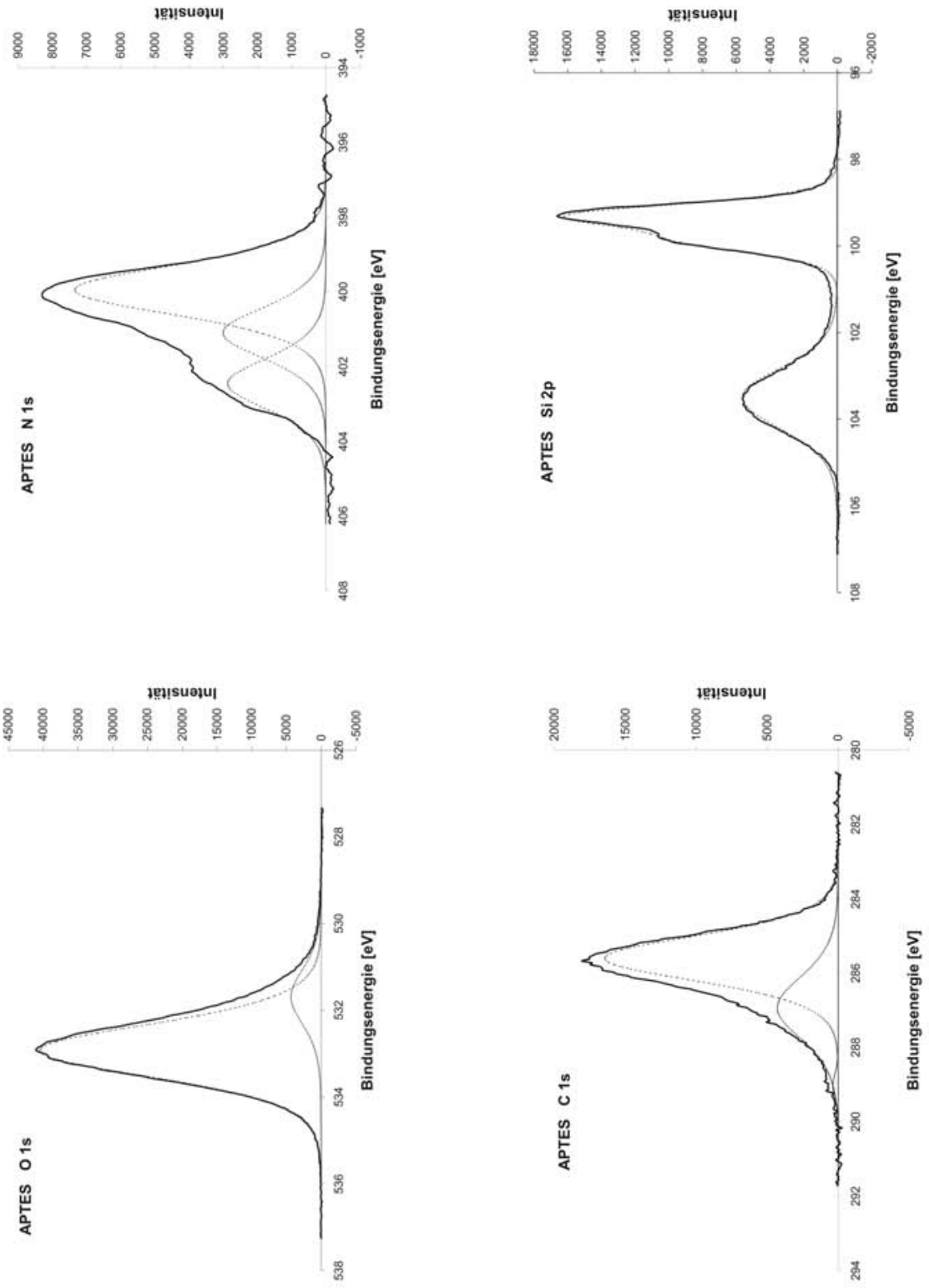

Figure B.6: Spectra of a silicon wafer after silanization with APTES

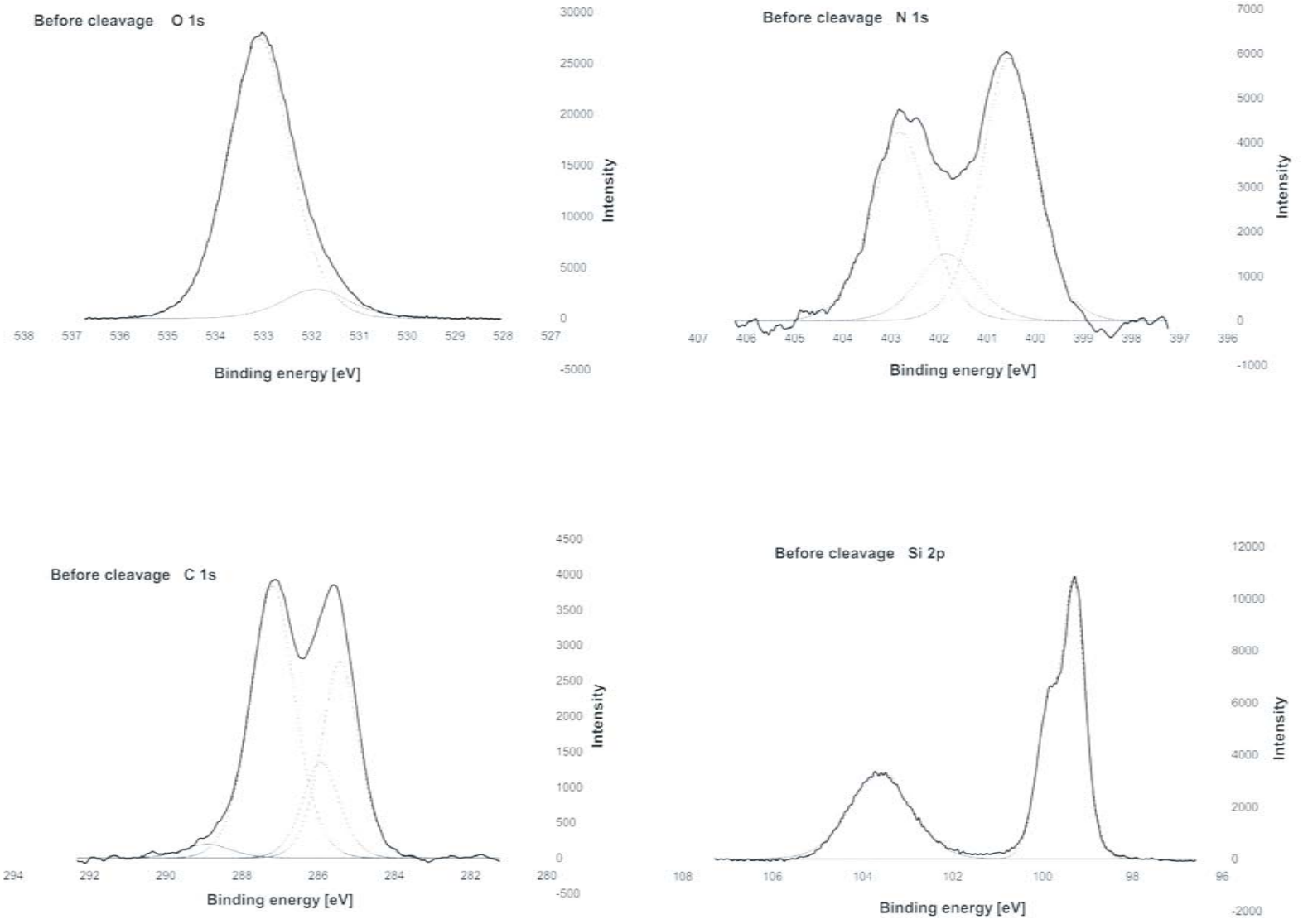

Figure B.7: Spectra of PEG covered wafer before cleavage of protection group

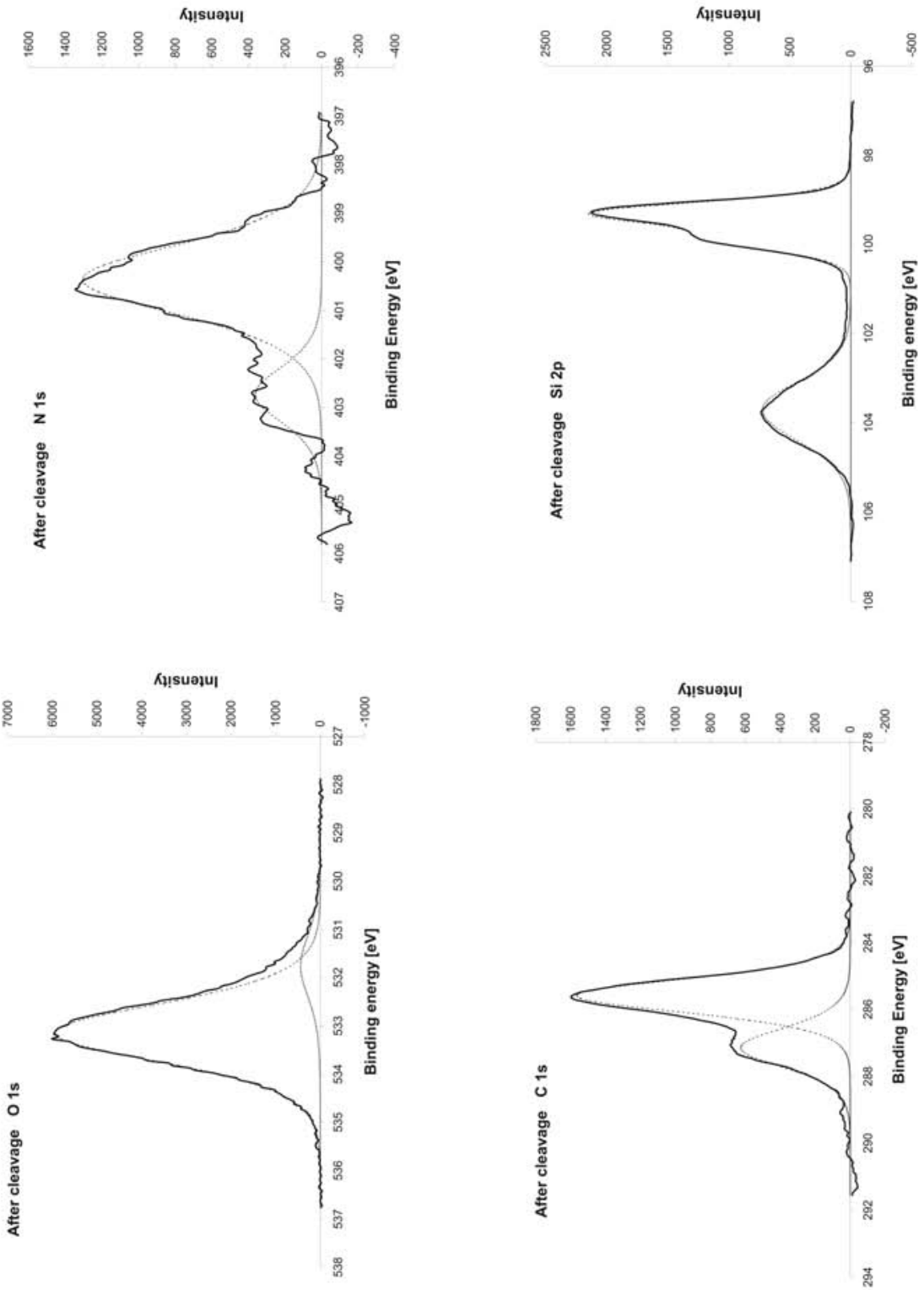

Figure B.8: Spectra of PEG covered wafer after cleavage of protection group

Danksagung

Bedanken möchte ich mich bei allen, die zum Gelingen dieser Arbeit beigetragen haben, insbesondere bei:

- Prof. Dr. E. Kroke und Prof. Dr. A. Offenhäusser für die interessante Aufgabenstellung und die Unterstützung dieser Arbeit
- Dr. D. Mayer für die ausgezeichnete Betreuung während dieser Arbeit
- D. Schwaab für das geduldige Anlernen und die umfangreiche Kenntnisweitergabe
- Dr. A. Yasuda, Dr. J. Wessels, Dr. B. Lüssem, A. Schreiber und Z. Karipidou für die fruchtbare Kooperation
- M. Prömpers für die Durchführung zahlreicher Reinraumarbeiten
- Dr. S. Ingebrandt für wertvolle Hinweise und Anregungen
- M. Banzet und D. Lomparski für oft benötigte und jederzeit gewährte praktische Hilfe
- S. Schaal , R. Helpenstein und T. Wilms für die Unterstützung bei der Durchführung praktischer Arbeiten
- Dr. A. Besmehn für die Durchführung der photoelektronenspektroskopischen Analyse
- Der Glastechnik-Werkstatt, besonders G. d'Orsaneo, der Konstruktions-Werkstatt, besonders D. Strobl, und dem Elektronik-Labor, besonders R. Otto, für die Anfertigung maßgeschneiderter Geräte.

Forschungszentrum Jülich
in der Helmholtz-Gemeinschaft

Jül-4249
Mai 2007
ISSN 0944-2952